ELEONORA PETRYAYEVA AND W. RUSS ALGAR*
DEPARTMENT OF CHEMISTRY, UNIVERSITY OF BRITISH COLUMBIA,
2036 MAIN MALL, VANCOUVER, BC V6T 1Z1, CANADA

IGOR L. MEDINTZ
CENTER FOR BIO/MOLECULAR SCIENCE AND ENGINEERING,
U.S. NAVAL RESEARCH LABORATORY CODE 6900,
4555 OVERLOOK AVENUE SW, WASHINGTON, DC 20375 USA

Quantum Dots in Bioanalysis: A Review of Applications Across Various Platforms for Fluorescence Spectroscopy and Imaging

Semiconductor quantum dots (QDs) are brightly luminescent nanoparticles that have found numerous applications in bioanalysis and bioimaging. In this review, we highlight recent developments in these areas in the context of specific methods for fluorescence spectroscopy and imaging. Following a primer on the structure, properties, and biofunctionalization of QDs, we describe select examples of how QDs have been used in combination with steady-state or time-resolved spectroscopic techniques to develop a variety of assays, bioprobes, and biosensors that function via changes in QD photoluminescence intensity, polarization, or lifetime. Some special attention is paid to the use of Förster resonance energy transfer–type methods in bioanalysis, including those based on bioluminescence and chemiluminescence. Direct chemiluminescence, electrochemiluminescence, and charge transfer quenching are similarly discussed. We further describe the combination of QDs and flow cytometry, including traditional cellular analyses and spectrally encoded barcode-based assay technologies, before turning our attention to enhanced fluorescence techniques based on photonic crystals or plasmon coupling. Finally, we survey the use of QDs across different platforms for biological fluorescence imaging, including epifluorescence, confocal, and two-photon excitation microscopy; single particle tracking and fluorescence correlation spectroscopy; super-resolution imaging; near-field scanning optical microscopy; and fluorescence lifetime imaging microscopy. In each of the above-mentioned platforms, QDs provide the brightness needed for highly sensitive detection, the photostability needed for tracking dynamic processes, or the multiplexing capacity needed to elucidate complex systems. There is a clear synergy between advances in QD materials and spectroscopy and imaging techniques, as both must be applied in concert to achieve their full potential.

Received 3 December 2012; accepted 18 December 2012.
* Author to whom correspondence should be sent. E-mail: algar@chem.ubc.ca.
DOI: 10.1366/12-06948

Index Headings: **Quantum dot; Fluorescence; Spectroscopy; Assay; Imaging; Microscopy; Flow cytometry; Single molecule; Förster resonance energy transfer (FRET); Multiplexing.**

INTRODUCTION

In 2002, *Applied Spectroscopy* published its first review on quantum dots (QDs), "Quantum Dots: A Primer," by Murphy and Coffer.[1] The applications of these luminescent nanocrystals have evolved tremendously over the last decade, particularly in the areas of bioimaging and bioanalysis. Since the seminal first demonstration of QDs for biological imaging in 1998,[2,3] thousands of new research articles on QDs have been published. Researchers have exploited the brightness, photostability, size-dependent optoelectronic properties, and superior multiplexing capability of QDs for a myriad of

applications.[4–15] Some of the more prominent applications include in vitro diagnostics, energy transfer–based sensing, cellular and in vivo imaging, and drug delivery and theranostics.[6,16,17] In parallel with these advances in bioimaging and bioanalysis, QD materials have also evolved to provide greater flexibility and capability. A wider range of nanocrystal materials, functional coatings, and bioconjugate techniques are available to facilitate new applications of QDs. As we have noted previously,[18] QDs have become bona fide multidisciplinary tools in much the same way as conventional fluorescent dyes, albeit not yet with the same extent of use. There has also been the realization that QDs should not be viewed as wholesale replacements for fluorescent dyes, but rather that QDs can be advantageous in many applications, disadvantageous in others, and even complementary to dyes in some cases.

The proliferation of QD materials across disciplines has been accompanied by a similar proliferation of more advanced spectroscopic technologies, as well as diminishing costs and greater commercial availability of important optical components (e.g., violet lasers, QD-specific filter sets). Indeed, use of the unique optical properties of QDs for bioanalysis and bioimaging is moot without a suitable measurement platform. Fortunately, new developments in applied spectroscopy and the biological applications of QDs are often synergistic. For example, the photoluminescence (PL) properties of QDs are ideal for maximizing the utility of spectral imaging and vice versa. Even the well-known blinking of QD PL, which can complicate single molecule tracking, becomes valuable for super-resolution imaging.[19] In this focal point review, we provide an expanded primer on QDs to complement that written by Murphy and Coffer,[1] briefly summarize the chemistry used to biofunctionalize QDs, and highlight some recent (2003–2012) biological applications of QDs in the context of specific spectroscopic techniques. These techniques include ensemble fluorescence measurements based on intensity, polarization, or lifetime; energy and charge transfer methods; flow cytometry and optical barcodes; enhanced fluorescence based on photonic crystals and plasmon coupling; epifluorescence, confocal, and two-photon excitation (2PE) microscopy; single particle tracking and fluorescence correlation spectroscopy; and super-resolution imaging and near-field scanning optical microscopy. Each example highlights how QDs help enable the full capability of a given spectroscopic or imaging technique, and vice versa.

OPTICAL PROPERTIES OF QUANTUM DOTS

What is a Quantum Dot? QDs are colloidal semiconductor nanocrystals with dimensions between about 1 and 10 nm. Excitons are generated in the nanocrystals upon the absorption of light, and electron-hole recombination leads to luminescence. Although depicted as spheres in most illustrations, QDs are crystalline materials with facets and a lattice structure analogous to the bulk semiconductor material. Depending on its size, each nanocrystal can comprise hundreds to thousands of atoms, a large fraction (>10%) of which are located at the nanocrystal surface (i.e., a high surface area-to-volume ratio). As described in more detail below, most of the QDs used in analytical applications are synthesized as core/shell structures, where the core nanocrystal is overcoated with another semiconductor material to protect and improve its optical properties. The "flagship" QD material is undoubtedly core/shell CdSe/ZnS.

Absorption and Photoluminescence. It was the unique photophysical properties of QDs that first generated excitement for biological imaging and analysis. QDs have become renowned for eye-catching photographs (Fig. 1A) of differentially sized QDs under ultraviolet (UV) illumination that show a bright rainbow of PL. The bright PL is the result of high quantum yields (Φ = 0.1–0.9) combined with large molar extinction coefficients (10^5–10^7 M^{-1} cm^{-1}). As shown in Figs. 1C and 1D, QDs have broad absorption spectra that continuously increase in magnitude from their first exciton peak to shorter wavelengths in the near-UV. QD PL spectra are shifted to slightly longer wavelengths than the first exciton absorption peak, such that an *effective* Stokes shift >100 nm can be achieved. The PL is also spectrally narrow, with an approximately Gaussian profile (full width at half-maximum [FWHM] of 25–35 nm). The stunning rainbow of QD PL arises from the fact that the peak emission wavelength shifts as a function of nanocrystal size and material. The QD size and PL color can be selected by controlling the temperature and duration of crystal growth during synthesis. Photographs of the type in Fig. 1A exemplify the utility of QDs for multiplexed analyses and multicolor imaging: a single light source can excite many colors of QD simultaneously (broad absorption), and each PL contribution can be readily resolved or deconvolved (narrow emission).

Other advantageous optical properties of QDs include excited state lifetimes that tend to be longer than those of fluorescent dyes (>10 ns), superior resistance to photobleaching and chemical degradation (due to the inorganic composition and confinement of the exciton), and two-photon absorption cross sections (10^3–10^4 GM) that are orders of magnitude larger than those of fluorescent dyes.[20] QDs are thus excellent probes for tracking dynamic processes over time, and for two-photon imaging of tissues or other complex biological specimens where near-infrared (NIR) excitation mitigates challenges associated with autofluorescence and attenuation of excitation light by strong protein absorbance (e.g., hemoglobin) in the visible region.[21,22]

Quantum Confinement and Core/Shell Structures. The size-dependence of QD PL is the result of *quantum confinement*. As a bulk material is reduced to nanoscale dimensions, the density of states decreases near the conduction band and valence band edges, resulting in the emergence of discrete excitonic states. The band gap energy further increases with decreasing nanocrystal size as the exciton is confined to smaller dimensions than its Bohr radius. The PL emission wavelength shifts since exciton recombination occurs between the band edge states. For example, bulk CdSe has a band gap energy of 1.76 eV and a Bohr exciton diameter of 9.6 nm,[23] whereas the band gap energy of 2–7 nm CdSe

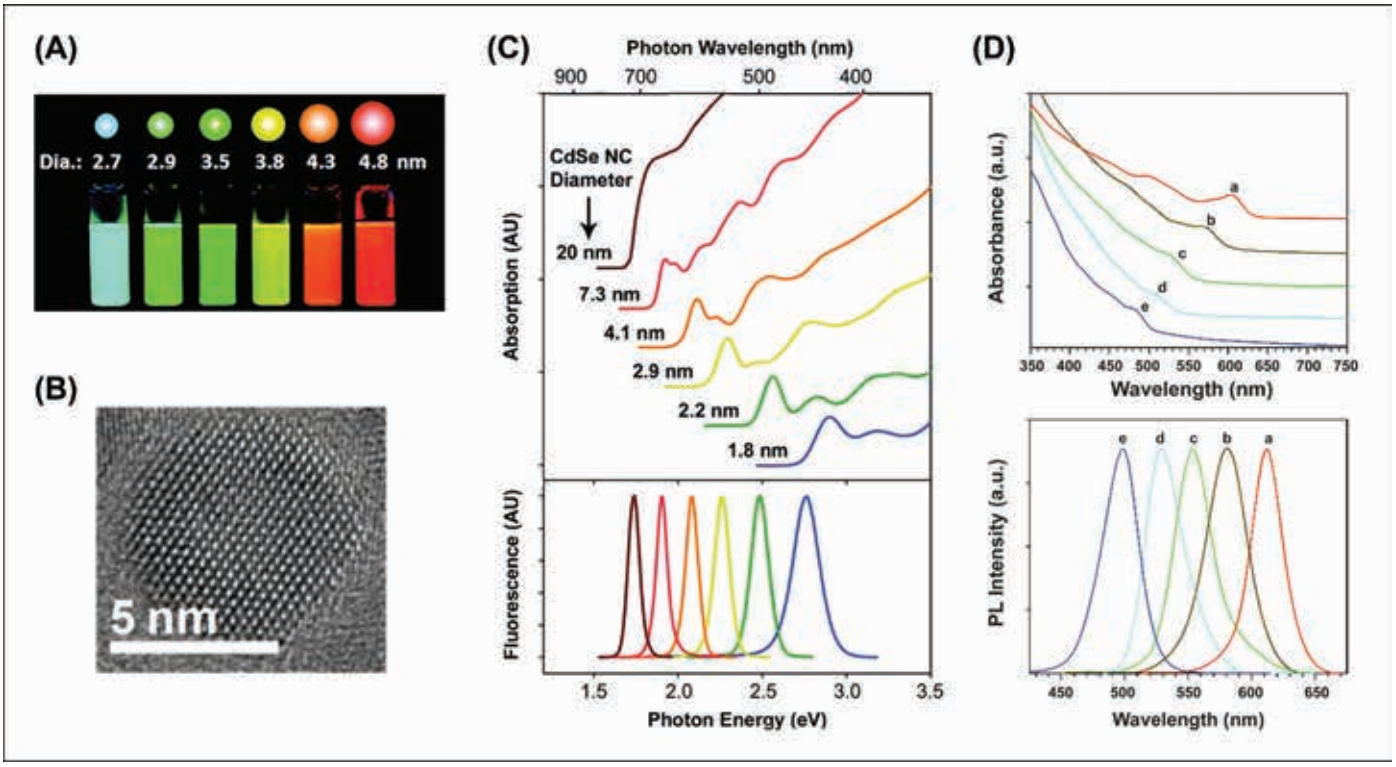

FIG. 1. **(A)** ***Size-tunable PL of CdSe QDs. The photograph was taken under UV illumination (365 nm).*** **(B)** ***Transmission electron microscopy image of a CdSe/ZnS QD. [(A) and (B) reproduced with permission from Ref. 18. Copyright American Chemical Society 2011.]*** **(C)** ***Size-dependent absorption and fluorescence spectra of CdSe QDs. [Reproduced with permission from Ref. 23. Copyright American Chemical Society 2010.]*** **(D)** ***Absorption and PL spectra of $Zn_xCd_{1-x}Se$ QDs with Zn mole fractions of (a) $x = 0$, (b) 0.28, (c) 0.44, (d) 0.55, and (e) 0.67. [Reproduced with permission from Ref. 56. Copyright American Chemical Society 2003.]***

nanocrystals decreases from 2.8 eV to 1.9 eV, with PL shifting between 450 and 650 nm. The range over which the band gap energy and PL wavelength can be tuned by quantum confinement depends on the material of the nanocrystal (vide infra) and its bulk band gap energy. PL emission centered at wavelengths between 380 and 2000 nm can be obtained with appropriate selection of the semiconductor material and nanocrystal size.[13]

Although a QD is approximately a physical representation of the particle-in-a-box concept, an important difference is that the core nanocrystal does not provide an infinite potential barrier for confinement of the exciton. Furthermore, the lattice structure of the nanocrystal abruptly terminates at its surface and can lead to localized "trap" states within the quantum confined band gap. Trap states can sometimes be observed as band gap emission, showing up as a broad peak on the bathochromic side of the expected band edge emission. These states, as well as leakage of the excitonic wavefunction outside the core nanocrystal, promote non-radiative pathways for recombination of the exciton.[23] To improve PL efficiency, the core nanocrystal can be coated with a few layers of a structurally similar semiconductor with a higher band gap energy, as is the case with widely used CdSe/ZnS and CdTe/ZnS QDs. Such an arrangement, where the core band edge states are both intermediate in energy to those of the shell, is referred to as a Type I heterostructure. This configuration is the most common in bioanalytical applications since it offers the best confinement of the exciton (Fig. 2A) and the highest rates of radiative recombination (i.e., brighter PL). Confinement is not complete, however, as shell growth is typically accompanied by a 5–10 nm bathochromic shift in the QD PL spectrum.

Other heterostructure configurations are designed to localize the electron, the holes, or both outside of the core nanocrystal. For example, in Type II heterostructures (e.g., CdTe/CdSe, CdSe/ZnTe),[24] the electron and hole are localized in the shell and core, respectively, or vice versa. This behavior arises from an offset between the band edge states of the core and shell (Fig. 2C). The exciton recombines across the core/shell interface and, consequently, the emission wavelength corresponds to an energy less than the band gap of either the core or shell material. The decreased overlap between the electron and hole wavefunctions also results in lower absorption coefficients and longer PL decay times. Type II QDs are potential NIR emitters and growth of a second Type I shell (e.g., CdSe/CdTe/ZnSe)[25] can enhance quantum yields; however, other Type I and alloyed NIR-emitting QDs (e.g., InAs/ZnSe, InAs/CdSe, InAs/InP, Cu:InP/ZnSe, $InAs_xP_{1-x}$/InP/ZnSe) are also being actively developed.[26–28] Quasi Type II QDs have only a small offset between, for example, the conduction band edge states of

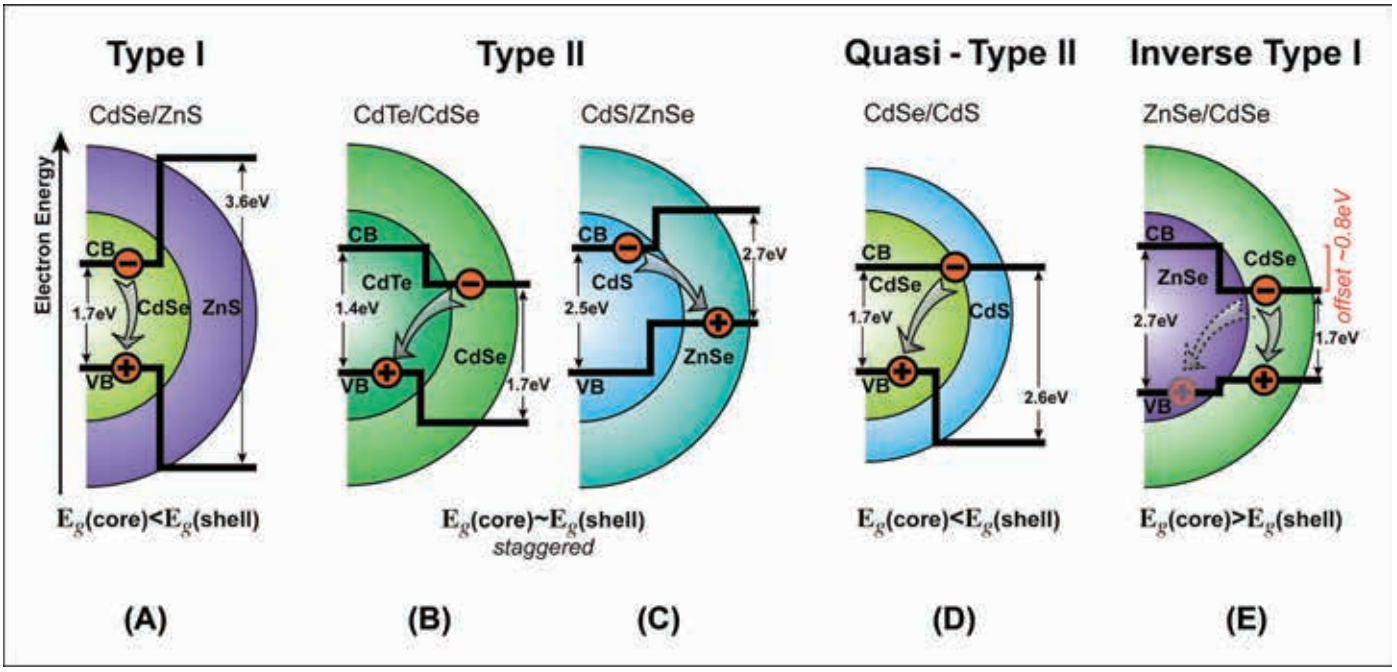

FIG. 2. Illustration of band gap engineering by selection of core and shell materials. The relative energy of conduction band and valence band edge states between the core and shell determines the localization of the electron and hole, and the nature of the transition associated with exciton recombination, offering an additional means of tuning the optical properties of QDs. **(A)** ***Type I QD with localization of both carriers in the core.*** **(B)** ***Type II QD with localization of the electron in the shell.*** **(C)** ***Type II QD with localization of the hole in the shell.*** **(D)** ***Quasi-Type II QD with localization of the electron in both and the core and shell.*** **(E)** ***Inverse-Type I QD with localization of both carriers in the shell.***

the core and shell, such that the electron is delocalized over the whole nanocrystal but the hole is confined to the core (Fig. 2D).[29] Inverse (or reverse) Type I QDs (e.g., CdS/CdSe, ZnSe/CdSe)[30] are designed to localize both the electron and hole into the shell. The band edge states for the shell are both intermediate to those of the core (Fig. 2E). These configurations also require a secondary Type I shell (e.g., ZnSe/InP/ZnS)[31] to enhance PL emission. Finally, lattice strain between the core and shell can be used to tune the optical properties of certain QDs. For example, growth of epitaxial shells of ZnS, ZnSe, CdS, or CdSe on small, soft CdTe cores can be used to shift band energies and thus PL emission. Compressive strain in the core increases the energy of its band edge states, whereas synergistic tensile strain in the shell decreases the energy of its band edge states.[32] The effect of growing thicker shells can be large enough to induce Type II band alignment in a Type I heterostructure such as CdTe/ZnSe.[32] To date, Type II QDs have not found widespread use in bioanalytical applications.

Surface States and Effects. The energies of band edge states are not the only determinants of QD PL. Even with growth of a Type I shell, surface states can still affect the PL of real QDs (i.e., imperfect structures). For example, the "blinking" or fluorescence intermittency of QDs, perhaps the second most renowned property after their size-tunable emission, is associated with surface states. Blinking can be observed at the single particle level, has a power law probability distribution, and is a consequence of either (i) charging and discharging of the core nanocrystal, or (ii) trapping of carriers at surface states before they can relax to emissive band edge core states.[33] Auger recombination is the predominant relaxation mechanism in charged QDs, resulting in very efficient PL quenching until the QD core is neutralized. Although detrimental in some applications of QDs, the observation of blinking is useful to confirm tracking of a single QD,[34,35] and it has enabled super-resolution imaging,[36] as described later in this review.

In addition to blinking, QDs sometimes exhibit other interesting optical phenomena under high-intensity excitation. These phenomena include bluing, photobrightening, and photodarkening, all of which are observable in the ensemble.[37] Bluing corresponds to an irreversible hypsochromic shift in the band edge emission and is the manifestation of photooxidative etching of the average nanocrystal size.[38] Brightening, or photoactivation, is an increase in the QD PL intensity under irradiation and is associated with changes in the properties of the QD surface. These changes have been suggested to include the passivation of defect states and dangling bonds,[37] or displacement of trapped charges,[39,40] each leading to a decrease in a "dark fraction" of non-luminescent QDs in the ensemble. The extent of photobrightening, as well as the opposite effect, photodarkening, depends on the duration and intensity of irradiation, although photodarkening seems to be induced at higher irradiation intensities,

above-gap excitation energies, and longer irradiation times. The competitive kinetics of photobrightening and photodarkening have been investigated and found to yield different steady-state QD PL intensities for different irradiation intensities.[40]

The aforementioned dark fraction, which has been observed experimentally via fluorescence coincidence analysis, is inversely correlated to the ensemble quantum yield.[41,42] It has been suggested that the mechanism for formation of the dark fraction is analogous to that for blinking behavior,[43] albeit that the dark fraction is not a by-product of blinking over extended timescales.[41,42] Interestingly, a decrease in the size of the dark fraction is responsible for the apparent increase in the ensemble QD quantum yield that is frequently observed upon "passivation" with adsorbed macromolecules such as proteins.[44]

The importance of the above-mentioned effects in analytical applications of QDs is variable, depending on both the characteristics of the batch of QDs used and the spectroscopic parameters of the experiment (e.g., laser power). Ensemble assay methodologies based on one-time measurements at low power excitation tend to be relatively immune, whereas single molecule tracking experiments with high-intensity excitation are the most susceptible to these effects. In either case, good or poor quality QDs can make a tremendous difference in the outcome of an experiment. Maintaining continuity in the properties of QD materials is thus an ongoing challenge in the field.

QUANTUM DOT MATERIALS

As alluded to above, QDs have been synthesized from a broad range of semiconductor materials. The most popular materials have been CdSe, CdTe, and their core/shell analogs, CdSe/ZnS and CdTe/ZnS. This popularity can be attributed to well-established synthetic protocols, emission that can be size-tuned over the visible/NIR region, and, not least of all, commercial availability. Traditionally, emission has been tuned on the basis of core nanocrystal size with these materials, and the role of the Type I shell has been to passivate dangling bonds on the surface of the core, better confine the exciton (vide supra) and enhance the QD's optical properties (e.g., the quantum yield can increase by 20–35%).[45,46] For this purpose, the growth of a thin shell is important. For example, with CdSe/ZnS QDs, the 12% lattice mismatch between CdSe and ZnS necessitates that growth of the ZnS shell be limited to a few atomic layers before lattice strain detrimentally affects the PL properties.[17] Thicker shells have been desirable to render QDs more robust or prevent blinking.[47] Effective approaches for growing thicker shells and relaxing lattice mismatch have included incorporating a small amount of Cd into the shell material,[48] and synthesis of gradient or multi-shell structures (e.g., CdSe/CdS/ZnS).[47,49,50] As an alternative to size-tuning of PL, QD core materials can also be alloyed. The PL emission of ternary alloyed QDs (e.g., $CdSe_xTe_{1-x}$, CdS_xSe_{1-x}, $Cd_xZn_{1-x}S$, $Cd_{1-x}Zn_xSe$) can be varied while maintaining a constant size (Fig. 1D),[51–56] and these materials are also commercially available.

In addition to II–VI semiconductors, other materials used for QD synthesis include III–V (e.g., InP)[57,58] or group IV (e.g., Si)[59,60] semiconductors. To some degree, the investigation of alternative materials to CdSe and CdTe has been driven by the perceived toxicity of Cd-based QDs (previous work[61–63] provides discussions on the complex issue of toxicity; QDs can be used in both toxic and nontoxic capacities). Although synthesis protocols for alternative materials are still being optimized to yield optical properties that match those of CdSe/ZnS and CdTe/ZnS QDs, there has been considerable progress. For example, InP/ZnS QDs[64] (with emission in the 480–750 nm range) and InP/ZnSe/ZnS QDs[65] have been reported with $\Phi = 0.4$–0.6 and a FWHM of 50–60 nm. In addition to the benefits of NIR emission for in vivo applications, QD size plays an important role in determining their fate in vivo. Renal clearance and minimal accumulation in organs (e.g., spleen, kidney, liver) are observed with nanoparticles <5.5 nm in hydrodynamic diameter.[66] Recently, Park et al. reported the synthesis of highly luminescent $CuIn_xSe_y$/ZnS core/shell QDs ($\Phi = 0.6$), with emission within the NIR biological window at 741 nm, a FWHM of 175 nm, and an average diameter of 5 nm.[67] With the exception of the large FWHM, these QDs are almost ideal for prospective in vivo applications. Some non–Cd QD materials (e.g., InP/ZnS, InGaP/ZnS) are currently available commercially.

Synthesis. Unfortunately, the laboratory synthesis of high-quality colloidal QDs is still largely restricted to experienced chemists. Despite numerous attempts in the literature to synthesize QDs in aqueous media by using convenient air-stable precursors, QDs with narrow FHWM (a function of the distribution of particle size, i.e., monodispersity) and high quantum yields have been almost exclusively obtained though solvothermal methods that use organometallic precursors and nonpolar organic solvents at high temperature and under inert atmosphere (i.e., pyrolysis of inorganic precursors).[68–70] The possible exception is the aqueous synthesis of CdTe QDs, where quantum yields have been reported to reach 82% but are typically closer to 40%.[71–73] These QDs can also be relatively monodisperse, with FWHM values typically in the range of 30–60 nm.

Functionalization of QDs. Although the optical properties of QD attract the lion's share of excitement, experts have now come to realize that the surface area of the QD is almost as valuable: A QD can serve as a nanoscale scaffold with physicochemical properties and biological activity that can be tailored through interfacial chemistry and bioconjugation. Functionalization is done in multiple steps, and the design and execution at each step are critical to the efficacy of the QD in its intended application.[18,74–78]

Interfacial Chemistry. Since most biological applications use core/shell QDs, the inorganic shell is generally the first site for modification. In particular, high-quality QDs prepared by solvothermal methods are coated with hydrophobic surfactants and require modification to render them water-soluble for biological applications. As shown in Figs. 3i to 3v, there are two well established routes to water-soluble QDs: (i) ligand exchange (i.e., replacement of the native surfactants), yielding more compact QDs; and (ii) encapsula-

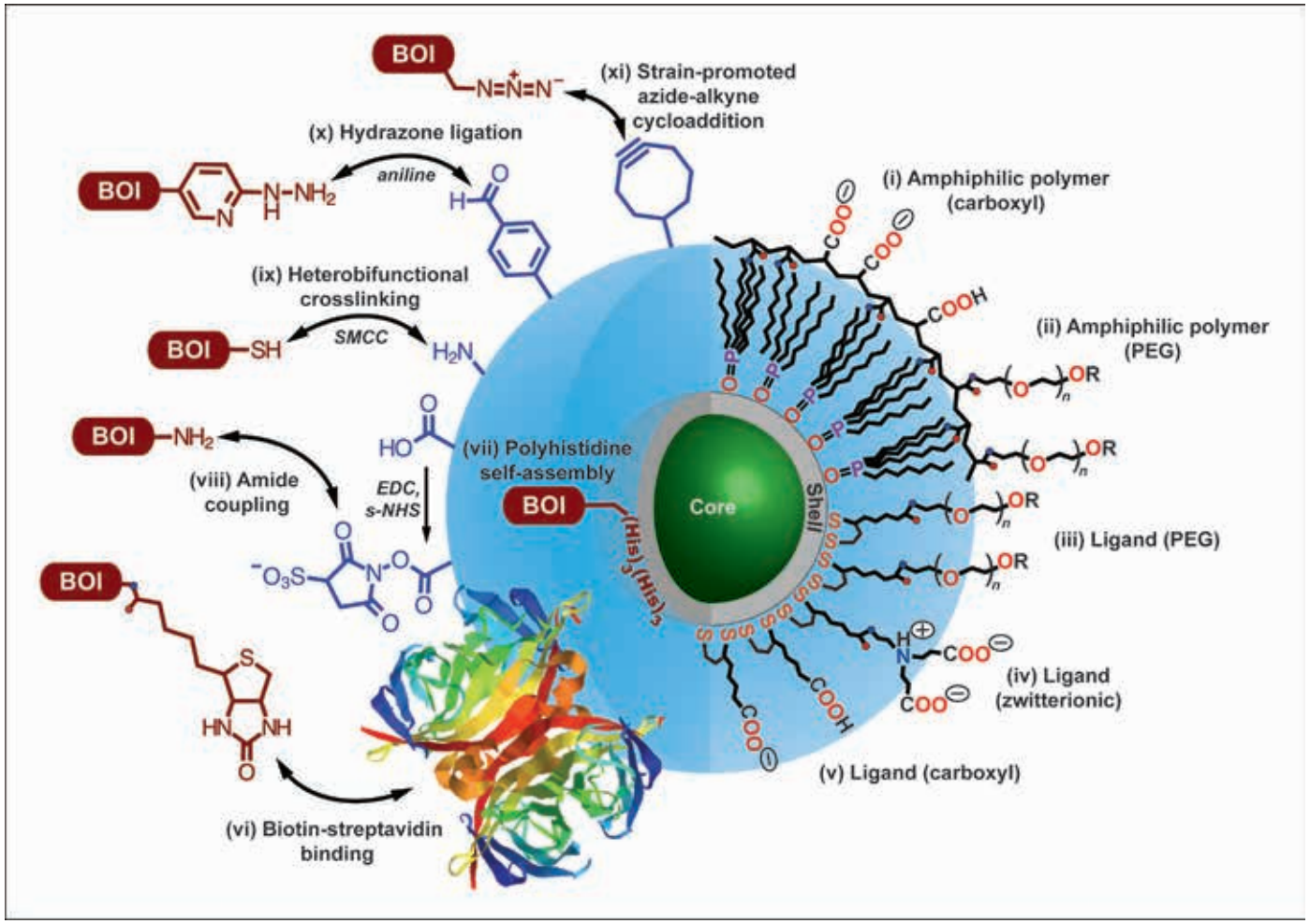

FIG. 3. ***Illustrative overview of the chemistry of core-shell QDs. Coatings for aqueous solubility are as follows:*** **(i)** ***amphiphilic polymer coating with carboxyl(ate) groups;*** **(ii)** ***amphiphilic polymer coating with PEG oligomers;*** **(iii)** ***dithiol ligand with a distal PEG oligomer;*** **(iv)** ***dithiol ligand with a distal zwitterionic functionality; and*** **(v)** ***dithiol ligand with a distal carboxyl(ate) group. Common R groups include carboxyl, amine, and methoxy, although many others can be introduced (e.g., see vi, x, xi). Methods for conjugating biomolecules of interest (BOI) are as follows:*** **(vi)** ***biotin-streptavidin binding;*** **(vii)** ***polyhistidine self-assembly to the inorganic shell of the QD;*** **(viii)** ***amide coupling using EDC/s-NHS activation;*** **(ix)** ***heterobifunctional crosslinking using succinimidyl-4-(N-maleimidomethyl)cyclohexane-1-carboxylate (SMCC; structure not shown);*** **(x)** ***aniline-catalyzed hydrazone ligation; and*** **(xi)** ***strain-promoted azide–alkyne cycloaddition. The double arrows are intended to represent conjugation between the functional groups and, in principle, their interchangeability (not reaction mechanisms or reversibility). Not drawn to scale.***

tion with an amphiphilic polymer (i.e., building around the native surfactants), typically yielding brighter QDs. Ideally, the core/shell QD PL properties are insensitive to interfacial chemistry; however, the typical few-atom-thick Type I shells do not fully isolate the nanocrystal core, and the optical properties of QDs are still somewhat affected by adsorbed molecules, pH, temperature, and other properties of the local environment.[79] This sensitivity is a consequence of imperfect confinement of the exciton, nonuniform coverage of the shell material on the core, or both.[48] Other important considerations for the hydrophilic modification of QDs include the net charge, colloidal stability (i.e., resistance to aggregation), long-term coating stability (i.e., stable association between the organic coating and inorganic QD), compatibility with bioconjugate chemistries (i.e., for attaching biomolecules of interest), and resistance to the nonspecific adsorption of proteins and other biomolecules in a sample matrix (i.e., non-fouling). In the following paragraphs, we describe the chemistry of coating QDs for aqueous solubility in more detail, focusing first on the interface exposed to bulk solution and then discussing the interface between the organic coating and the inorganic QD.

One of the most widely used methods for dispersing QDs in aqueous solution is to modify their outer surface with anionic carboxylate groups. At sufficiently basic pH and low ionic strength, electrostatic repulsion between QDs affords a stable colloidal suspension; however, efficient charge screening at high ionic strength, neutralization of the carboxylates at acidic pH, or both yield insoluble aggregates of QDs.[80,81] Car-

boxylate coatings (Figs. 3i and 3v) also tend to be prone to the nonspecific adsorption of proteins due to their charges. Popular alternatives to carboxylate coatings are those featuring poly(ethylene glycol) ([PEG]; Figs. 3ii and 3iii) oligomers or zwitterionic moieties (Fig. 3iv). Both PEGylated and zwitterionic coatings offer colloidal stability over broad ranges of pH and ionic strength, and minimal nonspecific adsorption for improved biocompatibility.[82,83] The advantage of zwitterionic coatings over those based on PEG is more compact size;[84,85] however, PEG oligomers can be modified with a variety of terminal functional groups (e.g., carboxylic acids, amines, hydroxyl, PEG, biotin) with minimal impact on the overall colloidal stability of the QDs.[86]

As noted above, there are two main methods for modifying QDs with functional groups such as carboxylic acids and PEG oligomers. The first of these methods is ligand exchange that involves the replacement of hydrophobic surfactants from QD synthesis with higher affinity hydrophilic ligands via mass action. The most common ligands are bifunctional molecules with thiol groups that coordinate to Zn^{2+} sites on the surface of the QD at one end, and display carboxylate or PEG groups at the other (Figs. 3iii to 3v). Although thiols will also coordinate to the Cd^{2+} at the surface of a bare CdSe core, the ZnS shell is less prone to oxidation and Zn^{2+} has higher binding affinity with basic ligands, improving the coating stability of the final aqueous QDs.[50] Coating stability is also improved by using bidentate ligands with two coordinating thiol groups. For example, an extensive library of bidentate ligands derived from dihydrolipoic acid have been reported, including those appended with functional group-terminated PEG oligomers[81] or compact zwitterionic moieties.[85] The major challenge of ligand exchange with thiols is a reduction in the quantum yield of the QD. Considerable efforts have been made to refine ligand exchange procedures to minimize such effects.[87–89] Commercially available QDs with hydrophobic surfactants are often made water soluble by ligand exchange with commercially available thiol ligands (e.g., 3-mercaptopropionic acid).[3]

Amphiphilic polymers are a second type of coating that can be applied to QDs, and that are designed to have a mixture of hydrophilic groups and hydrophobic alkyl side chains. The alkyl side chains interdigitate with alkyl-bearing surfactants from QD synthesis (e.g., trioctylphosphine oxide), leaving the hydrophilic groups at the surface of the now water-soluble QDs (Figs. 3i and 3ii). Common chemical strategies for preparing amphiphilic polymers include partial grafting of polyacrylic acid or poly(maleic anhydride) backbones with alkyl amines, where the remaining sites on the backbone are left as carboxylic acids or appended with PEG chains.[90–94] These polymer coatings better retain the original brightness of synthesized QDs since they build an additional layer onto the surface of the QD without altering coordination to the inorganic interface (i.e., less opportunity for forming surface traps). Polymer coatings also provide good long-term coating stability, but typically larger hydrodynamic radii than QDs coated with bifunctional ligands.[13] Water-soluble QDs with amphiphilic polymer coatings are available commercially, as are QDs coated with phospholipids that interact with the as-synthesized QDs in an analogous manner. Further details on the diversity of possible coatings for QDs, including those that are less widely used or still emerging (e.g., coordinating polymers[95,96]) can be found in several reviews.[6,18,86,97]

Bioconjugation of Quantum Dots. Bioconjugation strategies for QDs can be broadly classified into (i) covalent coupling and (ii) self-assembly/specific recognition; both strategies have been used to couple enzymes, proteins, peptides, antibodies, and oligonucleotides to QDs.[6,75] It is critical to note that, without suitable bioconjugation, the utility of QDs in bioimaging and bioanalysis will be greatly hindered, regardless of their highly favorable optical properties. Furthermore, irreproducibility in bioconjugation tends to translate into irreproducibility in experimental results. A key conceptual difference between QDs and fluorescent dyes is that QDs are effectively surfaces that can be modified with many biomolecules at many different sites, whereas fluorescent dyes typically have one reactive group that labels one of many sites on a biomolecule. This difference creates unique challenges for QDs and other nanoparticles, and these challenges have been thoroughly reviewed elsewhere.[75] Here, we briefly summarize some of the most general and pragmatic strategies for the bioconjugation of QDs, a few of which are illustrated in Figs. 3vi to 3xi.

Covalent conjugation methods provide a new chemical bond between a biomolecule of interest and the ligand or polymer coating of a QD. The robustness of the linkage is a function of both the bond stability and coating stability. The most common chemistry is to couple amine-bearing biomolecules to carboxylated QDs (or the opposite configuration) by using amide-bond forming, water-soluble activating reagents such as *N*-(3-dimethylaminopropyl)-*N′*-ethylcarbodiimide (EDC) and sulfo-*N*-hydroxysuccinimide (s-NHS) (Fig. 3viii).[10] This method is an effective "shotgun" method that works well in some applications and poorly in others. With many proteins, this chemistry neither provides good control over the number of proteins conjugated per QD nor their orientation (potentially affecting biological activity). Another common outcome is a fraction of crosslinked aggregates that tend to result from coupling between the large number of amine and carboxyl groups present on the surface of a protein. EDC chemistry is often most effective with monoreactive biomolecules, as is the case for many synthetic oligonucleotides and peptides. As an alternative to EDC, some commercial QD suppliers offer bioconjugation kits that target either amine or sulfhydryl groups on biomolecules, and that couple via hydrazone ligation (Fig. 3x) and heterobifunctional crosslinkers with maleimide groups (Fig. 3ix), respectively.[98] These reactions tend to offer somewhat better control over the final bioconjugates. The liabilities of conventional covalent conjugation methods have generated strong interest in developing highly chemoselective ligation reactions that provide excellent control over nanopar-

ticle bioconjugation.[75] The aforementioned hydrazone ligation[99] is one such example, as is copper-free strain-promoted azide-alkyne cycloaddition (Fig. 3xi; often called ''click chemistry'').[100,101] Both of these chemistries have commercially available "chemical handles" that can be used to modify amine-bearing QDs and biomolecules for subsequent ligation.[102]

Alternative bioconjugation strategies based on self-assembly and specific recognition take advantage of high-affinity noncovalent interactions to assemble biomolecules of interest to QDs. The best known example of specific recognition is the tight-binding (femtomolar dissociation constants) between biotin and the avidin family of tetravalent proteins (Fig. 3vi). Almost any biomolecule can be biotinylated using commercially available kits and reagents, assuming that it is not already sold with a biotin modification. Streptavidin-modified QDs are also available commercially, permitting widespread access to a diverse array of QD bioconjugates. This strategy permits a moderate level of control over the number of biomolecules assembled per QD (conjugate valence) and their orientations; however, there are limitations associated with the heterogeneous attachment of the streptavidin to the underlying QD coating.[103] To date, the bioconjugate method that has provided the best overall control is self-assembly between polyhistidine-appended biomolecules and the ZnS shell of ligand-coated QDs (Fig. 3vii; nanomolar dissociation constants), thereby providing excellent control over conjugate valence and orientation.[104] Both expressed proteins and commercially synthesized peptides can be readily obtained with polyhistidine tags. Relatively facile methods have also been developed for chemically ligating these tags to synthetic oligonucleotides.[105] Polyhistidine assembly has also been extended to commercial carboxylate polymer-coated QDs.[104] The primary advantage of polyhistidine self-assembly and biotin-streptavidin is that bioconjugation proceeds almost quantitatively without need for excess reagents and purification. A variety of other self-assembly/recognition methods have been developed, but they do not yet enjoy the same widespread use and accessibility; these methods have been reviewed elsewhere.[75]

Comparison of Luminescent Nanoparticles. The number of nanoparticle materials with bioanalytical utility has greatly increased. In the first half of the decade, review articles typically compared the optical properties of QDs with those of conventional organic fluorophores; however, it is now important to compare the properties of QDs with those of other luminescent nanoparticles, including nanodiamonds (NDs), carbon nanodots (C-dots), graphene oxide (GO), carbon nanotubes (CNTs), lanthanide-based upconversion nanoparticles (UCNPs), and fluorescent dye–doped silica nanoparticles (DSNPs). A summary comparison of the physical and optical properties of these luminescent NPs is given in Fig. 4. Note that each type of nanoparticle has its own benefits and liabilities, and each application will have its own "best" material. We briefly elaborate on some of the comparisons in Fig. 4 and note a recent review article for each material below:

- Organic fluorophores: monoreactive; prone to photobleaching, less facile multiplexing.[14]
- DSNPs: very bright, good resistance to photobleaching; much larger in size, less facile multiplexing.[106]
- NDs: excellent resistance to photobleaching, high quantum yield; emission is not easily tunable, low extinction coefficient.[107]
- GO: resistant to photobleaching, intrinsic aqueous solubility; broad PL emission is not easily tuned.[108]
- C-dots: non-blinking, excellent resistance to photobleaching; emission wavelength depends on excitation wavelength, poorly understood mechanism of PL.[109]
- CNTs: excellent resistance to photobleaching, NIR emission; challenging to obtain pure samples, weak PL intensity.[110]
- UCNPs: upconversion luminescence, more narrow emission lines; currently less developed coating and bioconjugate chemistry, multiple emission lines, larger size.[111]

Noble metal clusters (NCs) are another type of luminescent nanomaterial that has been gaining significant interest and deserves some special attention here. These NCs are sometimes referred to as "fluorescent noble metal QDs" due to their optical properties and discrete size-evolved electronic states. NCs contain between a few and a hundred atoms (e.g., Au, Ag, Pt), are smaller than 2 nm, exhibit no apparent plasmonic properties, and have excitation and emission bands similar to those of molecular dyes.[112] Some very promising work has been done toward the use of NCs for biological imaging and analysis.[112,113] For the purpose of this review, we treat NCs as a material distinct from semiconductor QDs. There are many practical reasons for this distinction, even if both sets of optical properties (e.g., size-dependent fluorescence) are rooted in confinement phenomena. For example, NCs are more akin to molecules than nanoparticles,[114] more sensitive to local environment,[115] synthesized quite differently,[112,113] and their properties cannot yet be rationally selected to the degree of semiconductor QDs.[113] Prospective biological applications of NCs have been reviewed elsewhere,[112,113,116] and they are not yet as developed as those with QDs.

BIOANALYSIS AND BIOIMAGING WITH QUANTUM DOTS

Spectrofluorometry. Most research and clinical laboratories have access to either a spectrofluorometer or fluorescence plate reader. These instruments are stalwarts of assay development and have been widely used with QDs. Here, we highlight in vitro bioanalyses based on simple fluorescence intensity measurements, and, more prominently, Förster-type energy transfer mechanisms, including fluorescence resonance energy transfer (FRET), bioluminescence energy transfer (BRET), and chemiluminescence energy transfer (CRET). Other transduction mechanisms include chemiluminescence (CL), electrochemiluminescence (ECL) and charge transfer (CT) quenching. In the following sections, we denote the peak PL wavelength of QDs by using a subscript number (e.g., QD_{525}); if no material is

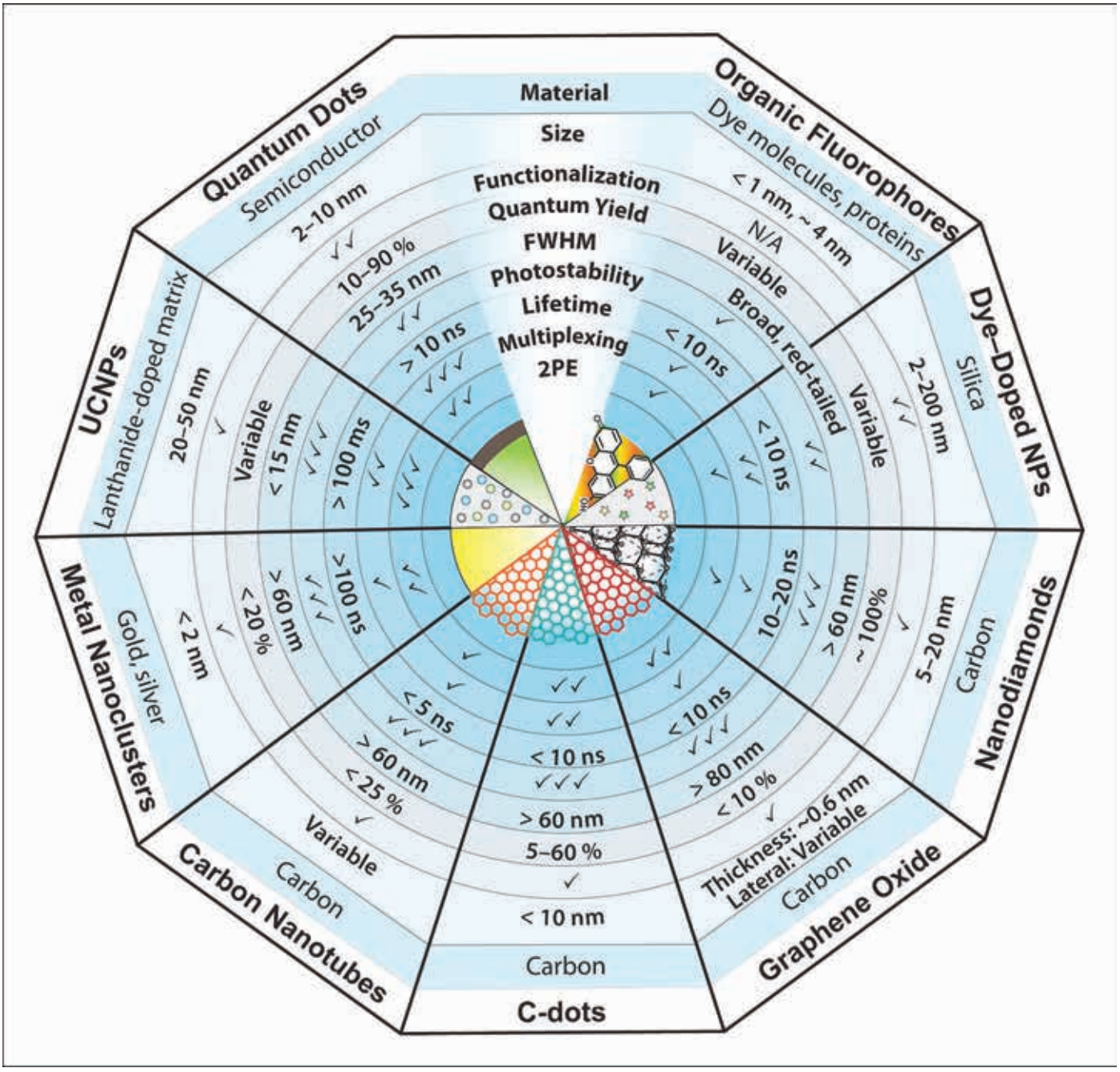

Fig. 4. Comparison of the physical and optical properties of luminescent nanoparticles and organic fluorophores. Check marks (✓) indicate the relative degree of favorability.

mentioned explicitly, the reader should assume the QD material is CdSe/ZnS.

Fluorescence Intensity. Compared with conventional organic dyes, the broad absorption and narrow emission of QDs offer significant advantages in multiplexed assays. Different colors of QD label are generally associated with different analytes of interest in a heterogeneous assay and are interrogated simultaneously. For example, Goldman et al. demonstrated the simultaneous detection of four toxins—cholera, ricin, shiga-like toxin 1, and staphylococcal enterotoxin B—in a sandwich immunoassay with QD labels.[117] The corresponding reporter antibodies were conjugated with QD_{510}, QD_{555}, QD_{590}, and QD_{610}, and offered limits of detection (LODs) in the range of 3–300 ng mL^{-1}. The assay was done in a single microtiter plate well with excitation at 330 nm. Many similar examples of spectral multiplexing based on QD PL intensity can be found in the literature.

Fluorescence Resonance Energy Transfer. A majority of FRET-based

bioanalyses use QDs as donors for organic dye acceptors, and these configurations have several advantages over more traditional dye–dye pairs. Strong QD absorption in the UV-blue region of the spectrum allows selection of an excitation wavelength that minimizes direct excitation of the acceptor dye. Furthermore, the narrow and size-tunable QD PL permits optimization of the spectral overlap integral with only limited crosstalk between donor and acceptor emission. The surface area of the QD also supports modification with multiple acceptor dyes, thus enhancing the rate and efficiency of energy transfer compared with a discrete donor–acceptor pair. A priori, the strong and broad light absorption by QDs also suggests that they would be ideal acceptors; however, efficient and unavoidable direct excitation of the QDs, coupled with their relatively long excited state lifetime, largely negates this advantage when paired with putative fluorescent dye donors (an excited state QD is not a good acceptor). The solution to this challenge has been to pair QDs as FRET acceptors with luminescent lanthanide complexes as donors.[12,118] Lanthanide ions (e.g., Tb^{3+}, Eu^{3+}) typically have excited state lifetimes on the order of 10^{-4}–10^{-3} s (cf. 10^{-9}–10^{-8} s for dyes and 10^{-8}–10^{-7} s for QDs). As such, directly excited QDs return to their ground state and become good acceptors following a microsecond delay after flash/pulsed excitation, whereas lanthanide ions remain in their excited state as good donors.[12,105] Förster distances can reach ~10 nm with lanthanide-QD FRET pairs and >7 nm with QD-dye pairs,[105] compared with <6 nm with conventional dye–dye pairs.

In bioanalytical applications, the great advantage of FRET is the ability to turn QD PL "on" or "off" in response to biorecognition events (e.g., ligand-receptor binding, enzyme activity, DNA hybridization) or other physicochemical stimuli (e.g., pH). Since measured signals are not strictly based on the accumulation of QDs, FRET methods can be applied in the ensemble and down to the level of single particles. Numerous configurations using QDs and FRET have been reported for the detection of metal ions,[102,119] small molecules,[44,120,121] toxins,[122] and drugs;[123] protease[124,125] and nuclease[126,127] activity; hybridization assays;[128,129] immunoassays;[130] and pH.[131,132] In each case, the underlying idea is that a donor/acceptor is added or removed from the vicinity of a FRET-paired QD, either physically (e.g., association or dissociation) or through a change in its resonance (i.e., a large spectral shift). FRET-based sensing has been thoroughly reviewed elsewhere,[4,16] and we have limited ourselves to a few more recent examples here.

Lowe et al. devised a QD-based method for the simultaneous detection of protease and kinase activity.[133] These two important classes of enzymes are frequently causative agents of disease, points for therapeutic intervention, or both. The method used a QD_{655}-Alexa Fluor 660 (A660) FRET-pair in combination with a QD_{525}-gold nanoparticle (Au NP) NSET-pair, as shown in Fig. 5A. Nano-surface energy transfer (NSET) is a dipole–dipole mechanism that is conceptually similar to FRET but occurs over distances approaching 20 nm.[134,135] A peptide substrate for urokinase-type plasminogen activator ([uPA], a serine protease) was labeled with a 1.4 nm Au NP at one terminus and biotinylated at its other terminus for binding with streptavidin-coated QD_{525}. The QD PL intensity was inversely proportional to the amount of proteolytic activity that cleaved the peptide substrate to prevent association between the Au NP and QD_{525} (i.e., loss of NSET). Similarly, a peptide substrate for human epidermal growth factor receptor 2 (HER2) kinase incorporated a terminal polyhistidine tag for self-assembly to ligand-coated QD_{655}, and a tyrosine residue that was phosphorylated by HER2 kinase in the presence of ATP as a cofactor. A660-labeled anti-phosphotyrosine formed an immunocomplex with the phosphorylated tyrosine and provided the proximity for FRET. The LOD was 50 ng mL^{-1} for uPA and 7.5 nM for HER2, values that were below the 200 ng mL^{-1} and 15 nM, respectively, clinical cutoffs for positive/negative breast cancer prognosis.

Although the current state-of-the-art for QD multiplexing is to use *N* colors of QD to detect *N* different analytes, Algar et al. have recently shown that time-gated FRET relays can be designed to detect two different analytes by using a single color of QD vector.[105,136] The time-gated relay comprised an approximately centrosymmetric array of luminescent Tb^{3+} complexes and fluorescent dyes (Alexa Fluor 647 [A647]) around a central QD_{620}. Due to the millisecond excited state lifetime of the Tb^{3+} complexes, two modes of interrogation were possible: prompt (~0 μs delay after flash excitation; 20 μs integration time) and gated (~55 μs delay after flash excitation; 1 ms integration time). On the prompt timescale, energy was transferred directly from the QD to the A647 and provided one detection channel. On the gated timescale, energy was transferred from the Tb^{3+} to the QD and then to the A647, with analysis of the overall gated PL data yielding a second detection channel based on Tb^{3+}-to-QD energy transfer. The time-gated FRET relay was applied in a model two-plex DNA hybridization assay (Fig. 5B),[105] and in two-plex assays for protease activity.[136] The latter assay included tracking the activation of an inactive pro-protease by another protease, where the activity of both the upstream *activating* protease and downstream *activated* protease were quantitatively measured. Although demonstrated with trypsin and chymotrypsinogen, this type of cascade occurs with many other proteases, such as the caspases and matrix metalloproteinases, which are involved in important biological signaling pathways and implicated in many diseases. An additional non-multiplexed application of the time-gated FRET relay involved decoupling Tb^{3+}-to-QD energy transfer from any biorecognition process, so as to shift the QD-to-A647 energy transfer from the nanosecond time domain to the microsecond time domain.[105] Such a configuration is expected to permit rejection of background scattering and autofluorescence (lifetime <20 ns) from complex biological samples, and proof-of-concept was demonstrated for sensing DNA hybridization and protease activity. Clearly, this configuration has important ramifications for zero background in vivo imaging.

Phase-sensitive detection and lock-in amplifiers are a well known tools of the spectroscopy trade and permit resolution

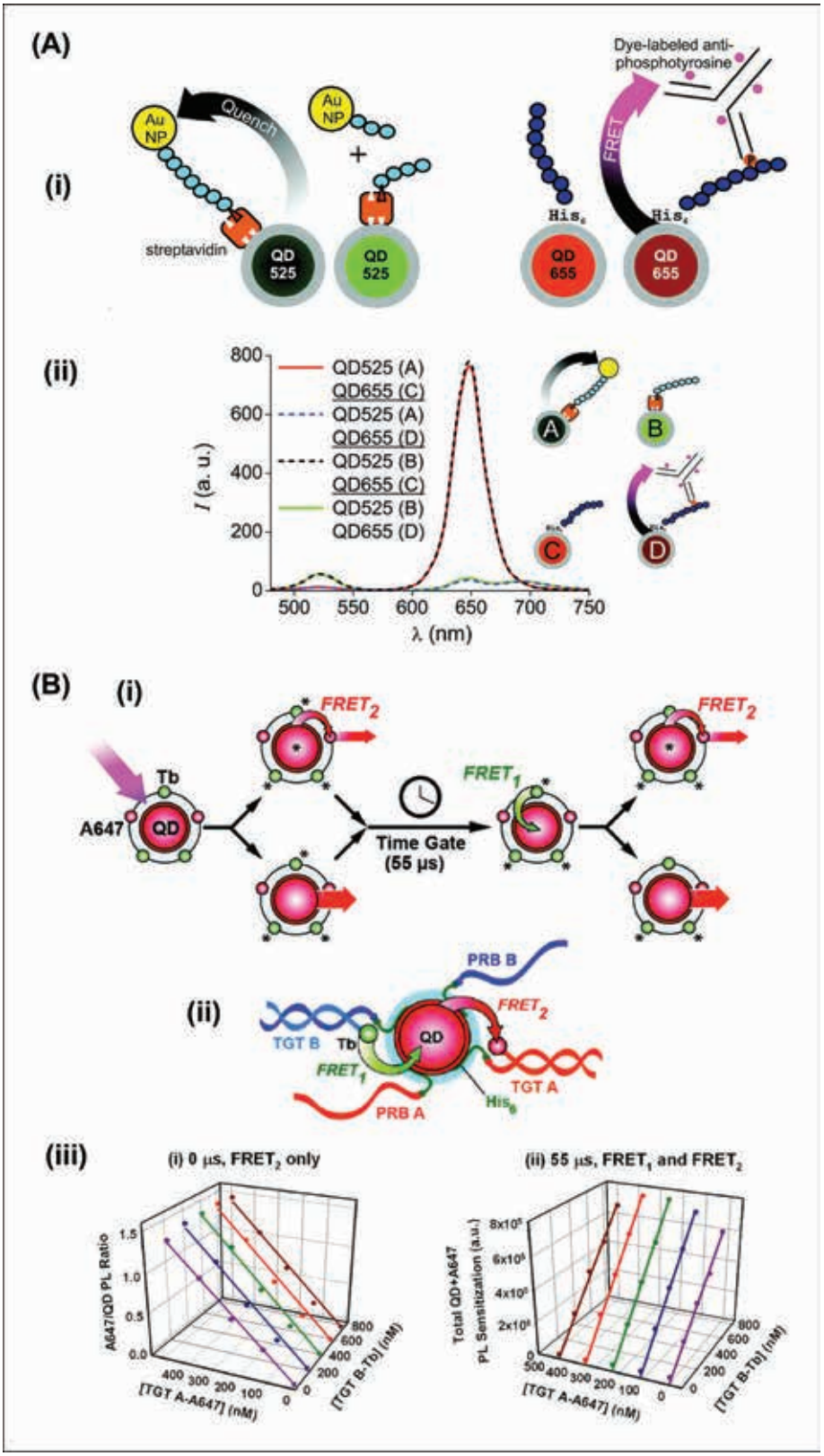

FIG. 5. **(A)** ***FRET/NSET-based two-plex detection of enzyme activity via two orthogonal self-assembly strategies with QDs (biotin-streptavidin and polyhistidine coordination).*** **(i)** ***Enzyme activity of uPA and HER2 kinase was monitored via the degree of retention of QD PL, which was quenched by the Au NP (NSET) or dye-labeled anti-phosphotyrosine antibody (FRET) in the absence of activity.*** **(ii)** ***QD PL in the absence or presence of each type of enzyme activity. [Reproduced with permission from Ref. 133. Copyright American Chemical Society 2012.]*** **(B)** ***Time-gated FRET relay for the two-plex detection of DNA hybridization using one QD vector.*** **(i)** ***Schematic of the time-gated FRET relay concept, showing energy transfer from a luminescent Tb^{3+} complex (Tb) to the QD, and from the QD to a fluorescent dye (A647).*** **(ii)** ***QD-probe oligonucleotide conjugates and hybridization to assemble the FRET relay.*** **(iii)** ***Orthogonal calibration curves for detection of the two DNA targets. [Reproduced with permission from Ref. 105. Copyright American Chemical Society 2012.]***

of weak signals in very noisy environments. These benefits of lock-in detection have been extended to fluorescence imaging.[137] Diaz et al. have suggested that photochromic FRET with QD donors are a means by which to reversibly modulate QD PL and reject background signals (Fig. 6).[138] To this end, QD_{540} were coated with an amphiphilic polymer functionalized with pendant diheteroarylethene photochromic dye molecules. The dyes were situated in the hydrophobic microenvironment around the QDs to facilitate optimal photoconversion upon modulation of excitation light (green vs. UV). Outer functional groups on the polymer were coupled with A647, which had constant fluorescence emission and was used as an internal standard. Under UV irradiation, the photochromic dye switched from an open to closed molecular form that was accompanied by the appearance of an absorption band in resonance with the QD PL. Consequently, the QD PL was quenched by 52% due to FRET. Under irradiation with green light, the closed form photochromic dye reverted to an open form with loss of the resonant absorption band and FRET. QD PL lifetimes decreased or increased commensurately with the FRET efficiency. Cyclic photomodulation of QD PL by alternating UV and visible excitation was reproducible over 15 cycles. Beyond intensity-based lock-in detection, these photoswitchable QDs may have applications in fluorescence lifetime imaging and super-resolution imaging.

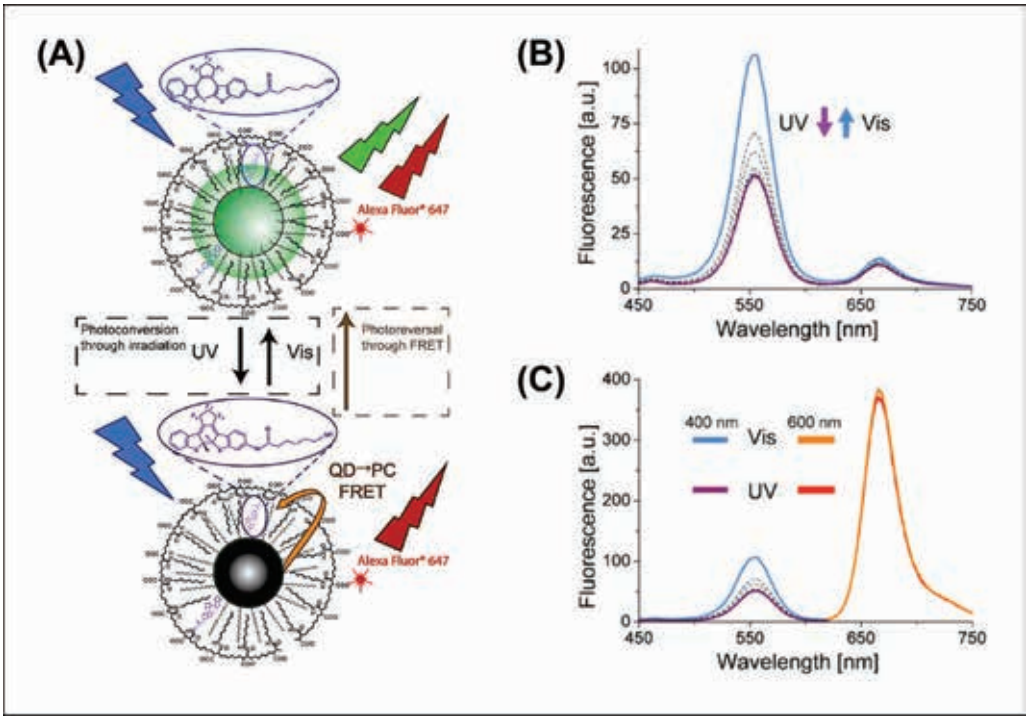

Fig. 6. **(A)** ***A photoswitchable QD that transfers energy via FRET to a photochromic acceptor and that uses A647 as an internal standard.*** **(B)** ***Fluorescence emission upon excitation at 400 nm after photoconversion with either UV or visible light.*** **(C)** ***Dual-color excitation at 400 nm and 600 nm to use A647 emission as an internal standard. [Reproduced with permission from Ref. 138. Copyright American Chemical Society 2012.]***

Bioluminescence Resonance Energy Transfer. Bioluminescence is the emission of light from an excited state product of a biochemical reaction; for example, via the luciferase enzyme–catalyzed oxidation of a luciferin substrate. This transient excited state can serve as a donor for Förster-type energy transfer provided that an acceptor is in sufficient proximity. The two most common BRET donors include *Renilla* luciferase (Rluc), which catalyzes the oxidation of coelenterazine with emission at ~480 nm; and Firefly luciferase, which catalyzes the oxidation of D-luciferin, with emission at ~560–580 nm.[139] Since these emission processes do not require incident light, it is possible to use QDs as efficient BRET acceptors. The broad absorption of QDs provides resonance with the blue-yellow emission of a BRET donor, and the tunable QD PL permits selection of a red or NIR acceptor emission that can be completely resolved from the BRET donor emission. This spectral separation is in contrast to organic fluorophores and fluorescent proteins that, due to their small Stokes shifts, tend to have nontrivial emission overlap with BRET donors.

Rao's group has done extensive work with QD-BRET, including developing Rluc-QD bioconjugates for multicolor, "self-illuminating" imaging in vivo,[140] and for multiplexed sensing of the proteolytic activity of matrix metalloproteinase-7 (MMP-7) and uPA in complex biological samples such as mouse serum and tumor secretions.[141] In the latter, two mutant Rluc enzymes were engineered with C-terminal amino acid sequences that were both a substrate for either uPA or MMP-7 and a linker for conjugation to QDs.[141] Conjugation of the Rluc to the QD provided the proximity necessary for efficient BRET (Fig. 7A). Hydrolysis of the substrate sequences by MMP-7 or uPA disrupted this proximity, resulting in a loss of BRET-sensitized QD emission. The LODs for multiplexed detection using QD_{655}-Rluc (MMP-7 substrate) and QD_{705}-Rluc (uPA substrate) conjugates were 1 and 500 ng mL^{-1}, respectively. QD-BRET is generally expected to provide a multiplexing capacity of two to four QD acceptors when paired with a given bioluminescent donor system.

Chemiluminescence Resonance Energy Transfer. Chemiluminescence is analogous to bioluminescence, excepting that no enzyme is involved in the chemical reaction that produces an excited state emitter. Also analogous to BRET, QDs are good CRET acceptors when in close proximity to a chemiluminogenic reaction (e.g., luminol/hydrogen peroxide [H_2O_2]) and can potentially offer multiplexing capacity of two to four acceptors. Willner's group has exploited catalytic hemin/G-quadruplex DNAzymes for the detection of DNA, metal ions, aptamer–substrate complexes, thrombin, glucose oxidase, and ATP by using QD-CRET.[142–145] The hemin/G-quadruplex DNAzyme exhibits peroxidase-like activity that can catalyze the chemiluminescent reaction between luminol and H_2O_2. For DNA detection, three different colors of QDs (PL at 490, 560, and 620 nm) were functionalized with three different hairpin oligonucleotide probes that were

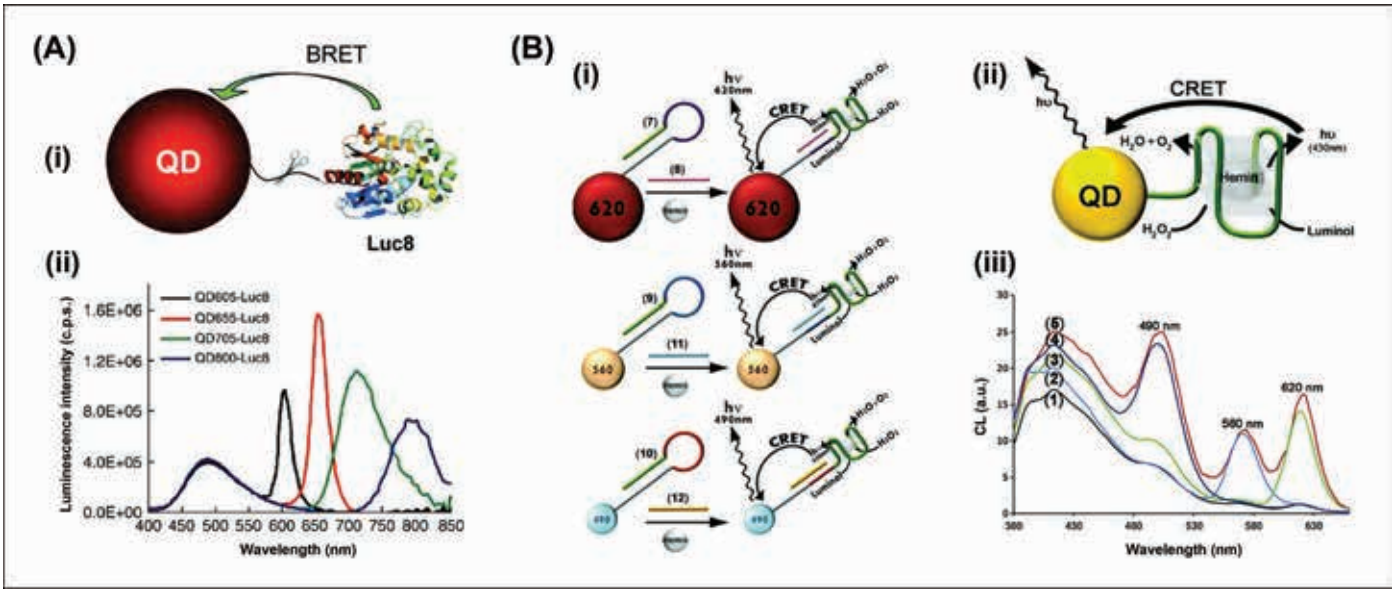

FIG. 7. **(A)** ***Example of QD-BRET:*** **(i)** ***construct with conjugated luciferase protein (Luc8) and*** **(ii)** ***BRET-sensitized PL from QD_{605}, QD_{655}, QD_{705}, and QD_{800} that can be combined for multiplexed bioanalysis and imaging. The scissors in (i) indicate how a peptidyl linker on the luciferase can be used for sensing protease activity. [Reproduced with permission from Ref. 141. Copyright American Chemical Society 2008 (i) and from Ref. 140. Copyright Macmillan Publishers Ltd: Nature Biotechnology 2006.]*** **(B)** ***Example of a QD-CRET construct for multiplexed detection of DNA:*** **(i)** ***QDs emitting at 620, 560, and 490 nm were functionalized with nucleic acid hairpin probe that, after hybridization with target, formed a catalytic hemin–G-quadruplex that*** **(ii)** ***oxidized luminol to generate CRET;*** **(iii)** ***the luminescence spectrum of a mixture of the three colors of QD conjugates after hybridization with varying amounts of their DNA targets. [Reproduced with permission from Ref. 144. Copyright American Chemical Society 2011.]***

complementary to three target oligonucleotide sequences of interest.[144] The stem segment contained a horseradish peroxidase–mimicking DNAzyme sequence, and the loop segment was complementary to the target. Hybridization caused opening of the hairpin structure such that self-assembly of the hemin/G-quadruplex DNAzyme was possible with evolution of chemiluminescence and CRET-sensitized QD emission. The three colors of QD provided three resolvable signals for the three targets of interest. Figure 7B illustrates this transduction strategy. A similar construct was developed for the detection of vascular endothelial growth factor (VEGF), a signaling protein overexpressed in cancer cells.[146] The VEGF induced assembly of the QD-hemin/G-quadruplex structure and CRET evolution. When compared with other transduction methods based on FRET (12 nM) and chemiluminescence (2.6 nM), detection of VEGF via CRET offered an improved LOD (875 pM).[146]

Chemiluminescence. In addition to serving as CRET acceptors, QDs can directly participate in CL reactions as the emitter. QD CL is generally obtained using H_2O_2 systems (e.g., H_2O_2, $NaHCO_3$-H_2O_2, pyrogallol-H_2O_2) that generate superoxide, $\bullet O_2^-$, and hydroxyl radicals, •OH, that inject an electron into the QD $1S_e$ quantum confined state and a hole into the $1S_h$ state, respectively. Subsequent electron–hole recombination generates QD luminescence. The QD CL intensity has been found to depend on the QD size and concentration, the oxidant and its concentration, surfactant, pH, and radical scavengers.[147,148] Despite the numerous advantages of CL-based biosensing (e.g., low background, low LOD, and a wide dynamic range), the use of QD CL remains limited with only a few proof-of-principle studies for the detection of metal ions,[149] phenolic compounds,[150] and immunoglobulin G.[150] Chen et al. demonstrated the detection of L-ascorbic acid, a CL inhibitor, in human serum by using CdSe/CdS QDs with a $NaHCO_3$–H_2O_2 system that forms peroxymonocarbonate, $HOOCO_2^-$, a reactive oxygen species.[151] Despite these proof-of-concept examples, the origin of QD CL (e.g., band gap states or band edge emission) is not entirely clear, and further study is needed to elucidate the mechanism before this transduction method can be used to its full potential.

Electrochemiluminescence. In ECL, a chemiluminescent reaction is initiated at the surface of an electrode. QDs can generate light under an alternating applied potential through an annihilation ECL mechanism where cationic and anionic QDs neutralize one another to yield a luminescent excited state.[152] However, QDs are more frequently combined with a coreactant to generate ECL. Common coreactants include sulfite (SO_3^{2-}) or O_2 for anodic ECL,[153–155] and H_2O_2 or peroxydisulfate ($S_2O_8^{2-}$) for cathodic ECL.[156,157] Under the applied potential, the coreactants are converted into radicals that transfer an electron or hole to the electrochemically generated QDs to yield ECL. In most applications, QDs are cast onto or composited with other materials at the surface of an electrode. The incorporation with other nanomaterials (e.g., carbon nanotubes, nanoflowers, graphene oxide, gold nanoparticles) is often observed to enhance ECL intensi-

ties.[158–161] The origin of ECL from QDs is strongly sensitive to surface chemistry and surface states. For example, in initial reports, ECL from CdSe QDs was observed from band gap states,[162] whereas ECL from CdSe/ZnS QDs corresponded to band-edge emission.[163] However, band-edge ECL has also been observed from CdSe and CdTe QDs lacking shell structures.[164–166] Further study is needed to gain better insight into the charge transfer reactions at the QD interface and the resulting ECL.

Various ECL-based assays have been developed for the detection of metal ions, small molecules, drugs, enzymes, and DNA hybridization and to monitor cell surface carbohydrate expression, as thoroughly reviewed elsewhere.[16,167,168] Transduction has primarily relied on analytes exerting a quenching effect on ECL, for example, via competitive charge transfer or resonance energy transfer (ECL-RET).[169,170] A critical limitation in QD-ECL–based transduction—and one that has persisted for more than a decade since the first observation of QD-ECL[171]—is the absence of spectrally multiplexed assays. If QDs are to ever replace conventional ECL reagents (e.g., luminol), it is essential that they provide a multiplexing advantage. The absence of multiplexed QD-ECL–based assays may reflect the limited understanding of the QD-ECL mechanism compared with, for example, well understood QD-FRET, an assay format increasingly used for multiplexed detection. Nonetheless, QD-ECL assays are making strides forward, particularly in the area of potential point-of-care devices. Shi and coworkers[172] recently reported QD-modified carbon tape electrodes on a low cost, paper-based platform for the

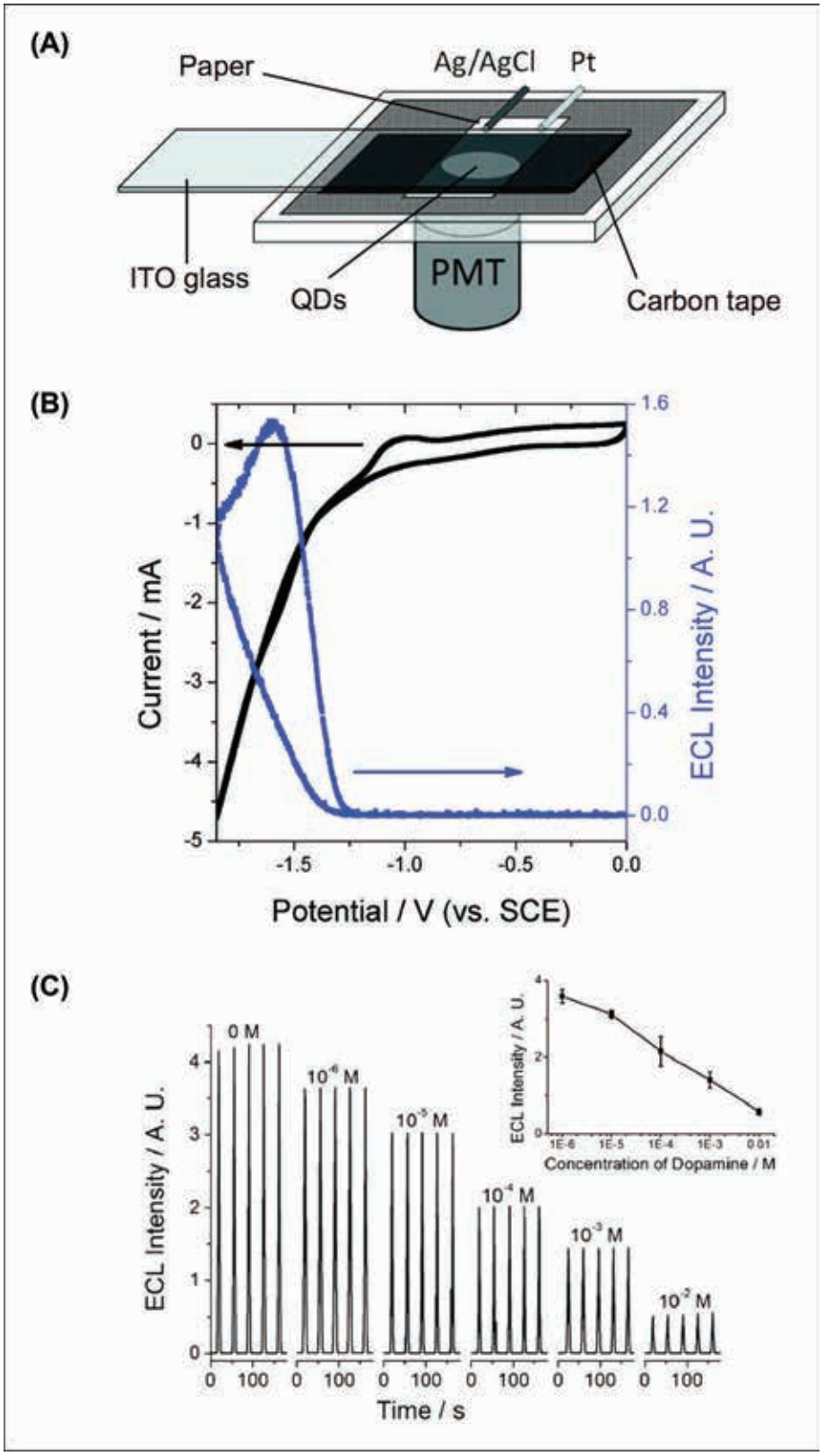

FIG. 8. ECL detection of dopamine using CdS QDs on carbon tape electrodes.* (A) *Instrument schematic.* (B) *ECL-potential curve and corresponding cyclic voltammogram of the CdS QD-modified carbon tape electrode.* (C) *ECL intensity as a function of dopamine concentration. Five cycles of detection are shown for each concentration. The inset shows the corresponding calibration curve. [Reproduced with permission from Ref. 172. Copyright American Chemical Society 2012.]

detection of dopamine (Fig. 8). The simple approach of drop casting CdS QDs on adhesive carbon tape provided reproducible ECL over 31 cycles of alternating cathodic and anodic potential (annihilation mechanism). Dopamine quenched the QD ECL and quantification was possible between 1 μM and 10 mM. Another recent study by Wu et al. described a multiplexed immunoassay for three cancer antigens—caricinoembryonic antigen, α-fetoproten, and prostate specific antigen—using ECL-RET on a microchip device with a 64-electrode array.[173] Although simultaneous detection of the three antigens was demonstrated, multiplexing was achieved on the basis of spatial registration rather than the spectral multiplexing capabilities of QDs. CdS nanorods and antigens were spotted on the electrode array within the microfluidic platform and generated cathodic ECL in the presence of $S_2O_8^{2-}$ coreactant. The electrochemically generated CdS excited state was able to transfer its energy to a tris(bipyridine)ruthenium(II) complex [$Ru(bpy)_3^{2+}$] acceptor that was a label on an antibody bound to the co-immobilized antigen. Any antigen present in a sample was detected via the increase in QD ECL intensity due to competitive binding with the $Ru(bpy)_3^{2+}$-labeled antibodies. The method was successful in identifying target cells from a complex cell mixture, and the amount of antigen detected on the cell surface was in good agreement with expectations.

Charge Transfer and Quantum Dots. Many redox-active dyes, metal complexes, and other molecules have a demonstrated ability to engage in charge transfer with QDs and quench their PL. These molecules have included Ru^{2+}-phenanthroline[174,175] and Ru^{2+}–polypyridine complexes,[176] ferrocene,[177,178] bipyridinium dyes,[179–182] and quinones,[183–185] among others.[186,187] As we discuss below, the modulation of CT quenching, like the modulation of FRET, can be used as an analytical signal in bioanalyses. Unlike FRET, however, the mechanism of PL quenching in these systems is not wholly understood. In general, quenching is thought to be due to photoinduced electron transfer (PET) between an excited state QD and a proximal molecule with an occupied or unoccupied state intermediate in energy to the valence and conduction band edge states of the QD, but many mechanistic details remain unclear. A significant challenge is reconciling analytically applied QD-CT systems that generally comprise aqueous core/shell QDs and redox active moieties as labels on biomolecules, with physical studies of QD-CT dynamics that use hydrophobic core-only QDs with adsorbed redox active moieties in organic solvent. Although the latter are important for applications of QDs in, for example, solar energy conversion,[188] the studies bypass much of the complexity inherent to bioanalytical systems.

In general, spectroscopic measurements (e.g., transient absorption) of nonaqueous, abiotic QD-CT systems support a PET mechanism, but there are many interesting observations that suggest more complex determinants of CT rates and PL quenching efficiencies. For example, electron transfer is typically faster with smaller QDs,[174,182,187] and this result has been attributed to a decrease in the free energy change for the CT reaction (i.e., energy gap between the QD conduction band state and proximal LUMO of the quencher) as the size of the QD increases.[182] However, other studies suggest a role for surface states in the CT mechanism: blinking dynamics and electron transfer rates have been correlated;[189] so-called "gray" states (quenched, but not nonemissive) have been observed with hole transfer to proximal dye molecules[189] and with hole-trapping during blinking;[190] and some of the core only QDs used in CT studies exhibit band gap PL[181] (for example). Stationary absorption spectra of a biotic QD-CT system, CdSe/ZnS QDs assembled with Ru^{2+}-phenanthroline (Ru-phen)–labeled peptides, have suggested hole transfer to surface states with one type of water-soluble ligand coating (negatively charged) and transfer to both surface and core states with another type of coating (neutral).[174] Here, PL quenching was attributed to charging-induced nonradiative relaxation pathways (e.g., Auger recombination or hole-trapping)[191] that became more efficient with decreasing nanocrystal size due to greater spatial overlap between the transferred charge and the exciton. Studies of abiotic QD-CT systems have begun to address the effect of ligands (e.g., length)[192] and the binding mode[193] of adsorbed redox active dyes to the QD surface; however, it is unclear how much insight abiotic studies will provide given the significantly different conditions of the experiments. Indeed, one study with hydrophobic CdSe/ZnS QDs found an electrochemical band gap (via cyclic voltammetry) that corresponded to the measured optical band gap, and observed efficient CT quenching of the QD PL by ferrocene;[194] another study with aqueous CdSe/ZnS QDs found only electrochemically active oxidation levels within the band gap and observed no apparent quenching by ferrocene.[174] There is clearly a need for more fundamental studies of the CT dynamics associated with QD bioconjugates.

The limited understanding of QD-CT systems notwithstanding, there is strong potential for the use of redox active molecules as dark quenchers for QDs. Compared with FRET, CT quenching is beneficial in that is does not have the requirement of spectral overlap and may offer greater ability to probe redox active biological processes. Another expected advantage of charge transfer is an exponential dependence of the quenching efficiency on the distance between the QD and redox-active moiety.[175] This sensitivity has been borne out in several unimolecular sensing constructs developed by Benson's group for the detection of maltose,[195,196] palmitate,[197] lead,[198] and thrombin.[175] These constructs have been reviewed elsewhere[16] and were based on conformational changes associated with receptor proteins or oligonucleotides/aptamers upon binding with their cognate target. The proteins and oligonucleotides were labeled with Ru-phen and conjugated to CdSe/ZnS QDs such that their conformational changes altered the separation between the QD and Ru-phen, resulting in changes in QD PL intensity. Unimolecular sensing configurations of this type cannot be so readily designed with FRET-based transduction, which is less sensitive to small changes in donor-acceptor separation (inverse sixth power-dependence). CT quenching can also be used in more conventional

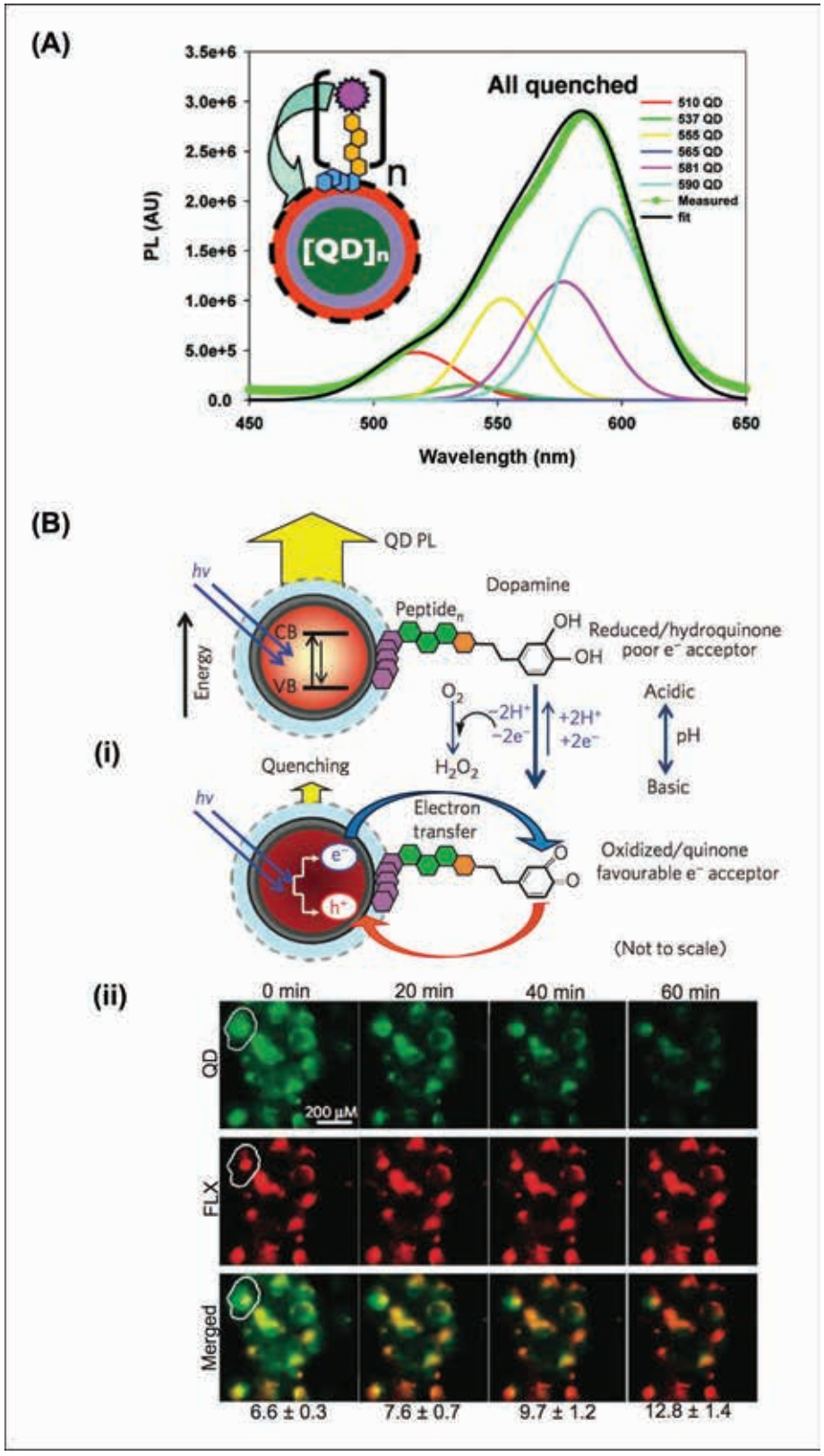

FIG. 9. **(A)** ***Resolution of six QD PL signals in a mixture where each QD was quenched to a different degree by Ru-phen. The measured composite spectrum is shown in green, and the best fit to the data is shown in black. Up to eight QD PL signals can be resolved. The inset is a cartoon representation of a Ru-phen–labeled peptide undergoing CT with a QD. [Reproduced with permission from Ref. 11. Copyright American Chemical Society 2009.]*** **(B)** ***A QD-CT pH sensor:*** **(i)** ***mechanism of CT quenching via electron transfer between the QD an a dopamine modified peptide;*** **(ii)** ***intracellular pH sensing over time via the microinjection of QD_{550}-dopamine conjugates (progressive quenching) and red fluorescent nanospheres (FLX; invariant) into COS-1 cells. [Adapted with permission from Ref. 183. Copyright Macmillan Publishers Ltd: Nature Materials 2010.]***

on-off formats common with FRET-based detection; for example, Medintz et al. self-assembled Ru-phen–labeled peptide substrates to CdSe/ZnS QDs as probes for the detection of the proteases chymotrypsin and thrombin.[174] Initially quenched due to the proximal Ru-phen, QD PL was recovered with proteolytic activity that cleaved the Ru-phen from the QD. Enzyme kinetic parameters were obtained by fitting the assay data with the Michaelis–Menten equation. Medintz et al. further demonstrated proof-of-concept for highly multiplexed CT quenching with eight colors of QDs (PL maxima at 510, 537, 555, 565, 581, 590, 610, and 635 nm), including a Gaussian deconvolution algorithm for resolution of each PL signal and their modulation by Ru-phen (Fig. 9A).[11]

In addition to sensing configurations that use hole accepting metal complexes to quench QD PL, there are examples that use electron accepting molecules, such as quinones, to monitor enzyme activity[199,200] and intracellular pH,[183] or bipyridinium, to monitor receptor–substrate interactions.[180] Initially, Yildiz et al. electrostatically adsorbed a bipyridinium dye to the surface of QDs and found that a macrocyclic receptor, cucurbit[7]uril, could disrupt the CT quenching interaction through competitive host–guest interactions.[180] Cui et al. reversed this approach by modifying CdTe QDs with thiolated cucurbit[6]uril (CB[6]) via self-assembly.[201] The CB[6] improved the colloidal stability of the QDs and, more pertinently, bound a nitrobenzene amine electron acceptor through a host–guest interaction, providing the proximity needed for CT

quenching. Both of the above-mentioned approaches are expected to be useful for monitoring molecular recognition processes or the dynamics of protein–ligand interactions.

Quinones are another potent electron acceptor for QDs.[183,199,200,202] Freeman et al. functionalized QD_{620} with peptides containing a phosphotyrosine residue (8 $\pm$ 2 per QD) to monitor the activity of alkaline phosphatase (ALP).[200] Initially, QDs were unquenched and retained their PL upon hydrolysis of the phosophotyrosine residue by ALP. However, in the presence of a reporter enzyme, tyrosinase, the resultant tyrosine residue is oxidized to a dopaquinone residue that quenched QD PL via CT. Quantification of ALP was demonstrated over the range 0.05–0.5 units in the presence of 25 units of tyrosinase. Similarly, direct modification of the QD surface with phosphotyrosine afforded detection of ALP over a range of 0.01–0.13 units. Medintz et al. developed an intracellular pH sensor by taking advantage of the pH-dependent conversion of dopamine from its hydroquinone form (acidic pH) to its quinone form (basic pH).[183] The quinone form efficiently quenches QDs via electron transfer. PEG-coated QD_{550} were functionalized with peptides modified at their N terminus with dopamine, resulting in progressive quenching of QD PL as the number of labeled peptides increased and the pH increased (pH 6–12). For more robust pH measurements, the dopamine-peptide–QD conjugates were mixed with pH-insensitive red fluorescent nanospheres to provide a reference signal. The mixture was microinjected into cells and by measuring the QD PL intensity relative to the red fluorescence nanospheres, it was possible to quantitatively track the gradual (60 min) increase in cytosolic pH after acidic extracellular medium (pH 6.5) was exchanged for basic extracellular medium (pH 11.5) in the presence of a cell-permeabilizing drug (Fig. 9B). Naturally, this QD-CT assembly also functions as an in vitro pH sensor, and can be interrogated on the basis of pH dependent changes in QD PL lifetime (measured relative to a pH insensitive dye such as Cy5).[183]

Fluorescence Polarization (FP). FP provides information about the Brownian motion-driven rotational dynamics of emitting fluorophores. These dynamics are a function of the size of a fluorophore bioconjugate, such that polarization increases as the molecular weight of the labeled biomolecule increases and rotation slows. Increases in polarization can thus signal biomolecular interactions (e.g., ligand-receptor binding) when one of the components is fluorescently labeled. The narrow size-tunable QD PL is also potentially ideal for developing multiplexed FP assays. For example, Tian et al. demonstrated an FP-based competitive immunoassay for the simultaneous detection of two tumor markers in human serum, carcinoembryonic antigen (CEA) and α-fetoprotein (AFP), by using CdTe/CdS QD_{520} and QD_{620} conjugated with these proteins.[203] Binding of the corresponding antibodies increased the effective size of the QD conjugates and increased the emission polarization. Notably, there are only a few examples of QD-based FP assays reported in the literature. This scarcity may be due to the intrinsically low polarization of QD emission: QDs have a so-called "bright plane" (emission orientated in any direction along this plane) and a "dark axis" (the c-axis) rather than a linear transition dipole like organic dyes.[204,205] Another potential challenge is the large geometric size (comparable to most proteins) and high molecular weight of QDs, which reduce the relative effect of individual binding events on rotational dynamics. The work by Tian et al. suggests that this shortcoming can be addressed by taking advantage of the multivalent nature of QD conjugates. Since multiple CEA or AFP proteins were conjugated per QD, multiple antibodies were bound per QD to provide a much larger change in rotational dynamics. Such formats may hold promise for further FP assays based on QDs.

Flow Cytometry and Optical Barcodes. In flow cytometry, single cells (or particles) are optically interrogated in an ordered flow stream, including side-scatter intensity; forward-scatter intensity; and, most pertinently, fluorescence intensity. The parallel detection of multiple fluorescent tags associated with cellular biomarkers (i.e., multiplexing) is critical to the utility of flow cytometry in high-throughput biomedical research and clinical diagnosis. In particular, this capability allows for complex studies that correlate the presence or absence of multiple cellular markers with specific immunophenotypes, responses to certain stimuli, or other investigations where distinct subpopulations of cells need to be resolved. By virtue of their brightness and multiplexing capability, QDs are a natural fit with flow cytometry. Indeed, the addition of QDs to the repertoire of fluorescent labels has increased the multiplexing capacity of flow cytometry to 17, as demonstrated by Roederer's laboratory.[206] Using a combination of nine organic fluorophores and eight colors of QD, antigen-specific T cells from a human immunodeficiency virus (HIV)-positive individual were immunophenotyped. The fluorescent probes consisted of QDs functionalized with either peptide-major histocompatibility complexes or antibodies, and organic fluorophores conjugated to antibodies. QD PL was detected using an octagonal array of photomultiplier tubes and dichroic/bandpass filters with laser excitation at 408 nm (Fig. 10A). The study found that T cells specific for a given pathogen, or even a particular epitope on that pathogen, can have different phenotypes, suggesting that the properties of individual T-cell clones could play a role in cell differentiation.[206] Kovtun et al. conjugated QD_{655} with agonists for dopamine transporter (DAT) to measure DAT activity and regulation in live cells with a flow-cytometric method.[207] Cells cultured in a microtiter plate were exposed to agonist candidates, incubated with a biotinylated reference agonist (competitive assay), washed, and incubated with QD_{655}-streptavidin conjugates. The cells were then collected from each well in the plate and analyzed via flow cytometry. The assay was able to determine half maximal inhibitory concentration values for agonists and indicate downregulation of DAT expression demonstrating direct pharmaceutical relevance.[207]

In addition to traditional flow cytometry applications, high-throughput multiplexed screening assays have been developed around flow cytometry instrumentation by using optically encoded bead technology.[208] Although

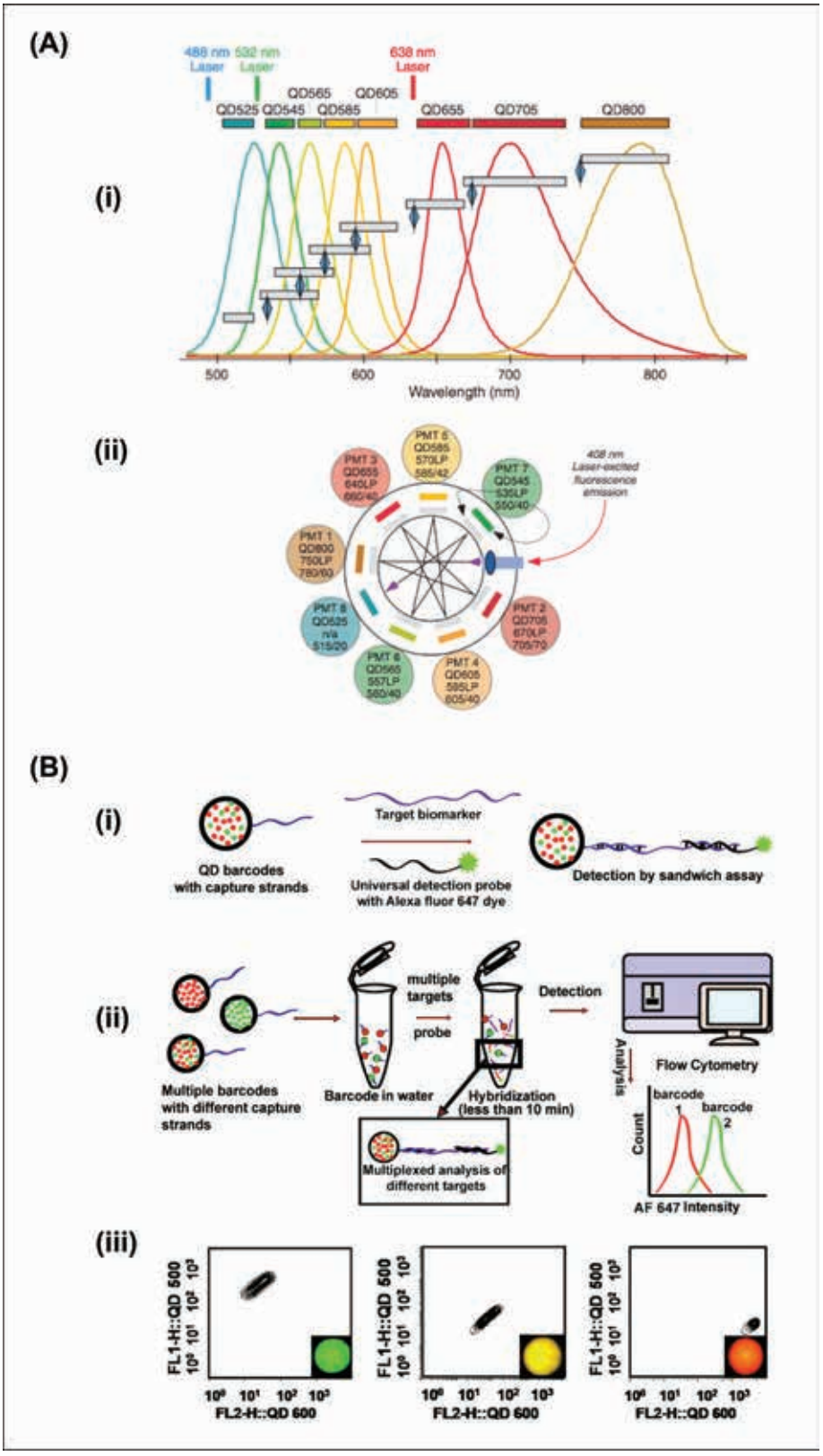

FIG. 10. **(A)** ***Schematic of an octagonal photomultiplier tube (PMT) array for eight-color flow cytometry using QD labels.*** **(i)** ***QD PL spectra and selection of optical components. Blue diamonds indicate the cut-on wavelengths of long-pass dichroic filters; gray bars indicate the transmission range of band pass filters. The colored bars above the spectra indicate the spectral detection range for each QD.*** **(ii)** ***Geometry of the detector array, illustrating the dichroic mirrors (gray) and bandpass filters (colored). [Adapted with permission from Ref. 206. Copyright Macmillan Publishers Ltd: Nature Medicine 2006.]*** **(B)** ***Example of a spectrally encoded barcode-based assay using QDs and a flow cytometer:*** **(i)** ***sandwich assay format with barcoded probe and universal reporter (A647);*** **(ii)** ***assay methodology;*** **(iii)** ***mapping of three different spectral barcodes based on the relative PL of QD_{500} and QD_{600}. The insets show color images of the three different barcodes. [Reproduced with permission from Ref. 214. Copyright American Chemical Society 2011.]***

possible (and commercialized) using fluorescent dyes,[209] QDs are a superior platform for optical encoding and multiplexed analysis by virtue of their spectrally narrow PL and the ability to excite multiple colors of QDs by using a single laser line.[210,211] QD-based barcodes are read using a combination of color and PL intensity; a barcode system with N resolvable levels of PL intensity and m different colors can theoretically provide $(N^m - 1)$ unique codes. For example, QD-barcodes designed with six colors and six intensity levels have a coding capacity $>45\,000$, and these codes can be read with 99.7% accuracy by using data processing algorithms.[212] Chan's group recently characterized a QD-barcode–based DNA hybridization assay, identifying optimal probe oligonucleotide and target sequence lengths for fast hybridization kinetics and good hybridization efficiency.[213] A model three-plex hybridization assay was designed using microbeads encoded with QD_{500} and QD_{600} at different ratios to obtain three unique codes, and the targets were non-purified, non-amplified DNA sequences from a restriction digest of plasmid DNA. The total sample preparation and analysis time was <1 h and the dynamic range was 0.02–100 fmol.[213] Chan's group also reported a similar flow cytometric method for rapid (<10 min), sensitive (femtomole level), and parallel detection of genetic markers for the infectious diseases HIV, hepatitis B, hepatitis C, syphilis, and malaria (Fig. 10B).[214] In another related study,

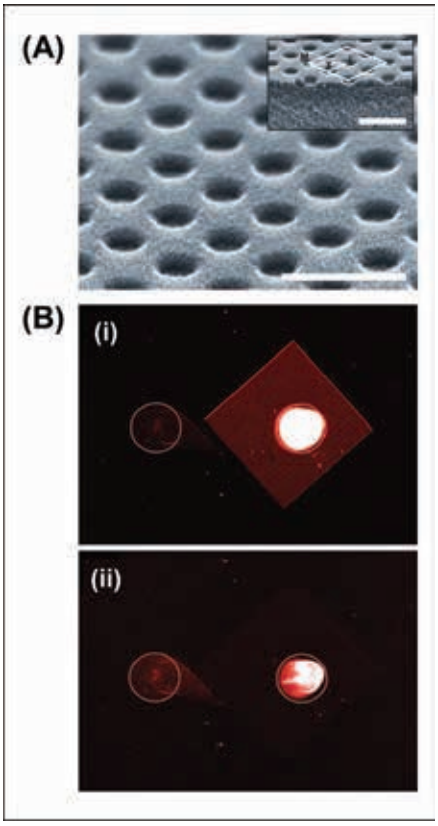

FIG. 11. **(A)** ***Scanning electron microscopy image of PC slab. The scale bars are 500 nm.*** **(B)** ***Enhancement of QD PL intensity:*** **(i)** ***108-fold when the PC is resonant with the excitation light;*** **(ii)** ***13-fold enhancement when the PC is not resonant with the excitation light. The circle on the left of each image shows the QD PL without a PC structure. [Adapted with permission from Ref. 218. Copyright Macmillan Publishers Ltd: Nature Nanotechnology 2007.]***

Xu et al. demonstrated a flow cytometric QD-barcode method for the simultaneous analysis of 10 single-nucleotide polymorphisims.[215] Continued development of QD-barcode assays is expected to result in improved methods for sensitive, high-throughput assays for broad panels of pathogen and disease markers.

Enhanced Fluorescence Techniques. ***Photonic Crystals.*** Photonic crystals (PCs) are structures that have sub-wavelength periodicity between two materials with different dielectric constants, resulting in a "photonic band gap" that does not allow propagation of certain wavelengths of light in some (or all) directions within the PC.[216] Cunningham's group has extensively developed PC slabs as substrates for a variety of assays with enhanced fluorescent detection capabilities.[217] The slabs comprise one- or two-dimensional (2D) grating patterns of titanium dioxide (TiO_2) on a quartz (SiO_2) substrate, and they can be engineered to have two optical resonances. For a given fluorophore, one of these resonances can be tuned to its excitation wavelength, thus permitting amplification of the electric near-field intensity at the surface of the PC (enhanced excitation); the second resonance can be tuned to the emission wavelength and redirect emitted fluorescence along the PC toward the optical detector via Bragg scattering (enhanced extraction). These two enhancement mechanisms are multiplicative and can increase fluorescence signals by 2–3 orders of magnitude.[217] For example, 2D PC slabs with resonances close to 488 nm (excitation) and 616 nm (emission) have been used to enhance the PL of red-emitting CdSe/ZnS QDs by a factor of 108 (Fig. 11).[218] The use of QDs in PC-based biosensing applications is underdeveloped. The potential challenge for spectral multiplexing is engineering multiple PC resonances for enhanced extraction of several colors of QD PL, although the broad QD absorption will permit effective use of the excitation enhancement across multiple colors. However, considering the well-established protocols for QD-based immunoassays,[219] and the ability to fabricate microtiter plates with embedded photonic crystals,[220] the future development of high-sensitivity, high-throughput screening methods with PCs and QDs can be anticipated.

Plasmon-Coupled Fluorescence. The immobilization of QDs on metallic heterostructures or thin films with plasmon resonances can provide significant enhancements in PL intensity.[221] These enhancements are a consequence of more intense local electric fields for excitation, increased radiative rates, and coupling to plasmon modes to yield directional, rather than isotropic, emission.[222,223] The magnitude of the enhancement depends on the size, shape, and type of metal substrate, as well as the distance between the emitter and the metal surface: short distances (e.g., <5 nm) induce fluorescence quenching through new non-radiative pathways, whereas intermediate distances (e.g., 10–20 nm) permit enhancement via the above-mentioned processes. The study and optimization of metal nanostructures to enhance fluorescence and other scattering processes are very active areas of research and have included investigations of QD PL enhancement. In one of the earliest reports, Kulakovich et al. used layer-by-layer assembly (LBL) to controllably place CdSe/ZnS QDs at fixed distances from Au NPs (12–15 nm diameter).[224] When the QDs were located 11 nm from the Au NPs, a PL enhancement factor of 5 was observed.[224] In a separate study, Chen et al. found an $\sim$two-fold PL enhancement when two colors of QD were LBL-assembled onto $\sim$100 nm Ag NPs at the optimum separation distance (Fig. 12A).[225] Subsequently, Song et al. fabricated a periodic silver nano-island ($\sim$100 nm) array that produced a 50-fold PL enhancement when the plasmonic features of the substrate were resonant with QD_{655} PL emission.[226] Pompa et al. observed a similar 30-fold enhancement in $QD_{550,598,625}$ PL when coupled to a periodic nano-pattern of gold triangles,[227] and Leong et al. observed a 15-fold enhancement when QD were sandwiched between a 2D array of gold nanodisks and colloidal Au NPs with controlled spacing.[228] The current understanding of plasmon enhanced fluorescence and the best methods for its implementation are far from complete; however, very sensitive assay methods with QD labels will undoubtedly be built around such plasmonic nanostructures and arrays. For example, a fluorescent dye–based immunoassay on a plasmonic nanostructure array has recently been reported to provide an $\sim 10^6$-fold improvement in the achievable LOD compared with a planar glass substrate.[229] Ultrasensitive multiplexed assays will be possible if similar enhancements can be obtained with QDs.

Traditional planar metal films, well known for surface plasmon resonance (SPR) assays and imaging, can also support plasmon enhanced QD PL. One of the first such examples was reported by Robelek et al., who demonstrated a multiplexed DNA hybridization assay by using SPR-enhanced fluorescence

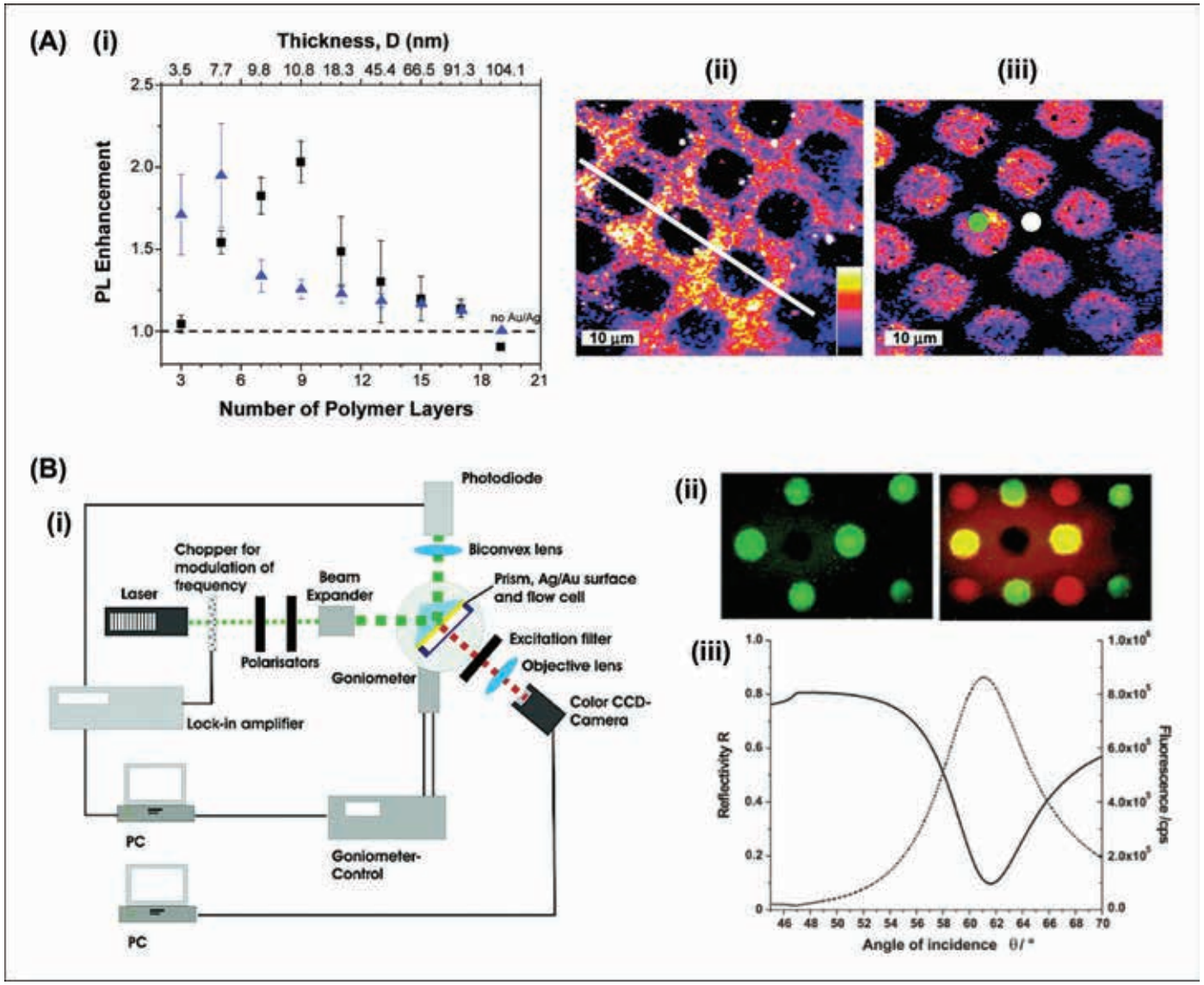

FIG. 12. **(A)** ***Plasmonic enhancement of QD PL.*** **(i)** ***Change in QD PL as a function of distance (controlled by LBL assembly of polymer layers) from a cross-hatched patterned array of Au (black squares) and Ag (blue triangles) NPs.*** **(ii)** ***False-colored QD PL image collected with 488 nm excitation, showing enhancement of QD PL on a cross-hatched pattern of Ag NPs.*** **(iii)** ***Image of the Ag NP pattern via reflection of the 488 nm excitation light, showing strong absorption by the Ag NPs. The white dot is a region with Ag NPs; the green dot is a region without. [Reproduced with permission from Ref. 225. Copyright American Chemical Society 2009.]*** **(B)** ***Surface plasmon–enhanced fluorescence imaging of a DNA array:*** **(i)** ***instrument schematic;*** **(ii)** ***images obtained from sequential hybridization of DNA targets labeled with green (left) and red (right) QDs; (iii) correlation between the SPR reflectivity (solid line) and QD PL intensity (dotted line) as a function of angle of incidence. [Reproduced with permission from Ref. 230. Copyright American Chemical Society 2004.]***

(Fig. 12B).[230] Two target oligonucleotide sequences, complementary to two different capture probes immobilized on the gold film, were labeled with QD_{565} and QD_{655}. Maximum PL intensity from the QDs was observed at the SPR angle (61°, 543 nm laser excitation), where excitation of surface plasmons was most efficient. Jin et al. reported an SPR-based immunoassay for prostate specific membrane antigens.[231] Plasmon-coupled PL provided a 7-fold enhancement in the measured PL compared with far-field excitation of PL, and this enhancement was attributed to directional emission at the SPR angle (47°, 405 nm laser excitation). Malic et al. also demonstrated SPR-based DNA hybridization assays and immunoassays by using NIR-emitting QDs as reporters.[232] However, in this work, the reflectivity was used as the analytical parameter (as in traditional SPR) rather than PL. The QDs provided a 25-fold signal amplification due to a putative combination of its optical mass (large size and high dielectric constant) and coupling of its emission into propagating surface plasmons. The minimum detectable DNA concentration was 100 fM. This type of experiment

must rely on spatial registration (i.e., discrete spots) and SPR imaging for multiplexing and thus does not take full advantage of the optical properties of QDs, but it is interesting from the perspective of multimodal detection (SPR and PL).

Microscopy and Imaging. Since the two seminal breakthroughs in 1998, when Bruchez et al. demonstrated multicolor imaging of fixed cells by using QDs (staining F-actin filaments and the nucleus),[2] and Chan and Nie demonstrated live cell imaging with receptor-mediated endocytosis of transferrin-QD conjugates,[3] QDs have steadily become a more prominent player in the microscopist's toolbox. In this section, we describe the utility of QDs in several microscopy techniques.

Epifluorescence Microscopy. Immunocytochemical (ICC) and immunohistochemical (IHC) labeling have been two of the most widespread applications of QDs in microscopy. Primary or secondary antibody-QD conjugates can be used for direct and indirect staining, respectively, albeit that the latter is often preferred due to the high cost of primary antibodies and the potential loss of activity upon conjugation. Several groups have reported labeling of fixed cells and tissue with QD-antibody conjugates. For example, Wu et al. demonstrated the use of QD probes for ICC labeling of different subcellular targets, including cell surface receptors (HER2), cytoskeletal components (actin and microtubules), and nuclear antigens associated with SK-BR-3 (human breast cancer) or 3T3 cells (mouse fibroblast).[10] QD-secondary antibody conjugates, or a combination of QD-streptavidin conjugates with biotinylated secondary antibody (or phalloidin for actin), were used for labeling. Turning to IHC, Chen et al. detected caveolin-1 and proliferating cell nuclear agent (PCNA) in a lung cancer tissue microarray.[233] Compared with conventional IHC, QD-based labeling improved detection rates from 47% to 57% for caveolin-1 and from 77% to 86% for PCNA. Similarly, QD-IHC has been shown to improve the sensitivity of quantitative detection of the HER2 breast cancer marker in formalin-fixed paraffin-embedded tissue specimens.[234] Ruan et al. found that QDs also provided excellent long-term stability (PL remained after 2–4 weeks) in addition to better sensitivity for IHC labeling of prostate stem cell antigen in specimens from prostate resections or prostatectomies.[235] QDs are also well suited to multiplexed staining of tissue biopsy specimens. Five-color molecular profiling of human prostate cancer cells by using QD-IHC has been described by Xing et al.,[236] who used one color of QD as an internal standard to target a housekeeping gene product that was expressed at a constant level. Four biomarkers—vimentin, N-cadherin, receptor activator of nuclear factor κB ligand, and E-cadherin—were labeled with secondary antibody conjugates of QD_{525}, QD_{565}, QD_{605}, and QD_{655}, respectively. An internal standard, elongation factor-1α, was labeled with QD_{705} (Fig. 13A). Here, epifluorescence was used in combination with spectral imaging (vide infra). In general, more insight can be obtained from the detection of more biomarkers in parallel, suggesting a key role for the multiplexing advantages of QDs in diagnostic pathology.

In addition to labeling fixed cells and tissues, epifluorescence microscopy and QDs have been widely applied for live cell labeling and imaging.[237] A report by Delehanty et al. demonstrated spatiotemporal multicolor labeling of live A594 cells (human alveolar adenocarcinoma) by using mixed delivery techniques over several days (Fig. 13B).[238] Initially, QD_{520} were delivered to cells by using a cationic polymer, and the cells were cultured for 3 days so that the QD_{520} were largely within late endosomes. QD_{635}-cell–penetrating peptide conjugates were then delivered to cells so as to label early endosomes, followed by cytosolic microinjection of QD_{550}-cyanine 3 (Cy3) conjugates and subsequent incubation with Cy5-QD_{635}-Arg-Gly-Asp (RGD) peptide conjugates to label $\alpha_V\beta_3$ integrins on the cell membrane. When combined with four narrow bandpass filters, these QD probes provided four distinct spectral windows for imaging each of the aforementioned cellular components with excitation at 457 nm. The QD_{550}-Cy3 and Cy5-QD_{635}-RDG conjugates were FRET pairs where the QDs were used as antennae to enable observation of Cy3/Cy5 PL with excitation at 457 nm (nonresonant with the dye absorption) and a reduction of dye photobleaching rates (indirect excitation via FRET).[238] QDs with emission wavelengths analogous to those of Cy3/Cy5 can also be used directly, as demonstrated with QD_{580} instead of Cy3. Additional examples of live cell imaging are discussed below in the context of other microscopy techniques.

Confocal Microscopy. Confocal microscopy is a high-resolution imaging technique that is capable of axial sectioning. It particularly benefits from the brightness of QDs due to its reduced light throughput compared with epifluorescence microscopy (the trade-off for higher resolution). Although less important for the spinning disk confocal format, the enhanced photostability of QDs is another significant advantage in the laser scanning format. Matsuno et al. used QDs and confocal laser scanning microscopy to generate three-dimensional (3D) images of the intracellular localization of either growth hormone or prolactin, along with its corresponding mRNA, by using combined immunohistochemical labeling (QD_{655}-antibody conjugates) and in situ hybridization (QD_{605}-oligonucleotide conjugates).[239] The spatial distributions of mRNA and its encoded protein provide insight into cellular protein synthesis. Chan et al. used similar methodology to simultaneously visualize vesicular monoamine transporter 2 mRNA and tyrosine hydroxylase protein within the cytoplasm of dopaminergic neurons.[240] Lee and coworkers used confocal imaging with QDs to observe agonist-induced endocytosis of two types of tagged G protein-coupled receptors (GPCRs): (i) influenza hemagglutinin (HA) peptide-tagged k-OR and (ii) green fluorescent protein (GFP)-tagged A3AR (adenosine receptors).[241] These GPCRs are overexpressed on the membrane of human osteosarcoma cells. The k-OR receptor was labeled with QD-anti-HA (antibody) conjugates, and the QD and GFP PL signals allowed real-time parallel visualization (Fig. 13C) of the internalization of both GPCR types when stimulated with agonists. This format is

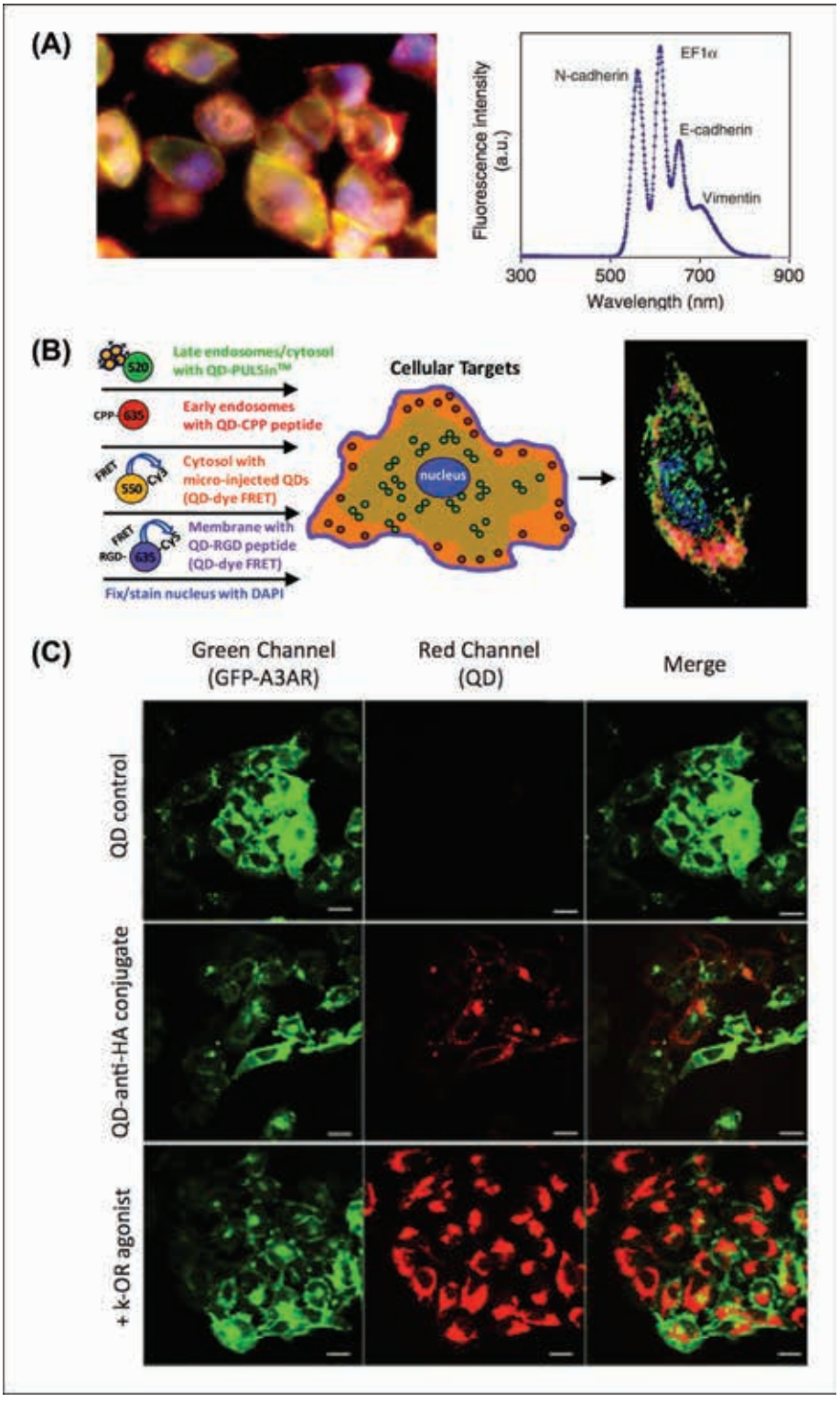

FIG. 13. **(A)** ***Four-plex profiling of tumor biomarkers. Fluorescence image (left) of highly metastatic prostate cancer cells acquired with a color charge-coupled device camera. The cells were labeled with QD_{565}-, QD_{605}-, QD_{655}-, and QD_{705}-antibody conjugates bound to N-cadherin, elongation factor (EF)–1α, E-cadherin, and vimentin, respectively. Single-cell PL data are shown on the right (acquired by spectral imaging). [Adapted with permission from Ref. 236. Copyright Macmillan Publishers Ltd: Nature Protocols 2007.]*** **(B)** ***Multicolor spatiotemporal strategy for labeling various subcellular compartments and structures with QDs and an example of a corresponding epifluorescence image. [Reproduced with permission from Ref. 238. Copyright American Chemical Society 2011.]*** **(C)** ***QD-based screening of GPCR agonists using QD-anti-HA conjugates with specific binding to HA-k-OR overexpressing cells (U2OS). Agonist-induced translocation of k-OR is clearly tracked by migration of membrane-bound QD conjugates to the cytoplasmic region. The cells also express a GFP-labeled adenosine receptor (A3AR). [Adapted with permission from Ref. 241. Copyright John Wiley and Sons 2012.]***

potentially useful for high-throughput screening of agonists for drug discovery (GPCRs are involved in several major diseases).[241]

Spectral Imaging. Spectral imaging includes both the hyperspectral and multispectral varieties, and offers superior informing power compared with conventional optical filter–based imaging. Image cubes (x, y, λ) are collected and comprise a stack of planar images acquired across a series of wavelengths, λ, or bands thereof (e.g., a PL spectrum at each image pixel). Even with emission overlap between different fluorophores, the use of spectral unmixing (i.e., deconvolution) and a library of reference spectra permits quantitative resolution of the unique fluorescence contribution from each emitter and discrimination of background autofluorescence. This technical capability is ideal for pairing with the multiplexing advantages of QDs to facilitate detection and visualization of multiple biomarkers in complex biological specimens. Recent studies have highlighted the utility of QD-based spectral imaging for studying human cancers. Li's group used multispectral imaging and IHC labeling with QD_{605}-streptavidin conjugates (via biotinylated secondary antibodies) to identify three molecular markers in breast cancer tissue: HER2, estrogen receptor, and progesterone receptor.[242,243] Five different molecular subtypes of breast cancer cell heterogeneity were identified and corresponded to different 5-year patient prognoses.[243] Spectral imaging was largely used to separate out tissue autofluorescence, and this separation was further aided by the brightness of QDs. In contrast, Nie's

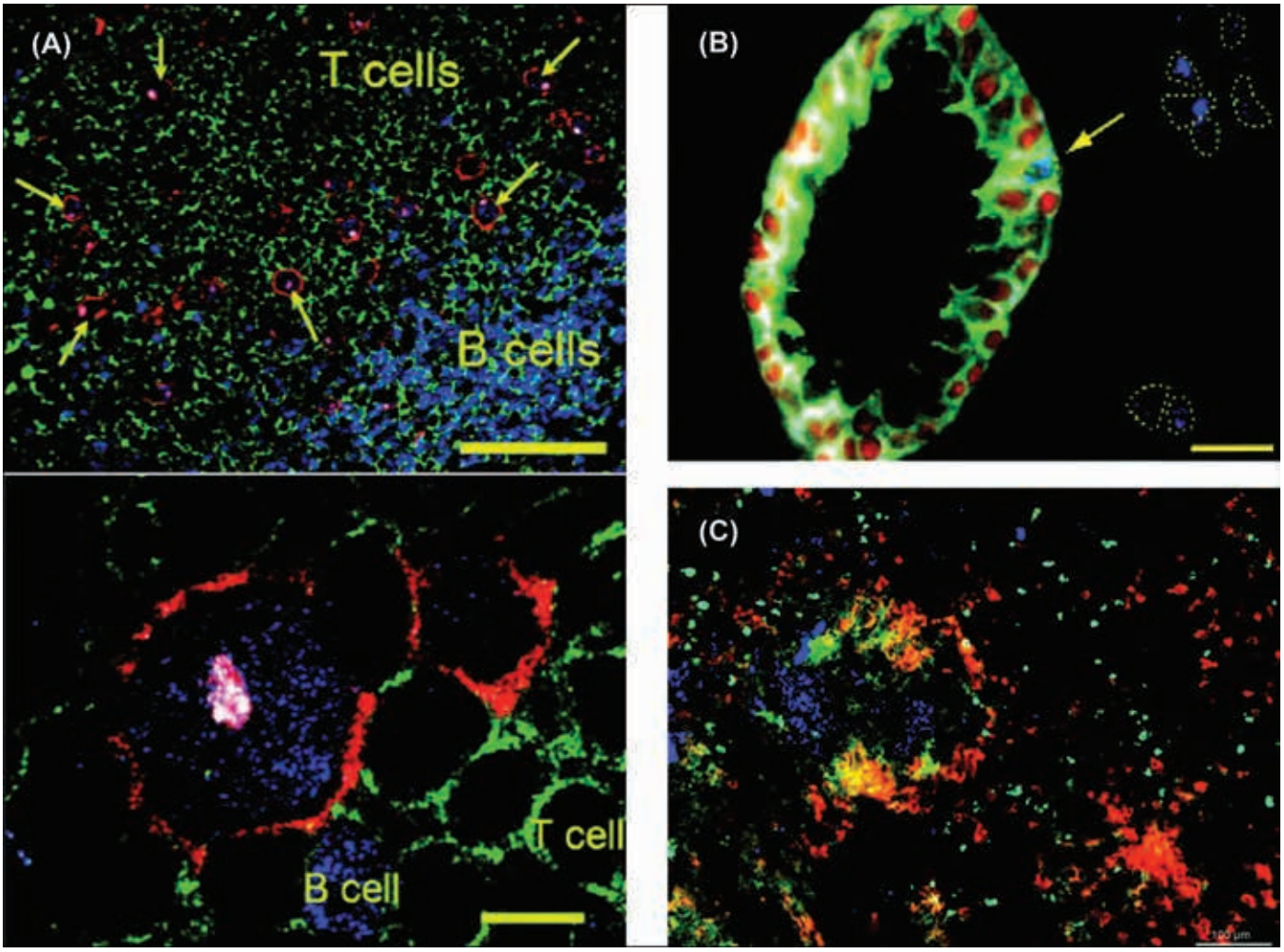

FIG. 14. **(A)** ***Multispectral imaging of QDs for detection of rare Hodgkin's and Reed–Sternberg (HRS) tumor cells in Hodgkin's lymphoma. The images show HRS malignant cells and infiltrating immune cells on lymph node tissue specimens. The HRS cells (arrows) exhibited characteristic staining pattern: membrane staining (CD30 positive, red), Golgi staining (CD15 positive, white), and nuclear staining (Pax5 positive, blue). Staining patterns were clearly distinct from infiltrating B cells (blue nuclear staining) and T cells (green membrane staining). The scale bar in the top image is 100 μm; the scale bar in the bottom image is 10 μm. [Reproduced with permission from Ref. 244. Copyright American Chemical Society 2010.]*** **(B)** ***Composite spectral image of a single malignant cell (arrow) in the basal layer of a largely benign prostate gland, surrounded by malignant cells (blue staining surrounded by dotted lines). The scale bar is 20 μm. Four different protein biomarkers, labeled with different colors of QD-antibody conjugates, are highlighted in green (E-cadherin), white (CK HMW), blue (AMACR), and red (p63). [Reproduced with permission from Ref. 245. Copyright American Chemical Society 2010.]*** **(C)** ***Five-color immunohistochemical labeling of a fixed mouse spleen tissue section with QD-antibody conjugates, imaged via multispectral imaging. A merged fluorescence-false color image is shown, highlighting the following cellular biomarkers: CD45/blue, CD31/yellow, CD11b/aqua, CD4/green, and CD11c/red. [Reproduced with permission from Ref. 98. Copyright American Chemical Society 2011.]***

group has used multispectral imaging with multiple colors of QD to reliably detect and characterize tumor cells in complex tissue microenvironments.[244,245] In one study, four protein biomarkers—CD15, CD30, CD45, and Pax5—were simultaneously mapped in lymph node biopsy specimens by using four colors of QD-secondary antibody conjugates (QD_{525}, QD_{565}, QD_{605}, and QD_{655}) as shown in Fig. 14A.[244] This method permitted reliable identification of low-abundance (~1%) Hodgkins's and Reed–Sternberg cells; identifying such cells is essential for differentiating Hodgkin's lymphoma from non-Hodgkin's lymphoma and benign lymphoid hyperplasia.[244] In another study, four protein markers associated with prostate cancer—E-cadhedrin, high-molecular-weight cytoketarin (CK HMW), p63, and α-methylacyl CoA racemase (AMACR)—were quantitatively mapped in biopsy specimens (Fig. 14B).[245] As in the previous study, the biomarkers were detected using four different colors of QD-secondary antibody conjugate (QD_{565}, QD_{605}, QD_{655}, QD_{705}), revealing molecular and morphological details that are unseen with traditional staining methods. One of the most important observations was that progressive changes in benign prostate

glands start with a single malignant cell and ultimately lead to a malignant gland.[245] Overall, spectral imaging with QDs is an ideal methodology for tackling the challenge of tumor heterogeneity that exists at the molecular, cellular, and tissue-architecture levels, as well as between individuals. A greater understanding of tumor growth mechanisms and more rigorous classification schemes are expected to lead to more effective stage-specific and personalized treatments of cancer. Jennings et al. demonstrated spectral imaging of fixed mouse spleen tissue sections IHC labeled with five colors of QD-antibody conjugate (QD_{525}, QD_{565}, QD_{605}, QD_{625}, QD_{650}).[98] B cells, T cells, leukocytes, thymocytes, and macrophages were labeled with the QDs via antibodies targeting CD45 (type C protein tyrosine phosphatase receptor), CD11c (integrin αX), CD31 (platelet endothelial cell adhesion molecule), CD4 (a glycoprotein), and CD11b (integrin αM) antigens, respectively (Fig. 14C).[98]

Another prospective application of spectral imaging with QDs is intracellular thermometry. QDs exhibit a bathochromic shift with increasing temperature due to alteration of electron lattice interactions.[246] Yang et al. used this effect to measure intracellular heat generation in NIH/3T3 murine fibroblast cells after Ca^{2+} stress and cold shock.[247] QD PL collected from the specimen through an inverted microscope was directed to a spectrograph to measure temperature-dependent spectral shifts, revealing an inhomogeneous intracellular temperature response. The importance of intracellular temperature measurements is described further in the section on fluorescence lifetime imaging microscopy (FLIM).

Two-Photon Fluorescence Microscopy. Another technique widely used for biological imaging is two-photon fluorescence microscopy (2PE). It offers high resolution, comparable to that of confocal microscopy, by limiting excitation of fluorescence to a small focal volume where there is sufficient flux of NIR photons for 2PE. The added advantage of 2PE is that NIR excitation penetrates more deeply into tissues and generates less autofluorescence than the visible excitation used in conventional (one-photon excitation [1PE]) confocal microscopy. Multiple fluorescent dyes can also be simultaneously interrogated due to frequent overlap in their 2PE spectra, even when their 1PE spectra have minimal overlap.[248] 2PE fluorescence microscopy, however, is still prone to photobleaching of dyes,[248] and such dyes already have limited brightness in 2PE due to their small two-photon absorption cross sections (typically <300 GM).[249] It is here that QDs are distinctly advantageous due to their resistance to photobleaching and remarkably large two-photon absorption cross sections (10^3–10^4 GM).[14,20]

One application of QDs in 2PE microscopy is high resolution cellular imaging with minimal autofluorescence background and photodamage. For example, Wang et al. imaged CdTe QDs in highly autofluorescent BY-2-T (tobacco) cells and found that the signal-to-noise (S/N) ratio, or QD PL-to-autofluorescence ratio, increased from ~3 to 11 when the switch was made from 1PE at 405 nm to 2PE at 800 nm.[250] This study also found that, unlike 1PE at 405 or 488 nm (2 mW), 2PE at 800 nm (20 mW) caused no discernible photodamage to QGY human hepatocellular carcinoma cells. Bharali et al. delivered folate-conjugated InP/ZnS QDs to KB cells (human epithelial) via receptor-mediated uptake and imaged their accumulation in multivesicular bodies with 2PE at 800 nm.[251] Geszke et al. similarly used folate conjugation and 2PE to deliver and image ZnS:Mn/ZnS QDs in T47D and MCF-7 breast cancer cells.[252] Tu et al. demonstrated that paramagnetic Mn-doped Si QDs could function as a non-cytotoxic, multimodal contrast agent for magnetic resonance imaging and 2PE fluorescence imaging of macrophage cells.[253] Selvin's group was able to extend their 2D, 1PE fluorescence-imaging-with-one-nanometer accuracy (FIONA) technique to 3D imaging by using 2PE in combination with QDs (Fig. 15).[254] 2PE FIONA was first validated by tracking the steps of individual QD_{655}-labeled myosin V motors on F-actin with nanometer accuracy (step size, 35.8 ± 6.3 nm for 2PE and 35.4 ± 7.0 nm for 1PE). Impressively, widefield illumination at 785 nm was used for the 2PE tracking and was uniquely enabled by the efficient 2PE of QDs. To achieve 3D imaging, widefield illumination was replaced with multipoint scanning (x-, y-, z-axes) of a 9×9 array of diffraction-limited focal spots by using a holographic beam-splitter. LamB receptors on live *Escherichia coli* cells were labeled with QD_{605} and found to occur as spatial helices or bands on the cell membrane. In a second experiment, basal breast cancer cells with membranous epidermal growth factor receptors (EGFR) were incubated with QD_{605}-epidermal growth factor conjugates to induce internalization. After fixing the cells, 3D-2PE FIONA was able to visualize individual QD-labeled EGFR endosomes with an (x, y, z) accuracy of ~ 2–3 nm. The 2PE-FIONA technique provided a five-fold enhancement in S/N compared with imaging with 1PE total internal reflection microscopy.[254]

Another useful application for QDs in 2PE microscopy is in vivo imaging. Larson et al. demonstrated in vivo 2PE imaging of mouse vasculature (i.e., angiography) in skin and adipose tissue by injection of amphiphilic polymer–coated CdSe/ZnS QD_{550} and 2PE at 880 nm.[20] Conventional fluorescein–dextran (70 kDa) angiography (2PE at 780 nm) revealed less detail than the QD-based angiography, even when using five-fold more excitation power at half the tissue depth. Collagen was imaged in parallel with the QDs via its second harmonic generation. Stroh et al. similarly demonstrated two-color 2PE (at 800 nm) imaging for tracking cells in vivo.[255] QD_{590} were conjugated with the HIV TAT protein to label bone marrow lineage–negative cells. The cells were co-injected with phospholipid-coated QD_{470} into a mouse with an MCaIV tumor, where the QD_{470} PL permitted imaging of blood flow and the QD_{590} PL permitted tracking of the recruitment of bone marrow–derived cells to the tumor. Although the NIR excitation used in 2PE microscopy addresses the penetration of tissue by excitation light, the depth of imaging remains limited (<500 μm)[21] by scattering and absorption of shorter wavelength fluorescence (e.g., visible wavelengths) emitted from within the tissue. Although the brightness of

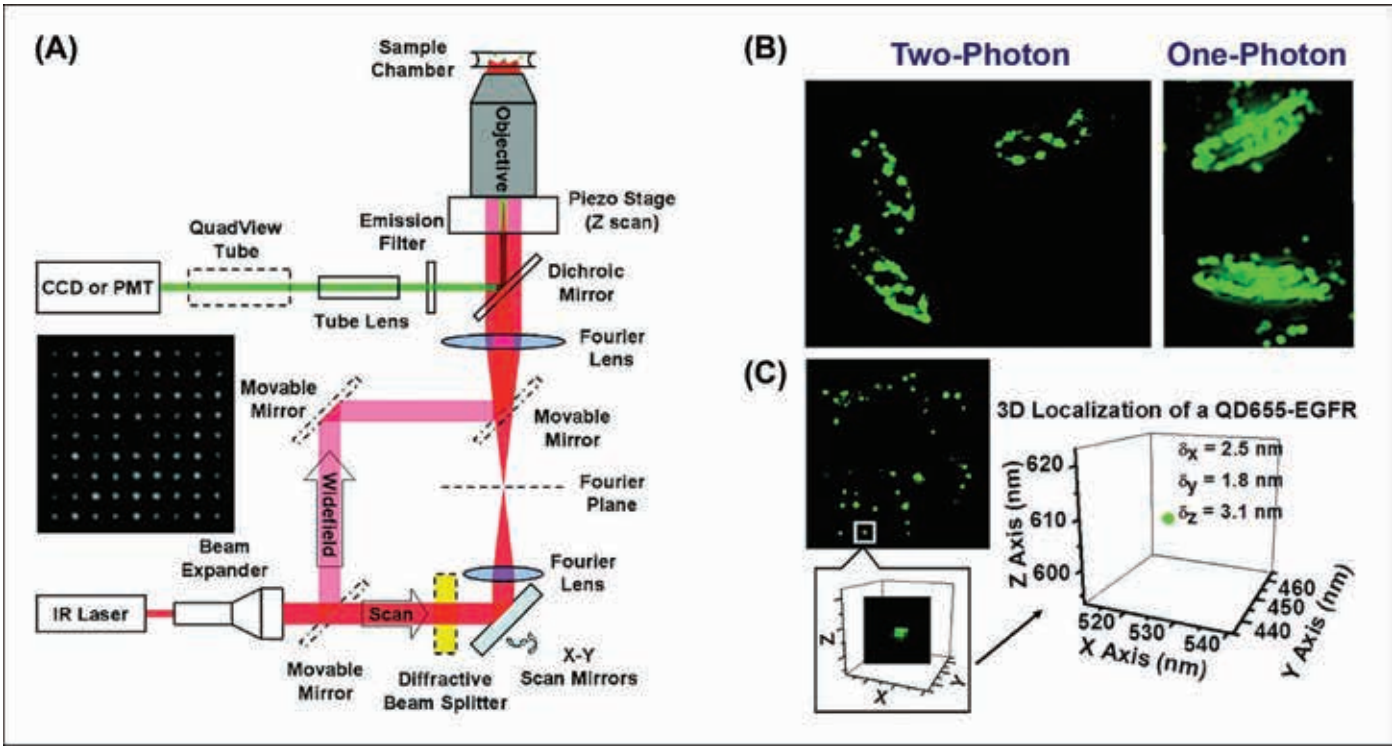

FIG. 15. 2PE-FIONA 3D imaging with QDs. **(A)** ***Instrument schematic. The holographic 9 × 9 excitation matrix used for 3D imaging is shown in the inset.*** **(B)** ***Images of live E. coli cells labeled with QD_{605}, illustrating the superior resolution of 2PE widefield imaging compared with 1PE widefield imaging.*** **(C)** ***3D localization of single QD_{655}-EGFR receptor conjugates on the membrane of a breast cancer cell. [Reproduced with permission from Ref. 254. Copyright American Chemical Society 2011.]***

QDs with NIR 2PE can help to address this challenge, another significant advantage of QDs in this regard is the ability to select certain sizes and materials to emit NIR PL. For example, CdTe QD_{800} can be imaged using 2PE at 900 nm, such that both the excitation and emission wavelengths fall within the tissue optical window between ~650 and 950 nm.[256] Measurements on tissue phantoms suggested imaging could be done at a depth of 1.6 mm, approximately twice the depth of imaging with 1PE of NIR $CdTe_xSe_{1-x}$/CdS ternary QDs (albeit that the latter was measured with real heart and femur tissue[257]).

Single Molecule/Particle Spectroscopy. ***Single Molecule/Particle Imaging.*** Single molecule spectroscopy provides access to physicochemical details that are lost when averaging over the ensemble; for example, revealing heterogeneous subpopulations or asynchronous dynamics.[258,259] Due to their brightness and resistance to photobleaching, QDs are ideal for single molecule or, more accurately, particle measurements. The propensity of QDs to blink is both a benefit and a liability as it confirms tracking of a single QD but also complicates the analysis of PL trajectories.[260] Since size polydispersity does not exist at the level of single QDs, the FWHM of their PL tends to decrease to ~15 nm.[260]

Single QD detection has been used to measure biomolecular interactions (e.g., DNA hybridization, DNA-protein binding, ligand-receptor binding), and to detect small molecules via two-color colocalization, FRET, and, more recently, charge transfer.[261–263] In the latter, CdSe/ZnS QD_{560} were functionalized with ferrocene-maltose binding protein (MBP) conjugates, resulting in CT quenching (Fig. 16A).[263] MBP undergoes a conformational change (scissoring) upon binding maltose, resulting in an increase in the distance between the ferrocene and the QD with a corresponding increase in the QD PL. By monitoring individual QDs, it was possible to detect maltose with a dynamic range spanning a remarkable five orders of magnitude (100 pM–10 μM). Interestingly, unlike single-pair FRET systems that show on-off switching of QD PL, the single QD-CT system exhibited constant emission with an increase in intensity upon binding maltose.[263] This behavior was attributed to a "gray" state associated with CT. Solution-phase single-pair FRET (spFRET) with QDs has also been used as a platform for sensitive assays. For example, Zhang et al. conjugated streptavidin-QD_{605} with biotinylated capture probe oligonucleotides for a sandwich DNA hybridization assay, where the reporter oligonucleotides were labeled with Cy5 acceptors.[264] spFRET was monitored by flowing the sample solution (mixed with QDs, capture and reporter oligonucleotides) through a glass microcapillary with laser excitation at 488 nm in a small observation volume. A fluorescence burst coincidence analysis between the donor and acceptor detection channels was used to observe FRET and measure DNA hybridization. The LOD was 4.8 fM target,

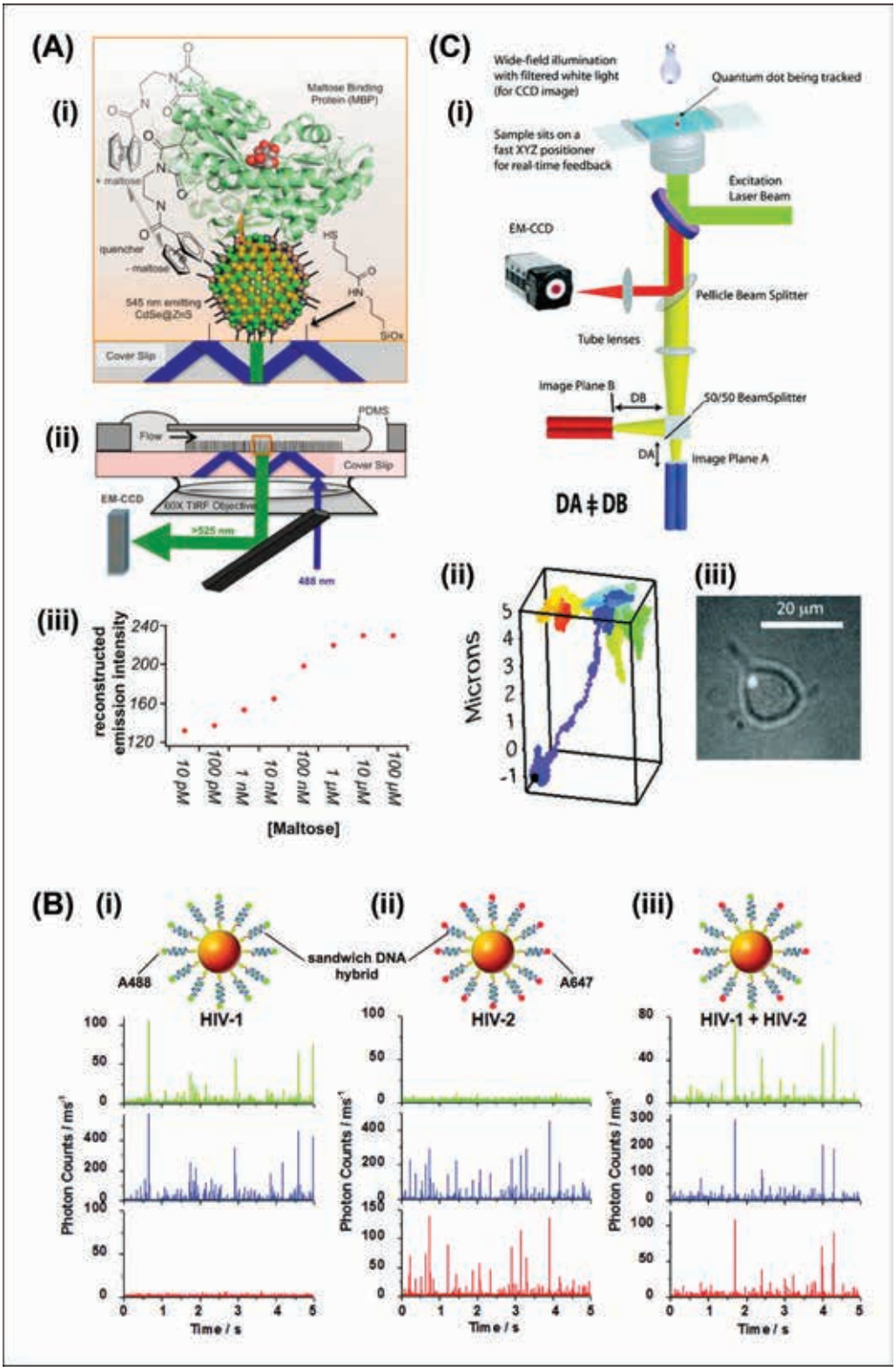

FIG. 16. **(A)** *Single molecule biosensing using QD-MBP-ferrocene conjugates:* **(i)** *schematic of the experiment illustrating the decrease in CT quenching efficiency upon binding maltose;* **(ii)** *schematic of the microfluidic channel used for sample delivery and the optical setup;* **(iii)** *titration curve for maltose detection spanning 100 pM–10 mM. [Reproduced with permission from Ref. 263. Copyright American Chemical Society 2012.]* **(B)** *Illustration of QD-DNA conjugates and representative 3C burst coincidence analysis results for the two-plex detection of DNA hybridization using single molecule fluorescence detection and spFRET:* **(i)** *HIV-1 gene detection, signaled by the coincidence of Alexa*

a value 100-fold better than the LOD associated with molecular beacons (0.48 pM). The assay was applied to the detection of Kras point mutations in clinical samples from patients with ovarian cancer.[264] Subsequently, Zhang and Hu extended this spectroscopic method to the multiplexed detection of the HIV-1 and HIV-2 genes, relying on a three-color (3C) burst coincidence analysis (Fig. 16B).[265] Here, two sandwich DNA hybridization assays were done in parallel using streptavidin-QD_{605}, two biotinylated capture probes targeting HIV-1 and HIV-2, and corresponding reporter oligonucleotides that were labeled with either Alexa Fluor® 488 (A488) or A647, respectively. Directly excited (488 nm laser line) fluorescence bursts from A488, when coincident with QD_{605} PL bursts, were indicative of presence of HIV-1 sequence. FRET-sensitized fluorescence bursts from A647, when coincident with QD PL bursts, were indicative of HIV-2.[265] This study is another example of taking advantage of the surface area offered by QDs to assemble multiple biomolecular probes.

In addition to bioanalytical applications, Pons et al. used spFRET between CdSe/ZnS QDs and dye-labeled polyhistidine-tagged MBP to confirm that biomolecules self-assemble to QDs according to a Poisson distribution.[266] That is, an ensemble with an average of N biomolecules (e.g., proteins, peptides, oligonucleotides) per QD is actually heterogeneous and comprises discrete subpopulations with $\ldots N-2$, $N-1$, N, $N+1$, $N+2 \ldots$ biomolecules per QD, where the abundance of each subpopulation is weighted according to Poisson statistics. With an average of four or more biomolecules per QD, the unconjugated subpopulation decreases to 2% of the ensemble.

Single QD tracking has also been used to study the diffusion dynamics of membrane proteins associated with neuronal cells, including the distribution and surface mobility of neuroreceptors for glycine,[267] γ-aminobutyric acid,[268] α7 neuronal nicotinic acetylcholine,[269] and 2-amino-3-(3-hydroxy-5-methyl-isoxazol-4-yl)propanoic acid,[270] at both synaptic and extrasynaptic sites. In another example, Tsien's group studied the vesicular secretion of neurotransmitters by loading individual synaptic vesicles with single QD_{605}.[271,272] Tracking of these QDs, in combination with a small pH-dependent change (15%) in QD PL intensity between vesicles (pH 5.5) and the extracellular matrix (pH 7.3), was used to distinguish between full collapse fusion (complete vesicle integration with membrane) and kiss-and-run ([K&R], transient vesicular fusion with membrane, retrieval, and release) mechanisms. It was found that K&R was more prominent under high-activity demand conditions. Lowe et al. investigated the selectivity mechanism of the nuclear pore complex in HeLa cells by tracking single QDs decorated with multiple copies of importin-β binding domain of snurportin-1, the import receptor for small molecule nucleoriboproteins.[273] The import or rejection of the QD cargos was monitored, and the authors were able to derive a model for cargo translocation that consisted of cargo capture, filtering, translocation, and release into the nucleus. Wells et al. demonstrated that QDs could be used to track the 3D molecular motions inside live cells and on their surface (Fig. 16C).[274] The imaging system used four diffraction-limited overlapping confocal volume elements, implemented with four optical fibers, and provided a localization accuracy of 50 nm along the x- and y-axes, and 80 nm along the z-axis, with 5 ms temporal resolution. Experimentally, QD-immunoglobulin E (IgE) conjugates were bound to high-affinity IgE receptors (FcεRI) on rat tumor mast cells. The motion of single QD-IgE-FcεRI complexes was tracked, revealing 3D surface topology of the cell membrane and permitting extraction of diffusion rates (0.21 $\mu m^2\ s^{-1}$). When the complexes were crosslinked with the addition of dinitrophenyl-bovine serum albumin antigen, it was possible to observe ligand-mediated endocytosis and measure the rate of vesicular transit (950 nm s^{-1}).[274]

Fluorescence Correlation Spectroscopy. Fluorescence (cross) correlation spectroscopy [F(C)CS] measures time-based intensity fluctuations in one or more fluorescence signals as single emitters diffuse in and out of a very small observation volume. Analogous to the single particle methods discussed under Single Molecule/Particle Imaging, the brightness of QDs and their photostability are significant advantages in F(C)CS, although their blinking behavior can again introduce extraneous fluctuations.[275,276] Nonetheless, FCS has become an important tool for physically characterizing QDs. It has been widely used to determine the hydrodynamic radii of QDs functionalized with different organic coatings or under different conditions, and it has been proposed as a method for accurately measuring QD concentrations and extinction coefficients.[275,277,278] In addition, Cramb's group has published several studies where QD-FCCS has been used to monitor ligand–receptor interactions. A pair of early studies investigated the streptavidin–biotin interaction in association with QDs (i.e., QD-streptavidin and QD-biotin conjugates).[279,280] It was found that the streptavidin–biotin dissociation constant ($K_d = k_{off}/k_{on}$) increased from 10^{-15} M with the native system to 10^{-10} M in association with QDs, where the association rate (k_{on}) decreased by 6 orders of magnitude and the dissociation rate increased by 1 order of magnitude.[280] 2PE-FCCS was also used to interrogate the binding kinetics between the agonist Leu-enkephalin (BLEK) and human μ

Fluor 488 (A488) and QD PL;* (ii) *HIV-2 gene detection signaled by the coincidence of A647 and QD PL; and* (iii) *simultaneous detection of HIV-1 and HIV-2 genes via the coincidence of A488, QD, and A647 PL. [Adapted with permission from Ref. 265. Copyright American Chemical Society 2010.]* (C) *3D tracking of single QDs using an optical fiber–based confocal imaging system:* (i) *instrument schematic;* (ii) *3D trajectory for a QD–IgE-FceRI conjugate over 250 s, where early times are indicated in red and late times are indicated in blue;* (iii) *image of the cell for which the trajectory was generated. [Reproduced with permission from Ref. 274. Copyright American Chemical Society 2010.]

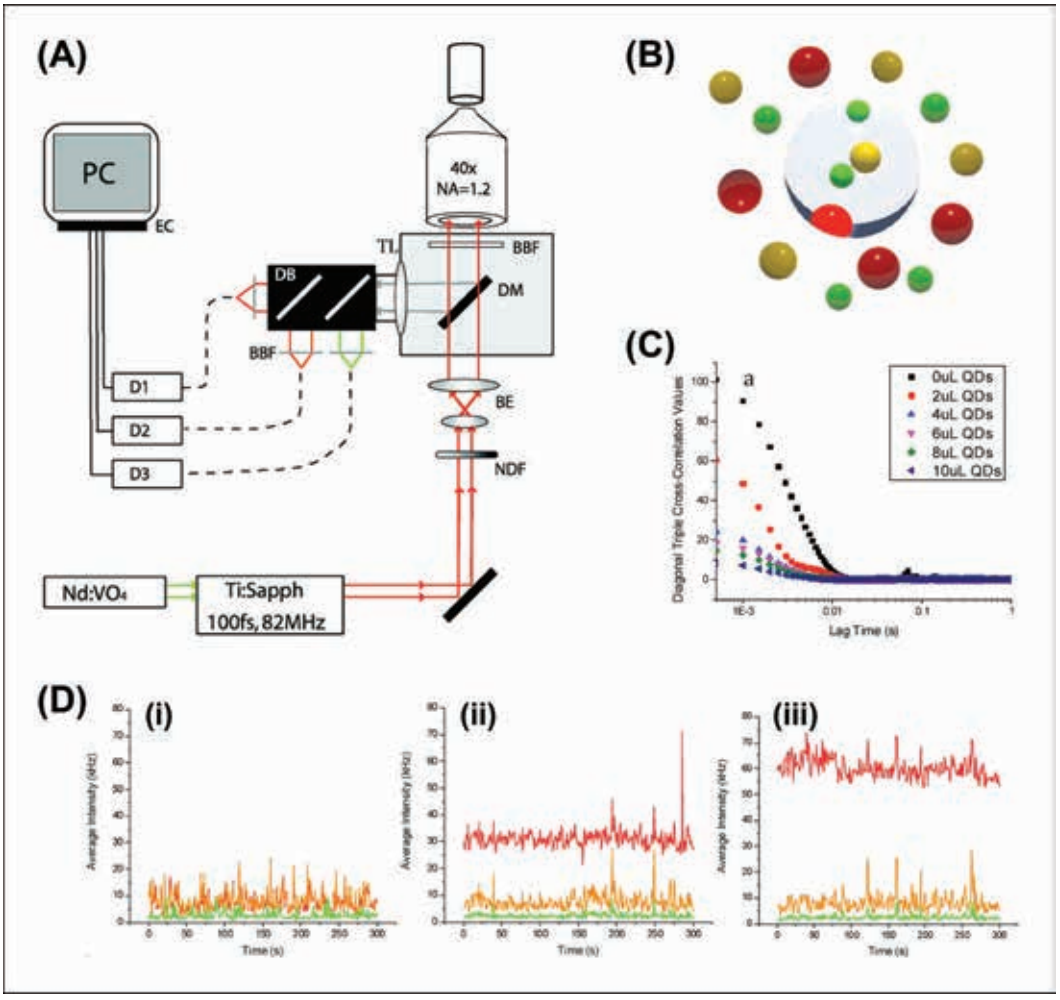

FIG. 17. Three-color FCCS using QDs. **(A)** ***Instrument diagram.*** **(B)** ***Schematic of QD nanobarcode.*** **(C)** ***Diagonal triple cross-correlation function decays for QD_{655} at different concentrations.*** **(D)** ***Count rate trajectories collected for QD_{525} (green), QD_{605} (orange), and increasing amounts of QD_{655} (red):*** **(i)** ***0 μL,*** **(ii)** ***6 μL, and*** **(iii)** ***10 μL. [Reproduced with permission from Ref. 283. Copyright American Chemical Society 2012.]***

opioid receptor (hMOR) in cell membrane nanopatches.[281] QD_{605} were conjugated with BLEK to bind the hMOR receptors, and the FCCS data were converted into fractional receptor occupancy for Hill plot analysis and extraction of K_d. Interestingly, the conjugation of BLEK to comparatively large QDs did not affect its binding properties. Cramb's group has developed 3C-FCCS that is greatly facilitated by the multiplexing advantages of QDs (Fig. 17).[281–283] Polymer spheres barcoded with QD_{525}, QD_{605}, and QD_{655} could be successfully identified and quantitated in the presence of more than an 800-fold excess of free QDs, and the size of the triply labeled spheres could be determined.[281] 3C-FCCS was also able to identify and determine the size of DNA trimers (~80 nm) labeled with the three colors of QD.[282] The technique does not require long acquisition times (<1 min) and is expected to be useful for measuring molecular exchanges in signal transduction pathways, or the assembly of tripartite biomolecular complexes.

Wiseman's group has used QDs as labels in image correlation spectroscopy (ICS) for measuring biomolecular diffusion constants.[284–286] Although the blinking of QDs affects diffusion measurements made with temporal ICS, reciprocal space (k-space) ICS (kICS) can separate PL fluctuation contributions due to blinking and transport.[284,285] kICS has been used to measure the diffusion coefficient of QD-labeled glycosyl phosphatidylinositol–anchored protein CD73 in the membrane of live fibroblast cells.[284] Furthermore, by taking advantage of changes in blinking autocorrelation as a function of QD clustering, it was possible to observe T-cell receptor clustering upon activation with antigen.[286]

Super-Resolution Imaging. Optical microscopy is an unrivaled tool for obtaining structural and molecular information at the micrometer scale. However, the opportunity for insight at the nanometer scale, where complex and important biochemistry remains to be

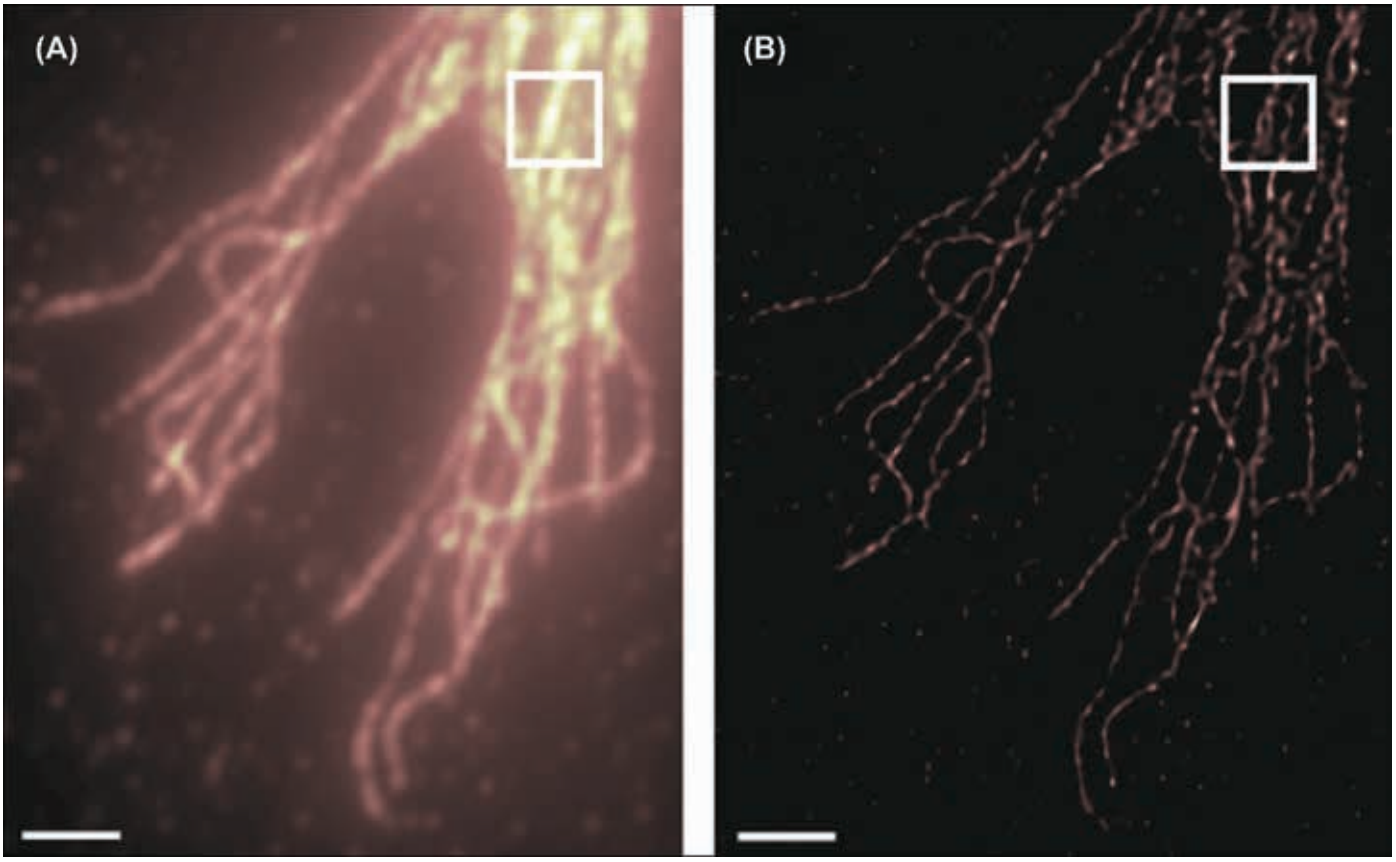

FIG. 18. 3D SOFI of the α-tubulin network in 3T3 cells labeled with QD_{625}: **(A)** *Time-averaged image from all frames and* **(B)** *SOFI image. The scale bar is 2 μm. [Reproduced with permission from Ref. 36. Copyright the authors 2009.]*

elucidated, is limited by the Abbé diffraction limit (~λ/2 or typically 200–300 nm). To address this shortcoming, a variety of super-resolution imaging techniques have emerged. One group of these techniques, referred to as single molecule localization methods, includes stochastic optical reconstruction microscopy (STORM), photoactivated localization microscopy, and super-resolution optical fluctuation imaging (SOFI). These methods rely on the switching of individual fluorophores between bright and dark states, which has a natural parallel with the blinking behavior of QDs. Indeed, Lidke et al. used an independent component analysis method to resolve two closely spaced (23 nm) QD emitters, based on their blinking, with a standard wide-field microscope.[19] Chien et al. similarly used the blinking of QDs to image microtubules in fixed CHO (Chinese hamster ovary) cells with 30 nm resolution and an acquisition time that was less than 1 min.[287] QDs were also used to develop the SOFI imaging technique that records a movie to capture fluorescence intermittency (i.e., blinking) over time and statistically analyzes the signal fluctuations.[36] Since the blinking of QDs follows power law statistics and occurs over all time scales, arbitrary frame rates can be used. The advantages of the technique include a five-fold improvement in resolution and reduced background, as demonstrated by labeling the α-tubulin network of fixed 3T3 fibroblast cells with QD_{625}-secondary antibody conjugates (Fig. 18).[36] There is an ongoing effort to combine QDs and STORM for in vivo super-resolution imaging.[288,289]

Near-Field Scanning Optical Microscopy. Near-field scanning optical microscopy (NSOM) is a scanning probe imaging technique that provides optical resolution below the diffraction limit, with simultaneous topographic information. Cai's group has combined QDs and NSOM for high-resolution (~50–100 nm) imaging of cell surface receptors in several studies.[290–292] For example, one study focused on imaging antigen-specific T-cell receptor (TCR) response to activation and expansion.[290] Vγ2Vδ2 T-cell surface receptors specifically bind phosphoantigens, resulting in T-cell expansion (i.e., rapid proliferation of clonal T cells) as part of an immune response. QD_{655} were conjugated with anti-TCR antibodies and used to label the TCRs on T cells obtained from macaques. The NSOM-measured distribution of QD PL across individual cells was correlated to the cell surface distribution of TCRs. Before activation and expansion, a larger number of smaller TCR sites were associated with Vγ2Vδ2 T cells ($\sim 5 \pm 1 \times 10^3$, primarily 50 nm in size) and more uniformly distributed compared with a nonengaging αβ T-cell phenotype ($\sim 2 \pm 1 \times 10^3$, >90 nm in size). After activation (i.e., infection of the ma-

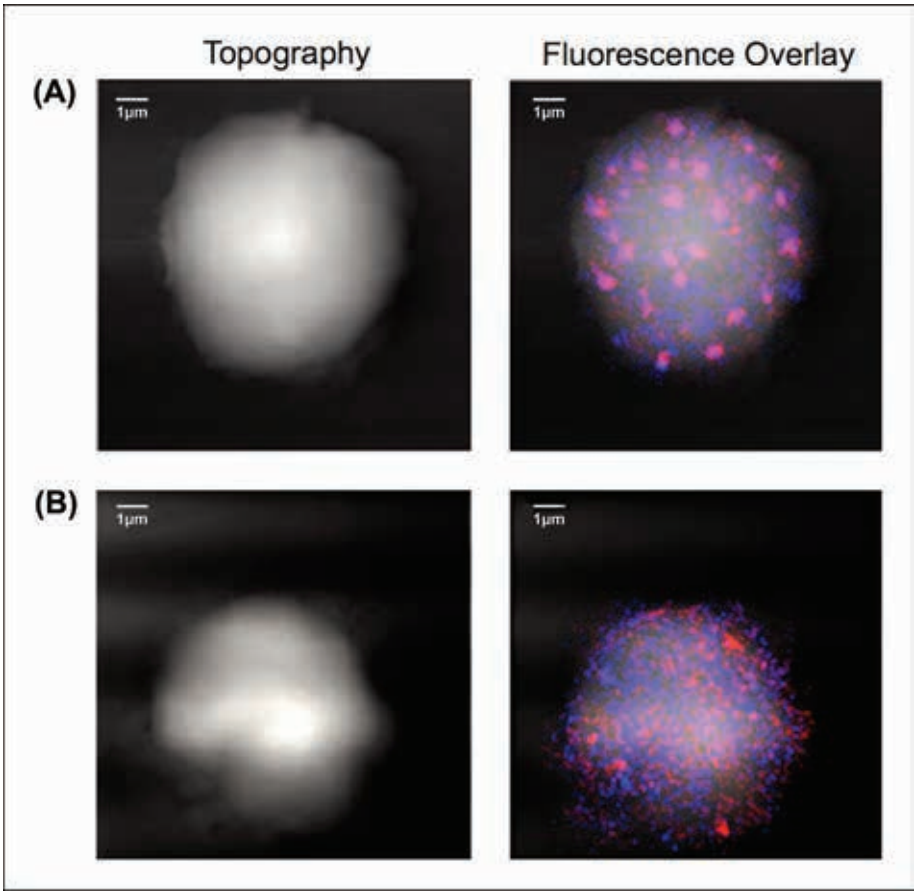

FIG. 19. NSOM images of T cell receptors (TCR/CD3) labeled with QD-antibody conjugates: **(A)** *CD4 T cells co-stimulated with anti-CD3 and anti-CD28 antibodies; and* **(B)** *CD4 T cells stimulated with anti-CD28 only. Scale bars are 1 μm. The images on the left show topographic data, the images in the right show the merged topographic-QD PL data. PL from QD-labeled CD3 is shown in blue; PL from QD-labeled CD4 is shown in red; colocalization of both PL signals appears violet. The co-stimulation of cells (A) shows increased co-clustering of CD3-CD4 nanodomains on the membrane. Figure reprinted with permission under the Creative Commons Attribution License from ref. 293. Copyright 2009 the authors.*

caques), the TCRs aggregated on the Vγ2Vδ2 T-cell membrane, and this pattern was sustained in daughter cells. The aggregated receptors recognized phosphoantigen and imbued the Vγ2Vδ2 T cells with much more potent effector function, suggesting an important role for TCR aggregation in immune response.[290] In these experiments, the QD_{655} were found to be a much more effective label than several common fluorescent dyes, permitting repeated imaging of cells by virtue of their resistance to both photobleaching and chemical degradation. Building on this approach, these authors subsequently used two-color NSOM to visualize the clustering and interactions of membrane receptors during TCR/CD3-mediated signaling in T cells.[293] Images of QD_{605} and QD_{650} PL were combined with topographical information (Fig. 19) and indicated co-clustering of CD3 with CD4 or CD8 co-receptors during T-cell activation. The authors also noted that co-stimulation of CD28 receptors significantly enhanced the clustering of TCR/CD3 with CD4 co-receptors, but not CD8 co-receptors. Cai's group also used QD-antibody conjugates and NSOM to investigate the distribution of CD4 receptor proteins on T-helper cell surfaces[291] and hyaluronan receptor CD44 on the surface of mesenchymal stem cells.[292] In the latter, blinking was suggested to be useful for identifying single QDs, and preferential enrichment of QD-antibody conjugates was observed on cell filopodia (a sensory organelle important in migration and adhesion).[292] The enrichment corresponded to clusters of CD44 domains (200–600 nm in size) that were primarily observed at the peaks and ridges of cell surface topography plots. Such detail would not have been discerned without the dual topographical and optical capability of the NSOM technique, facilitated by the use of QDs.

Fluorescence Lifetime and Fluorescence Lifetime Imaging Microscopy. Although QD PL intensity measurements are straightforward and versatile, reliable quantitative measurements are very challenging when the concentration of QDs is not controlled. Such is almost always the case when, for example, QDs are delivered to cells, QDs are immobilized at an interface, or QDs are subject to dilution in flow systems. Although ratiometric PL intensity methods address this challenge, ratiometric QD probes are not available for every application. Fluorescence (or PL) lifetime analysis is independent of QD concentration and is also very well suited to quantitative measurements when concentration is uncertain. In addition to being a measure of FRET and CT quenching efficiency, changes in QD PL properties, such as lifetime, can reflect physicochemical changes in the local microenvironment (e.g., temperature, pH) by virtue of changes in radiative and non-radiative rates.[294,295] Jaque's group has investigated this phenomenon for thermometry applications and found that optimum temperature sensitivity can be obtained with smaller sized QDs and the use of CdTe over CdSe.[296] Spectral shifts are accompanied by changes in PL lifetime where, for example, CdTe QD_{515} (1 nm in diameter) exhibited a thermal sensitivity of $-0.017\ °C^{-1}$ (measured as the *relative* change in lifetime per degree Celsius) between 27 and 50 °C. This sensitivity was comparable to rhodamine B–doped microspheres ($0.0016\ °C^{-1}$) and Kiton red dye ($0.011\ °C^{-1}$),[296] suggesting that QDs might be useful probes for FLIM-based measurement of intracellular temperature. Such measurements are important for identifying "hot" malignant cells (higher metabolic

activity compared with healthy cells) and monitoring hyperthermic treatment of those cells.

FLIM can also be used for visualization and quantitative sensing with QD probes based on FRET or CT quenching. For example, Pai and Cotlet modified vaterite ($CaCO_3$) microparticles with CdSe/ZnS QD_{525}-TDTomato (fluorescent protein) conjugates and measured the QD-TDTomato FRET efficiency (~67%) via two-color FLIM.[297] Although only a proof-of-concept study, this format could be readily extended to sensing proteolytic activity by expressing the fluorescent protein with a peptide linker that was a substrate for a protease of interest.[125,141] Ruedas-Rama et al. developed a FLIM-based chloride ion (Cl^-) sensor based on the CT quenching interaction between CdSe/ZnS QD_{610} and lucigenin, a chloride-sensitive indicator dye.[298] The lucigenin was conjugated to the QDs to provide the proximity for CT quenching, resulting in a marked decrease in the QD PL intensity and its lifetime (from 20 to 9 ns). However, Cl^- dynamically quenches lucigenin, and the collisional lucigenin–Cl^- interaction competed with the QD–lucigenin CT interaction. Increasing concentrations of Cl^- led to a progressive recovery of the QD PL lifetime, including a linear response for 0.5–50 mM Cl^- in a complex solution mimicking an intracellular matrix.[298] FLIM-based sensing of Cl^- was demonstrated, but once again only as a proof-of-concept. Nevertheless, as FLIM with fluorescent proteins and organic dyes continues to grow in importance for cellular imaging and sensing,[299–301] the utility of combining QDs with FLIM will also grow.

SUMMARY AND OUTLOOK

The role for QDs in bioanalysis and bioimaging has grown considerably over the last decade, and this growth can be expected to continue. QDs have emerged as much more than an alternative to fluorescent dyes, providing the means to address new challenges in biochemical and biophysical research. As the applications of QDs have expanded, there has been a progressive evolution of QD materials and bioconjugates, permitting even greater tailoring of the physical and optical properties of QDs. This review has summarized the important properties of QDs and highlighted several QD-based methods in bioanalysis and bioimaging. These methods rely on QD PL intensity, polarization, or lifetime for detection, as well as modulation of these properties via Förster-type energy transfer (FRET, BRET, CRET), CL and ECL, CT quenching, and coupling with plasmonic structures or photonic crystals. Fluorometers, plate readers, flow cytometers, and other steady-state or time-resolved spectroscopic platforms have been used to develop assays around QDs, whereas imaging methods have included the use of epifluorescence, confocal and 2PE microscopy, spectral imaging, single particle tracking, FCS, super-resolution imaging, NSOM, and FLIM. In each of the above-mentioned methods, QDs offer nontrivial advantages: the brightness needed for sensitive detection, the photostability needed for tracking dynamic processes, the multiplexing capability needed to elucidate complex systems, or the nanoscale interface needed for biomolecular engineering of novel probes and biosensors. Although QD materials have been commercialized for research and development purposes, one of the challenges moving forward will be to translate the fruits of these labors into commercialized, QD-enabled technologies; for example, assay kits and diagnostic platforms. In the interim, QDs will continue their rise to prominence as powerful and versatile tools for bioanalysis and bioimaging.

ACKNOWLEDGMENTS

Eleonora Petryayeva is grateful to the Natural Sciences and Engineering Research Council of Canada for support through a postgraduate fellowship. W. Russ Algar and Eleonora Petryayeva acknowledge the University of British Columbia for financial support of this research. Igor L. Medintz acknowledges the Office of Naval Research, the Naval Research Laboratory (NRL), the NRL Nanosciences Institute, the Defense Advanced Research Projects Agency, and the Defense Threat Reduction Agency Joint Science and Technological Office (DTRA-JSTO) Military Interdepartmental Purchase Requisition B112582M.

1. C.J. Murphy, J.L. Coffer. "Quantum Dots: A Primer". Appl. Spectrosc. 2002. 56(1): 16A-27A.
2. M. Bruchez, M. Moronne, P. Gin, S. Weiss, A.P. Alivisatos. "Semiconductor Nanocrystals as Fluorescent Biological Labels". Science. 1998. 281(5385): 2013-2016.
3. W.C.W. Chan, S.M. Nie. "Quantum Dot Bioconjugates for Ultrasensitive Nonisotopic Detection". Science. 1998. 281(5385): 2016-2018.
4. I.L. Medintz, H. Mattoussi. "Quantum Dot-Based Resonance Energy Transfer and Its Growing Application in Biology". Phys. Chem. Chem. Phys. 2009. 11(1): 17-45.
5. M.K. Wagner, F. Li, J.J. Li, X.F. Li, X.C. Le. "Use of Quantum Dots in the Development of Assays for Cancer Biomarkers". Anal. Bioanal. Chem. 2010. 397(8): 3213-3224.
6. H. Mattoussi, G. Palui, H.B. Na. "Luminescent Quantum Dots as Platforms for Probing in Vitro and in Vivo Biological Processes". Adv. Drug Delivery Rev. 2012. 64(2): 138-166.
7. C. Frigerio, D.S.M. Ribeiro, S.S.M. Rodrigues, V.L.R.G. Abreu, J.A.C. Barbosa, J.A.V. Prior, K.L. Marques, J.L.M. Santos. "Application of Quantum Dots as Analytical Tools in Automated Chemical Analysis: A Review". Anal. Chim. Acta. 2012. 735: 9-22.
8. M.F. Frasco, N. Chaniotakis. "Bioconjugated Quantum Dots as Fluorescent Probes for Bioanalytical Applications". Anal. Bioanal. Chem. 2010. 396(1): 229-240.
9. X. Michalet, F.F. Pinaud, L.A. Bentolila, J.M. Tsay, S. Doose, J.J. Li, G. Sundaresan, A.M. Wu, S.S. Gambhir, S. Weiss. "Quantum Dots for Live Cells, in Vivo Imaging, and Diagnostics". Science. 2005. 307(5709): 538-544.
10. X.Y. Wu, H.J. Liu, J.Q. Liu, K.N. Haley, J.A. Treadway, J.P. Larson, N.F. Ge, F. Peale, M.P. Bruchez. "Immunofluorescent Labeling of Cancer Marker Her2 and Other Cellular Targets with Semiconductor Quantum Dots". Nat. Biotechnol. 2003. 21(1): 41-46.
11. I.L. Medintz, D. Farrell, K. Susumu, S.A. Trammell, J.R. Deschamps, F.M. Brunel, P.E. Dawson, H. Mattoussi. "Multiplex Charge-Transfer Interactions between Quantum Dots and Peptide-Bridged Ruthenium Complexes". Anal. Chem. 2009. 81(12): 4831-4839.
12. D. Geissler, L.J. Charbonniere, R.F. Ziessel, N.G. Butlin, H.G. Lohmannsroben, N. Hildebrandt. "Quantum Dot Biosensors for Ultrasensitive Multiplexed Diagnostics". Angew. Chem. Int. Ed. 2010. 49(8): 1396-1401.
13. I.L. Medintz, H.T. Uyeda, E.R. Goldman, H. Mattoussi. "Quantum Dot Bioconjugates for Imaging, Labelling and Sensing". Nat. Mater. 2005. 4(6): 435-446.
14. U. Resch-Genger, M. Grabolle, S. Cavaliere-Jaricot, R. Nitschke, T. Nann. "Quantum Dots versus Organic Dyes as Fluorescent Labels". Nat. Methods. 2008. 5(9): 763-775.
15. W.C.W. Chan, D.J. Maxwell, X.H. Gao, R.E. Bailey, M.Y. Han, S.M. Nie. "Luminescent Quantum Dots for Multiplexed Biological Detection and Imaging". Curr. Opin. Biotechnol. 2002. 13(1): 40-46.
16. W.R. Algar, A.J. Tavares, U.J. Krull. "Beyond Labels: A Review of the Application of Quantum Dots as Integrated Components of Assays, Bioprobes, and Biosensors Utilizing

Optical Transduction". Anal. Chim. Acta. 2010. 673(1): 1-25.
17. S.J. Rosenthal, J.C. Chang, O. Kovtun, J.R. McBride, I.D. Tomlinson. "Biocompatible Quantum Dots for Biological Applications". Chem. Biol. 2011. 18(1): 10-24.
18. W.R. Algar, K. Susumu, J.B. Delehanty, I.L. Medintz. "Semiconductor Quantum Dots in Bioanalysis: Crossing the Valley of Death". Anal. Chem. 2011. 83(23): 8826-8837.
19. K. Lidke, B. Rieger, T. Jovin, R. Heintzmann. "Superresolution by Localization of Quantum Dots Using Blinking Statistics". Opt. Express. 2005. 13(18): 7052-7062.
20. D.R. Larson, W.R. Zipfel, R.M. Williams, S.W. Clark, M.P. Bruchez, F.W. Wise, W.W. Webb. "Water-Soluble Quantum Dots for Multiphoton Fluorescence Imaging in Vivo". Science. 2003. 300(5624): 1434-1436.
21. F. Helmchen, W. Denk. "Deep Tissue Two-Photon Microscopy". Nat. Methods. 2005. 2(12): 932-940.
22. R.H. Na, I.M. Stender, L.X. Ma, H.C. Wulf. "Autofluorescence Spectrum of Skin: Component Bands and Body Site Variations". Skin Res. Technol. 2000. 6(3): 112-117.
23. A.M. Smith, S. Nie. "Semiconductor Nanocrystals: Structure, Properties, and Band Gap Engineering. Acc". Chem. Res. 2009. 43(2): 190-200.
24. S. Kim, B. Fisher, H.J. Eisler, M. Bawendi. "Type-II Quantum Dots: CdTe/CdSe(Core/Shell) and CdSe/ZinTe(Core/Shell) Heterostructures". J. Am. Chem. Soc. 2003. 125(38): 11466-11467.
25. B. Blackman, D. Battaglia, X. Peng. "Bright and Water-Soluble Near IR-Emitting CdSe/CdTe/ZnSe Type-II/Type-I Nanocrystals, Tuning the Efficiency and Stability by Growth". Chem. Mater. 2008. 20(15): 4847-4853.
26. R. Xie, X. Peng. "Synthetic Scheme for High-Quality InAs Nanocrystals Based on Self-Focusing and One-Pot Synthesis of InAs-Based Core–Shell Nanocrystals". Angew. Chem. Int. Ed. 2008. 47(40): 7677-7680.
27. R. Xie, X. Peng. "Synthesis of Cu-Doped InP Nanocrystals (d-dots) with ZnSe Diffusion Barrier as Efficient and Color-Tunable NIR Emitters.". J. Am. Chem. Soc. 2009. 131(30): 10645-10651.
28. S.W. Kim, J.P. Zimmer, S. Ohnishi, J.B. Tracy, J.V. Frangioni, M.G. Bawendi. "Engineering InAsxP1-x/InP/ZnSe III-V Alloyed Core/Shell Quantum Dots for the Near-Infrared". J. Am. Chem. Soc. 2005. 127(30): 10526-10532.
29. R.G. Xie, K. Chen, X.Y. Chen, X.G. Peng. "InAs/InP/ZnSe Core/Shell/Shell Quantum Dots as Near-Infrared Emitters: Bright, Narrow-Band, Non-Cadmium Containing, and Biocompatible". Nano Res. 2008. 1(6): 457-464.
30. X. Zhong, R. Xie, Y. Zhang, T. Basché, W. Knoll. "High-Quality Violet- to Red-Emitting ZnSe/CdSe Core/Shell Nanocrystals". Chem. Mater. 2005. 17(16): 4038-4042.
31. S. Kim, J. Park, T. Kim, E. Jang, S. Jun, H. Jang, B. Kim, S.-W. Kim. "Reverse Type-I ZnSe/InP/ZnS Core/Shell/Shell Nanocrystals: Cadmium-Free Quantum Dots for Visible Luminescence". Small. 2011. 7(1): 70-73.
32. A.M. Smith, A.M. Mohs, S. Nie. "Tuning the Optical and Electronic Properties of Colloidal Nanocrystals by Lattice Strain". Nat. Nanotechnol. 2009. 4(1): 56-63.
33. C. Galland, Y. Ghosh, A. Steinbruck, M. Sykora, J.A. Hollingsworth, V.I. Klimov, H. Htoon. "Two Types of Luminescence Blinking Revealed by Spectroelectrochemistry of Single Quantum Dots". Nature. 2011. 479(7372): 203-U275.
34. S. Clarke, F. Pinaud, O. Beutel, C.J. You, J. Piehler, M. Dahan. "Covalent Monofunctionalization of Peptide-Coated Quantum Dots for Single-Molecule Assays". Nano Lett. 2010. 10(6): 2147-2154.
35. M.V. Ehrensperger, C. Hanus, C. Vannier, A. Triller, M. Dahan. "Multiple Association States between Glycine Receptors and Gephyrin Identified by SPT Analysis". Biophys. J. 2007. 92(10): 3706-3718.
36. T. Dertinger, R. Colyer, G. Iyer, S. Weiss, J. Enderlein. "Fast, Background-Free, 3D Super-Resolution Optical Fluctuation Imaging (SOFI)". P. Natl. Acad. S. USA. 2009. 106(52): 22287-22292.
37. S.F. Lee, M.A. Osborne. "Brightening, Blinking, Bluing and Bleaching in the Life of a Quantum Dot: Friend or Foe?". ChemPhysChem. 2009. 10(13): 2174-2191.
38. K.X. Hay, V.Y. Waisundara, Y. Zong, M.-Y. Han, D. Huang. "CdSe Nanocrystals as Hydroperoxide Scavengers: A New Approach to Highly Sensitive Quantification of Lipid Hydroperoxides". Small. 2007. 3(2): 290-293.
39. A. Javier, G.F. Strouse. "Activated and Intermittent Photoluminescence in Thin CdSe Quantum Dot Films". Chem. Phys. Lett. 2004. 391(1-3): 60-63.
40. J.U. Sutter, D.J.S. Birch, O.J. Rolinski. "The Effect of Intensity of Excitation on CdSe/ZnS Quantum Dots: Opportunities in Luminescence Sensing". Appl. Phys. Lett. 2011. 98(2): 021108.
41. J. Yao, D.R. Larson, H.D. Vishwasrao, W.R. Zipfel, W.W. Webb. "Blinking and Nonradiant Dark Fraction of Water-Soluble Quantum Dots in Aqueous Solution". P. Natl. Acad. S. USA. 2005. 102(40): 14284-14289.
42. T. Pons, I.L. Medintz, D. Farrell, X. Wang, A.F. Grimes, D.S. English, L. Berti, H. Mattoussi. "Single-Molecule Colocalization Studies Shed Light on the Idea of Fully Emitting versus Dark Single Quantum Dots". Small. 2011. 7(14): 2101-2108.
43. N. Durisic, P.W. Wiseman, P. Grutter, C.D. Heyes. "A Common Mechanism Underlies the Dark Fraction Formation and Fluorescence Blinking of Quantum Dots". ACS Nano. 2009. 3(5): 1167-1175.
44. I.L. Medintz, A.R. Clapp, H. Mattoussi, E.R. Goldman, B. Fisher, J.M. Mauro. "Self-Assembled Nanoscale Biosensors Based on Quantum Dot FRET Donors". Nat. Mater. 2003. 2(9): 630-638.
45. M.A. Hines, P. Guyot-Sionnest. "Synthesis and Characterization of Strongly Luminescing ZnS-Capped CdSe Nanocrystals". J. Phys. Chem. 1996. 100(2): 468-471.
46. B.O. Dabbousi, J. RodriguezViejo, F.V. Mikulec, J.R. Heine, H. Mattoussi, R. Ober, K.F. Jensen, M.G. Bawendi. "(CdSe)ZnS Core-Shell Quantum Dots: Synthesis and Characterization of a Size Series of Highly Luminescent Nanocrystallites". J. Phys. Chem. B. 1997. 101(46): 9463-9475.
47. X.Y. Wang, X.F. Ren, K. Kahen, M.A. Hahn, M. Rajeswaran, S. Maccagnano-Zacher, J. Silcox, G.E. Cragg, A.L. Efros, T.D. Krauss. "Non-Blinking Semiconductor Nanocrystals". Nature. 2009. 459(7247): 686-689.
48. J. McBride, J. Treadway, L.C. Feldman, S.J. Pennycook, S.J. Rosenthal. "Structural Basis for Near Unity Quantum Yield Core/Shell Nanostructures". Nano Lett. 2006. 6(7): 1496-1501.
49. D.V. Talapin, I. Mekis, S. Gotzinger, A. Kornowski, O. Benson, H. Weller. "CdSe/CdS/ZnS and CdSe/ZnSe/ZnS Core-Shell-Shell Nanocrystals". J. Phys. Chem. B. 2004. 108(49): 18826-18831.
50. R.G. Xie, U. Kolb, J.X. Li, T. Basche, A. Mews. "Synthesis and Characterization of Highly Luminescent CdSe-Core CdS/Zn0.5Cd0.5S/ZnS Multishell Nanocrystals". J. Am. Chem. Soc. 2005. 127(20): 7480-7488.
51. M.D. Regulacio, M.Y. Han. "Composition-Tunable Alloyed Semiconductor Nanocrystals. Acc". Chem. Res. 2010. 43(5): 621-630.
52. N. Al-Salim, A.G. Young, R.D. Tilley, A.J. McQuillan, J. Xia. "Synthesis of CdSeS Nanocrystals in Coordinating and Noncoordinating Solvents: Solvent's Role in Evolution of the Optical and Structural Properties". Chem. Mater. 2007. 19(21): 5185-5193.
53. L.A. Swafford, L.A. Weigand, M.J. Bowers, J.R. McBride, J.L. Rapaport, T.L. Watt, S.K. Dixit, L.C. Feldman, S.J. Rosenthal. "Homogeneously Alloyed CdSxSe1-x Nanocrystals: Synthesis, Characterization, and Composition/Size-Dependent Band Gap". J. Am. Chem. Soc. 2006. 128(37): 12299-12306.
54. R.E. Bailey, S. Nie. "Alloyed Semiconductor Quantum Dots: Tuning the Optical Properties Without Changing the Particle Size". J. Am. Chem. Soc. 2003. 125(23): 7100-7106.
55. X. Zhong, Y. Feng, W. Knoll, M. Han. "Alloyed ZnxCd1-xS Nanocrystals with Highly Narrow Luminescence Spectral Width". J. Am. Chem. Soc. 2003. 125(44): 13559-13563.
56. X. Zhong, M. Han, Z. Dong, T.J. White, W. Knoll. "Composition-Tunable ZnxCd1-xSe Nanocrystals with High Luminescence and Stability". J. Am. Chem. Soc. 2003. 125(28): 8589-8594.
57. O.I. Micic, S.P. Ahrenkiel, A.J. Nozik. "Synthesis of Extremely Small InP Quantum Dots and Electronic Coupling in Their Disordered Solid Films". Appl. Phys. Lett. 2001. 78(25): 4022-4024.
58. D. Battaglia, X. Peng. "Formation of High Quality InP and InAs Nanocrystals in a Noncoordinating Solvent". Nano Lett. 2002. 2(9): 1027-1030.
59. A. Shiohara, S. Prabakar, A. Faramus, C.-Y. Hsu, P.-S. Lai, P.T. Northcote, R.D. Tilley. "Sized Controlled Synthesis, Purification,

and Cell Studies with Silicon Quantum Dots". Nanoscale. 2011. 3(8): 3364-3370.
60. F. Erogbogbo, K.T. Yong, I. Roy, R. Hu, W.C. Law, W.W. Zhao, H. Ding, F. Wu, R. Kumar, M.T. Swihart, P.N. Prasad. "In Vivo Targeted Cancer Imaging, Sentinel Lymph Node Mapping and Multi-Channel Imaging with Biocompatible Silicon Nanocrystals". ACS Nano. 2011. 5(1): 413-423.
61. L.Y.T. Chou, W.C.W. Chan. "Nanotoxicology No Signs of Illness". Nat. Nanotechnol. 2012. 7(7): 416-417.
62. S. Ghaderi, B. Ramesh, A.M. Seifalian. "Fluorescence Nanoparticles "Quantum Dots as Drug Delivery System and Their Toxicity: A Review". J. Drug Targeting. 2011. 19(7): 475-486.
63. F.M. Winnik, D. Maysinger. "Quantum Dot Cytotoxicity and Ways To Reduce It". Acc. Chem. Res. 2012. DOI: 10.1021/ar3000585.
64. S. Xu, J. Ziegler, T. Nann. "Rapid Synthesis of Highly Luminescent InP and InP/ZnS Nanocrystals". J. Mater. Chem. 2008. 18(23): 2653-2656.
65. T. Greco, C. Ippen, A. Wedel. "InP/ZnSe/ZnS Core-Multishell Quantum Dots for Improved Luminescence Efficiency". Proc. SPIE. 2012. 8424: 842439.
66. H.S. Choi, W. Liu, P. Misra, E. Tanaka, J.P. Zimmer, B.I. Ipe, M.G. Bawendi, J.V. Frangioni. "Renal Clearance of Quantum Dots". Nat. Biotechnol. 2007. 25(10): 1165-1170.
67. J. Park, C. Dvoracek, K.H. Lee, J.F. Galloway, H.-e. C. Bhang, M.G. Pomper, P.C. Searson. "CuInSe/ZnS Core/Shell NIR Quantum Dots for Biomedical Imaging". Small. 2011. 7(22): 3148-3152.
68. Z.A. Peng, X.G. Peng. "Formation of High-Quality CdTe, CdSe, and CdS Nanocrystals Using CdO as Precursor". J. Am. Chem. Soc. 2001. 123(1): 183-184.
69. L.H. Qu, Z.A. Peng, X.G. Peng. "Alternative Routes Toward High Quality CdSe Nanocrystals". Nano Lett. 2001. 1(6): 333-337.
70. W.W. Yu, X.G. Peng. "Formation of High-Quality CdS and UII-VI Semiconductor Nanocrystals in Noncoordinating Solvents: Tunable Reactivity of Monomers". Angew. Chem. Int. Ed. 2002. 41(13): 2368-2371.
71. W.J. Zhang, G.J. Chen, J. Wang, B.C. Ye, X.H. Zhong. "Design and Synthesis of Highly Luminescent Near-Infrared-Emitting Water-Soluble CdTe/CdSe/ZnS Core/Shell/Shell Quantum Dots". Inorg. Chem. 2009. 48(20): 9723-9731.
72. Z.T. Deng, O. Schulz, S. Lin, B.Q. Ding, X.W. Liu, X.X. Wei, R. Ros, H. Yan, Y. Liu. "Aqueous Synthesis of Zinc Blende CdTe/CdS Magic-Core/Thick-Shell Tetrahedral-Shaped Nanocrystals with Emission Tunable to Near-Infrared". J. Am. Chem. Soc. 2010. 132(16): 5592.
73. Z.M. Yuan, Q. Ma, A.Y. Zhang, Y.Q. Cao, J. Yang, P. Yang. "Synthesis of Highly Luminescent CdTe/ZnO Core/Shell Quantum Dots in Aqueous Solution". J. Mater. Sci. 2012. 47(8): 3770-3776.
74. W.J. Parak, T. Pellegrino, C. Plank. "Labelling of Cells with Quantum Dots". Nanotechnology. 2005. 16(2): R9-R25.
75. W.R. Algar, D.E. Prasuhn, M.H. Stewart, T.L. Jennings, J.B. Blanco-Canosa, P.E. Dawson, I.L. Medintz. "The Controlled Display of Biomolecules on Nanoparticles: A Challenge Suited to Bioorthogonal Chemistry". Bioconjugate Chem. 2011. 22(5): 825-858.
76. K.E. Sapsford, W.R. Algar, L. Berti, K.B. Gemmill, B. Casey, E. Oh, M.H. Stewart, I.L. Medintz. "Functionalizing Nanoparticles with Biological Molecules: Developing Chemistries that Facilitate Nanotechnology". Chem. Rev., paper in press, 2012.
77. K.E. Sapsford, K.M. Tyner, B.J. Dair, J.R. Deschamps, I.L. Medintz. "Analyzing Nanomaterial Bioconjugates: A Review of Current and Emerging Purification and Characterization Techniques". Anal. Chem. 2011. 83(12): 4453-4488.
78. I. Medintz. "Universal Tools for Biomolecular Attachment to Surfaces". Nat. Mater. 2006. 5(11): 842-842.
79. P.A.S. Jorge, M.A. Martins, T. Trindade, J.L. Santos, F. Farahi. "Optical Fiber Sensing Using Quantum Dots". Sensors. 2007. 7(12): 3489-3534.
80. K. Susumu, H.T. Uyeda, I.L. Medintz, T. Pons, J.B. Delehanty, H. Mattoussi. "Enhancing the Stability and Biological Functionalities of Quantum Dots via Compact Multifunctional Ligands". J. Am. Chem. Soc. 2007. 129(45): 13987-13996.
81. K. Susumu, B.C. Mei, H. Mattoussi. "Multifunctional Ligands based on Dihydrolipoic Acid and Polyethylene Glycol to Promote Biocompatibility of Quantum Dots". Nat. Protoc. 2009. 4(3): 424-436.
82. B.C. Mei, K. Susumu, I.L. Medintz, J.B. Delehanty, T.J. Mountziaris, H. Mattoussi. "Modular Poly(ethylene glycol) Ligands for Biocompatible Semiconductor and Gold Nanocrystals with Extended pH and Ionic Stability". J. Mater. Chem. 2008. 18(41): 4949-4958.
83. W. Liu, M. Howarth, A.B. Greytak, Y. Zheng, D.G. Nocera, A.Y. Ting, M.G. Bawendi. "Compact Biocompatible Quantum Dots Functionalized for Cellular Imaging". J. Am. Chem. Soc. 2008. 130(4): 1274-1284.
84. E. Muro, T. Pons, N. Lequeux, A. Fragola, N. Sanson, Z. Lenkei, B. Dubertret. "Small and Stable Sulfobetaine Zwitterionic Quantum Dots for Functional Live-Cell Imaging". J. Am. Chem. Soc. 2010. 132(13): 4556.
85. K. Susumu, E. Oh, J.B. Delehanty, J.B. Blanco-Canosa, B.J. Johnson, V. Jain, W.J. Hervey, W.R. Algar, K. Boeneman, P.E. Dawson, I.L. Medintz. "Multifunctional Compact Zwitterionic Ligands for Preparing Robust Biocompatible Semiconductor Quantum Dots and Gold Nanoparticles". J. Am. Chem. Soc. 2011. 133(24): 9480-9496.
86. Y.J. Zhang, A. Clapp. "Overview of Stabilizing Ligands for Biocompatible Quantum Dot Nanocrystals". Sensors. 2011. 11(12): 11036-11055.
87. D. Liu, P.T. Snee. "Water-Soluble Semiconductor Nanocrystals Cap Exchanged with Metalated Ligands". ACS Nano. 2011. 5(1): 546-550.
88. Y.J. Zhang, A.M. Schnoes, A.R. Clapp. "Dithiocarbamates as Capping Ligands for Water-Soluble Quantum Dots". ACS Appl. Mater. Interfaces. 2010. 2(11): 3384-3395.
89. D.J. Zhou, Y. Li, E.A.H. Hall, C. Abell, D. Klenerman. "A Chelating Dendritic Ligand Capped Quantum Dot: Preparation, Surface Passivation, Bioconjugation and Specific DNA detection". Nanoscale. 2011. 3(1): 201-211.
90. E.E. Lees, T.L. Nguyen, A.H.A. Clayton, P. Mulvaney, B.W. Muir. "The Preparation of Colloidally Stable, Water-Soluble, Biocompatible, Semiconductor Nanocrystals with a Small Hydrodynamic Diameter". ACS Nano. 2009. 3(5): 1121-1128.
91. W.W. Yu, E. Chang, J.C. Falkner, J.Y. Zhang, A.M. Al-Somali, C.M. Sayes, J. Johns, R. Drezek, V.L. Colvin. "Forming Biocompatible and Nonaggregated Nanocrystals in Water Using Amphiphilic Polymers". J. Am. Chem. Soc. 2007. 129(10): 2871-2879.
92. T. Pellegrino, L. Manna, S. Kudera, T. Liedl, D. Koktysh, A.L. Rogach, S. Keller, J. Radler, G. Natile, W.J. Parak. "Hydrophobic Nanocrystals Coated with an Amphiphilic Polymer Shell: A General Route to Water Soluble Nanocrystals". Nano Lett. 2004. 4(4): 703-707.
93. C. Luccardini, C. Tribet, F. Vial, V. Marchi-Artzner, M. Dahan. "Size, Charge, and Interactions with Giant Lipid Vesicles of Quantum Dots Coated with an Amphiphilic Macromolecule". Langmuir. 2006. 22(5): 2304-2310.
94. D. Janczewski, N. Tomczak, M.Y. Han, G.J. Vancso. "Synthesis of Functionalized Amphiphilic Polymers for Coating Quantum Dots". Nat. Protoc. 2011. 6(10): 1546-1553.
95. I. Yildiz, B. McCaughan, S.F. Cruickshank, J.F. Callan, F.M. Raymo. "Biocompatible CdSe−ZnS Core−Shell Quantum Dots Coated with Hydrophilic Polythiols". Langmuir. 2009. 25(12): 7090-7096.
96. W.H. Liu, A.B. Greytak, J. Lee, C.R. Wong, J. Park, L.F. Marshall, W. Jiang, P.N. Curtin, A.Y. Ting, D.G. Nocera, D. Fukumura, R.K. Jain, M.G. Bawendi. "Compact Biocompatible Quantum Dots via RAFT-Mediated Synthesis of Imidazole-Based Random Copolymer Ligand". J. Am. Chem. Soc. 2010. 132(2): 472-483.
97. J.K. Oh. "Surface Modification of Colloidal CdX-Based Quantum Dots for Biomedical Applications". J. Mater. Chem. 2010. 20(39): 8433-8445.
98. T.L. Jennings, S.G. Becker-Catania, R.C. Triulzi, G. Tao, B. Scott, K.E. Sapsford, S. Spindel, E. Oh, V. Jain, J.B. Delehanty, D.E. Prasuhn, K. Boeneman, W.R. Algar, I.L. Medintz. "Reactive Semiconductor Nanocrystals for Chemoselective Biolabeling and Multiplexed Analysis". ACS Nano. 2011. 5(7): 5579-5593.
99. D.E. Prasuhn, J.B. Blanco-Canosa, G.J. Vora, J.B. Delehanty, K. Susumu, B.C. Mei, P.E. Dawson, I.L. Medintz. "Combining Chemoselective Ligation with Polyhistidine-Driven Self-Assembly for the Modular Display of Biomolecules on Quantum Dots". ACS Nano. 2010. 4(1): 267-278.
100. H.S. Han, N.K. Devaraj, J. Lee, S.A. Hilderbrand, R. Weissleder, M.G. Bawendi.

"Development of a Bioorthogonal and Highly Efficient Conjugation Method for Quantum Dots Using Tetrazine-Norbornene Cycloaddition". J. Am. Chem. Soc. 2010. 132(23): 7838.
101. A. Bernardin, A. Cazet, L. Guyon, P. Delannoy, F. Vinet, D. Bonnaffe, I. Texier. "Copper-Free Click Chemistry for Highly Luminescent Quantum Dot Conjugates: Application to in Vivo Metabolic Imaging". Bioconjugate Chem. 2010. 21(4): 583-588.
102. D.E. Prasuhn, A. Feltz, J.B. Blanco-Canosa, K. Susumu, M.H. Stewart, B.C. Mei, A.V. Yakovlev, C. Loukov, J.M. Mallet, M. Oheim, P.E. Dawson, I.L. Medintz. "Quantum Dot Peptide Biosensors for Monitoring Caspase 3 Proteolysis and Calcium Ions". ACS Nano. 2010. 4(9): 5487-5497.
103. K. Boeneman, J.R. Deschamps, S. Buckhout-White, D.E. Prasuhn, J.B. Blanco-Canosa, P.E. Dawson, M.H. Stewart, K. Susumu, E.R. Goldman, M. Ancona, I.L. Medintz. "Quantum Dot DNA Bioconjugates: Attachment Chemistry Strongly Influences the Resulting Composite Architecture". ACS Nano. 2010. 4(12): 7253-7266.
104. A.M. Dennis, D.C. Sotto, B.C. Mei, I.L. Medintz, H. Mattoussi, G. Bao. "Surface Ligand Effects on Metal-Affinity Coordination to Quantum Dots: Implications for Nanoprobe Self-Assembly". Bioconjugate Chem. 2010. 21(7): 1160-1170.
105. W.R. Algar, D. Wegner, A.L. Huston, J.B. Blanco-Canosa, M.H. Stewart, A. Armstrong, P.E. Dawson, N. Hildebrandt, I.L. Medintz. "Quantum Dots as Simultaneous Acceptors and Donors in Time-Gated Forster Resonance Energy Transfer Relays: Characterization and Biosensing". J. Am. Chem. Soc. 2012. 134(3): 1876-1891.
106. S.W. Bae, W.H. Tan, J.I. Hong. "Fluorescent Dye-Doped Silica Nanoparticles: New Tools for Bioapplications". Chem. Commun. 2012. 48(17): 2270-2282.
107. V.N. Mochalin, O. Shenderova, D. Ho, Y. Gogotsi. "The Properties and Applications of Nanodiamonds". Nat. Nanotechnol. 2012. 7(1): 11-23.
108. K.P. Loh, Q.L. Bao, G. Eda, M. Chhowalla. "Graphene Oxide as a Chemically Tunable Platform for Optical Applications". Nat. Chem. 2010. 2(12): 1015-1024.
109. S.N. Baker, G.A. Baker. "Luminescent Carbon Nanodots: Emergent Nanolights". Angew. Chem. Int. Ed. 2010. 49(38): 6726-6744.
110. H.C. Wu, X.L. Chang, L. Liu, F. Zhao, Y.L. Zhao. "Chemistry of Carbon Nanotubes in Biomedical Applications". J. Mater. Chem. 2010. 20(6): 1036-1052.
111. F. Wang, D. Banerjee, Y.S. Liu, X.Y. Chen, X.G. Liu. "Upconversion Nanoparticles in Biological Labeling, Imaging, and Therapy". Analyst. 2010. 135(8): 1839-1854.
112. Y.C. Shiang, C.C. Huang, W.Y. Chen, P.C. Chen, H.T. Chang. "Fluorescent Gold and Silver Nanoclusters for the Analysis of Biopolymers and Cell Imaging". J. Mater. Chem. 2012. 22(26): 12972-12982.
113. L. Shang, S.J. Dong, G.U. Nienhaus. "Ultra-Small Fluorescent Metal Nanoclusters: Synthesis and Biological Applications". Nano Today. 2011. 6(4): 401-418.
114. J. Zheng, P.R. Nicovich, R.M. Dickson. "Highly Fluorescent Noble-Metal Quantum Dots". Annu. Rev. Phys. Chem. 2007. 58: 409-431.
115. I. Diez, R.H.A. Ras. "Fluorescent Silver Nanoclusters". Nanoscale. 2011. 3(5): 1963-1970.
116. Y.Z. Lu, W. Chen. "Sub-Nanometre Sized Metal Clusters: from Synthetic Challenges to the Unique Property Discoveries". Chem. Soc. Rev. 2012. 41(9): 3594-3623.
117. E.R. Goldman, A.R. Clapp, G.P. Anderson, H.T. Uyeda, J.M. Mauro, I.L. Medintz, H. Mattoussi. "Multiplexed Toxin Analysis Using Four Colors of Quantum Dot Fluororeagents". Anal. Chem. 2004. 76(3): 684-688.
118. F. Morgner, S. Stufler, D. Geissler, I.L. Medintz, W.R. Algar, K. Susumu, M.H. Stewart, J.B. Blanco-Canosa, P.E. Dawson, N. Hildebrandt. "Terbium to Quantum Dot FRET Bioconjugates for Clinical Diagnostics: Influence of Human Plasma on Optical and Assembly Properties". Sensors. 2011. 11(10): 9667-9684.
119. C.S. Wu, M.K.K. Oo, X.D. Fan. "Highly Sensitive Multiplexed Heavy Metal Detection Using Quantum-Dot-Labeled DNAzymes". ACS Nano. 2010. 4(10): 5897-5904.
120. R. Freeman, Y. Li, R. Tel-Vered, E. Sharon, J. Elbaz, I. Willner. "Self-Assembly of Supramolecular Aptamer Structures for Optical or Electrochemical Sensing". Analyst. 2009. 134(4): 653-656.
121. E.R. Goldman, I.L. Medintz, J.L. Whitley, A. Hayhurst, A.R. Clapp, H.T. Uyeda, J.R. Deschamps, M.E. Lassman, H. Mattoussi. "A Hybrid Quantum Dot−Antibody Fragment Fluorescence Resonance Energy Transfer-Based TNT Sensor". J. Am. Chem. Soc. 2005. 127(18): 6744-6751.
122. K.E. Sapsford, J. Granek, J.R. Deschamps, K. Boeneman, J.B. Blanco-Canosa, P.E. Dawson, K. Susumu, M.H. Stewart, I.L. Medintz. "Monitoring Botulinum Neurotoxin A Activity with Peptide-Functionalized Quantum Dot Resonance Energy Transfer Sensors". ACS Nano. 2011. 5(4): 2687-2699.
123. K.R. Lee, I.-J. Kang. "Effects of Dopamine Concentration on Energy Transfer Between Dendrimer–QD and Dye-Labeled Antibody". Ultramicroscopy. 2009. 109(8): 894-898.
124. I.L. Medintz, A.R. Clapp, F.M. Brunel, T. Tiefenbrunn, H.T. Uyeda, E.L. Chang, J.R. Deschamps, P.E. Dawson, H. Mattoussi. "Proteolytic Activity Monitored by Fluorescence Resonance Energy Transfer Through Quantum-Dot-Peptide Conjugates". Nat. Mater. 2006. 5(7): 581-589.
125. K. Boeneman, B.C. Mei, A.M. Dennis, G. Bao, J.R. Deschamps, H. Mattoussi, I.L. Medintz. "Sensing Caspase 3 Activity with Quantum Dot-Fluorescent Protein Assemblies". J. Am. Chem. Soc. 2009. 131(11): 3828.
126. S. Huang, Q. Xiao, Z.K. He, Y. Liu, P. Tinnefeld, X.R. Su, X.N. Peng. "A High Sensitive and Specific QDs FRET Bioprobe for MNase". Chem. Commun. 2008. (45): 5990-5992.
127. M. Suzuki, Y. Husimi, H. Komatsu, K. Suzuki, K.T. Douglas. "Quantum Dot FRET Biosensors That Respond to pH, to Proteolytic or Nucleolytic Cleavage, to DNA Synthesis, or to a Multiplexing Combination". J. Am. Chem. Soc. 2008. 130(17): 5720-5725.
128. V.J. Bailey, H. Easwaran, Y. Zhang, E. Griffiths, S.A. Belinsky, J.G. Herman, S.B. Baylin, H.E. Carraway, T.H. Wang. "MS-qFRET: A Quantum Dot-Based Method for Analysis of DNA Methylation". Genome Res. 2009. 19(8): 1455-1461.
129. W.R. Algar, U.J. Krull. "Towards Multi-Colour Strategies for the Detection of Oligonucleotide Hybridization Using Quantum Dots as Energy Donors in Fluorescence Resonance Energy Transfer (FRET)". Anal. Chim. Acta. 2007. 581(2): 193-201.
130. M.D. Kattke, E.J. Gao, K.E. Sapsford, L.D. Stephenson, A. Kumar. "FRET-Based Quantum Dot Immunoassay for Rapid and Sensitive Detection of *Aspergillus amstelodami*". Sensors. 2011. 11(6): 6396-6410.
131. A.M. Dennis, W.J. Rhee, D. Sotto, S.N. Dublin, G. Bao. "Quantum Dot-Fluorescent Protein FRET Probes for Sensing Intracellular pH". ACS Nano. 2012. 6(4): 2917-2924.
132. R.C. Somers, R.M. Lanning, P.T. Snee, A.B. Greytak, R.K. Jain, M.G. Bawendi, D.G. Nocera. "A Nanocrystal-Based Ratiometric pH Sensor for Natural pH Ranges". Chem. Sci. 2012. 3(10): 2980-2985.
133. S.B. Lowe, J.A.G. Dick, B.E. Cohen, M.M. Stevens. "Multiplex Sensing of Protease and Kinase Enzyme Activity via Orthogonal Coupling of Quantum Dot–Peptide Conjugates". ACS Nano. 2011. 6(1): 851-857.
134. T.L. Jennings, M.P. Singh, G.F. Strouse. "Fluorescent Lifetime Quenching near d = 1.5 nm Gold Nanoparticles: Probing NSET Validity". J. Am. Chem. Soc. 2006. 128(16): 5462-5467.
135. T. Pons, I.L. Medintz, K.E. Sapsford, S. Higashiya, A.F. Grimes, D.S. English, H. Mattoussi. "On the Quenching of Semiconductor Quantum Dot Photoluminescence by Proximal Gold Nanoparticles". Nano Lett. 2007. 7(10): 3157-3164.
136. W.R. Algar, A.P. Malanoski, K. Susumu, M.H. Stewart, N. Hildebrandt, I.L. Medintz. "Multiplexed Tracking of Protease Activity Using a Single Color of Quantum Dot Vector and a Time-Gated Förster Resonance Energy Transfer Relay". Anal. Chem. 2012. 84(22): 10136-10146.
137. G. Marriott, S. Mao, T. Sakata, J. Ran, D.K. Jackson, C. Petchprayoon, T.J. Gomez, E. Warp, O. Tulyathan, H.L. Aaron, E.Y. Isacoff, Y.L. Yan. "Optical Lock-in Detection Imaging Microscopy for Contrast-Enhanced Imaging in Living Cells". P. Natl. Acad. S. USA. 2008. 105(46): 17789-17794.
138. S.A. Diaz, L. Giordano, T.M. Jovin, E.A. Jares-Erijman. "Modulation of a Photoswitchable Dual-Color Quantum Dot Containing a Photochromic FRET Acceptor and an Internal Standard". Nano Lett. 2012. 12(7): 3537-3544.
139. Z.Y. Xia, J.H. Rao. "Biosensing and Imaging Based on Bioluminescence Resonance Ener-

gy Transfer". Curr. Opin. Biotechnol. 2009. 20(1): 37-44.
140. M.K. So, C.J. Xu, A.M. Loening, S.S. Gambhir, J.H. Rao. "Self-Illuminating Quantum Dot Conjugates for in Vivo Imaging". Nat. Biotechnol. 2006. 24(3): 339-343.
141. Z.Y. Xia, Y. Xing, M.K. So, A.L. Koh, R. Sinclair, J.H. Rao. "Multiplex Detection of Protease Activity with Quantum Dot Nanosensors Prepared by Intein-Mediated Specific Bioconjugation". Anal. Chem. 2008. 80(22): 8649-8655.
142. X.Q. Liu, R. Freeman, E. Golub, I. Willner. "Chemiluminescence and Chemiluminescence Resonance Energy Transfer (CRET) Aptamer Sensors Using Catalytic Hemin/G-Quadruplexes". ACS Nano. 2011. 5(9): 7648-7655.
143. A. Niazov, R. Freeman, J. Girsh, I. Willner. "Following Glucose Oxidase Activity by Chemiluminescence and Chemiluminescence Resonance Energy Transfer (CRET) Processes Involving Enzyme-DNAzyme Conjugates". Sensors. 2011. 11(11): 10388-10397.
144. R. Freeman, X.Q. Liu, I. Winner. "Chemiluminescent and Chemiluminescence Resonance Energy Transfer (CRET) Detection of DNA, Metal Ions, and Aptamer-Substrate Complexes Using Hemin/G-Quadruplexes and CdSe/ZnS Quantum Dots". J. Am. Chem. Soc. 2011. 133(30): 11597-11604.
145. E. Golub, A. Niazov, R. Freeman, M. Zatsepin, I. Willner. "Photoelectrochemical Biosensors Without External Irradiation: Probing Enzyme Activities and DNA Sensing Using Hemin/G-Quadruplex-Stimulated Chemiluminescence Resonance Energy Transfer (CRET) Generation of Photocurrents". J. Phys. Chem. C. 2012. 116(25): 13827-13834.
146. R. Freeman, J. Girsh, A.F.J. Jou, J.A.A. Ho, T. Hug, J. Dernedde, I. Willner. "Optical Aptasensors for the Analysis of the Vascular Endothelial Growth Factor (VEGF)". Anal. Chem. 2012. 84(14): 6192-6198.
147. H. Chen, L. Lin, Z. Lin, G.S. Guo, J.M. Lin. "Chemiluminescence Arising from the Decomposition of Peroxymonocarbonate and Enhanced by CdTe Quantum Dots". J. Phys. Chem. A. 2010. 114(37): 10049-10058.
148. Z.P. Wang, J. Li, B. Liu, J.Q. Hu, X. Yao, J.H. Li. "Chemiluminescence of CdTe Nanocrystals Induced by Direct Chemical Oxidation and Its Size-Dependent and Surfactant-Sensitized Effect". J. Phys. Chem. B. 2005. 109(49): 23304-23311.
149. X.Z. Li, J. Li, J.L. Tang, J. Kang, Y.H. Zhang. "Study of Influence of Metal Ions on CdTe/H2O2 Chemiluminescence". J. Lumin. 2008. 128(7): 1229-1234.
150. Z.P. Wang, J. Li, B. Liu, J.H. Li. "CdTe Nanocrystals Sensitized Chemiluminescence and the Analytical Application". Talanta. 2009. 77(3): 1050-1056.
151. H.I. Chen, R.B. Li, L. Lin, G.S. Guo, J.M. Lin. "Determination of l-Ascorbic Acid in Human Serum by Chemiluminescence Based on Hydrogen Peroxide-Sodium Hydrogen Carbonate-CdSe/CdS Quantum Dots System". Talanta. 2010. 81(4-5): 1688-1696.
152. J.P. Lei, H.X. Ju. "Fundamentals and Bioanalytical Applications of Functional Quantum Dots as Electrogenerated Emitters of Chemiluminescence". TrAC, Trends Anal. Chem. 2011. 30(8): 1351-1359.
153. X. Liu, L. Guo, L. Cheng, H. Ju. "Determination of Nitrite Based on Its Quenching Effect on Anodic Electrochemiluminescence of CdSe Quantum Dots". Talanta. 2009. 78(3): 691-694.
154. L. Zhang, L. Shang, S. Dong. "Sensitive and Selective Determination of Cu2+ by Electrochemiluminescence of CdTe Quantum Dots''. Electrochem. Commun. 2008. 10(10): 1452-1454.
155. X. Liu, H. Ju. "Coreactant Enhanced Anodic Electrochemiluminescence of CdTe Quantum Dots at Low Potential for Sensitive Biosensing Amplified by Enzymatic Cycle". Anal. Chem. 2008. 80(14): 5377-5382.
156. H. Han, Z. Sheng, J. Liang. "Electrogenerated Chemiluminescence from Thiol-Capped CdTe Quantum Dots and Its Sensing Application in Aqueous Solution". Anal. Chim. Acta. 2007. 596(1): 73-78.
157. H. Huang, Y. Tan, J. Shi, G. Liang, J.-J. Zhu. "DNA Aptasensor for the Detection of ATP Based on Quantum Dots Electrochemiluminescence". Nanoscale. 2010. 2(4): 606-612.
158. G.F. Jie, P. Liu, L. Wang, S.S. Zhang. "Electrochemiluminescence Immunosensor Based on Nanocomposite Film of CdS Quantum Dots-Carbon Nanotubes Combined with Gold Nanoparticles-Chitosan". Electrochem. Commun. 2010. 12(1): 22-26.
159. R. Zhang, L. Fan, Y. Fang, S. Yang. "Electrochemical Route to the Preparation of Highly Dispersed Composites of ZnO/Carbon Nanotubes with Significantly Enhanced Electrochemiluminescence from ZnO''. J. Mater. Chem. 2008. 18(41): 4964-4970.
160. T. Wang, S.Y. Zhang, C.J. Mao, J.M. Song, H.L. Niu, B.K. Jin, Y.P. Tian. "Enhanced Electrochemiluminescence of CdSe Quantum Dots Composited with Graphene Oxide and Chitosan for Sensitive Sensor. Biosens". Bioelectron. 2012. 31(1): 369-375.
161. J. Wang, Y. Shan, W.-W. Zhao, J.-J. Xu, H.-Y. Chen. "Gold Nanoparticle Enhanced Electrochemiluminescence of CdS Thin Films for Ultrasensitive Thrombin Detection". Anal. Chem. 2011. 83(11): 4004-4011.
162. N. Myung, Z.F. Ding, A.J. Bard. "Electrogenerated Chemiluminescence of CdSe Nanocrystals". Nano Lett. 2002. 2(11): 1315-1319.
163. N. Myung, Y. Bae, A.J. Bard. "Effect of Surface Passivation on the Electrogenerated Chemiluminescence of CdSe/ZnSe Nanocrystals". Nano Lett. 2003. 3(8): 1053-1055.
164. S.K. Poznyak, D.V. Talapin, E.V. Shevchenko, H. Weller. "Quantum Dot Chemiluminescence". Nano Lett. 2004. 4(4): 693-698.
165. Y. Bae, N. Myung, A.J. Bard. "Electrochemistry and Electrogenerated Chemiluminescence of CdTe Nanoparticles". Nano Lett. 2004. 4(6): 1153-1161.
166. H. Jiang, H. Ju. "Electrochemiluminescence Sensors for Scavengers of Hydroxyl Radical Based on Its Annihilation in CdSe Quantum Dots Film/Peroxide System". Anal. Chem. 2007. 79(17): 6690-6696.
167. H.P. Huang, J.J. Li, J.J. Zhu. "Electrochemiluminescence Based on Quantum Dots and Their Analytical Application". Anal. Methods. 2011. 3(1): 33-42.
168. J. Li, S.J. Guo, E.K. Wang. "Recent Advances in New Luminescent Nanomaterials for Electrochemiluminescence Sensors''. RSC Advances. 2012. 2(9): 3579-3586.
169. X. Liu, H. Jiang, J. Lei, H. Ju. "Anodic Electrochemiluminescence of CdTe Quantum Dots and Its Energy Transfer for Detection of Catechol Derivatives". Anal. Chem. 2007. 79(21): 8055-8060.
170. X. Liu, L. Cheng, J. Lei, H. Ju. "Dopamine Detection Based on Its Quenching Effect on the Anodic Electrochemiluminescence of CdSe Quantum Dots''. Analyst. 2008. 133(9): 1161-1163.
171. Z.F. Ding, B.M. Quinn, S.K. Haram, L.E. Pell, B.A. Korgel, A.J. Bard. "Electrochemistry and Electrogenerated Chemiluminescence from Silicon Nanocrystal Quantum Dots''. Science. 2002. 296(5571): 1293-1297.
172. C.G. Shi, X. Shan, Z.Q. Pan, J.J. Xu, C. Lu, N. Bao, H.Y. Gu. "Quantum Dot (QD)-Modified Carbon Tape Electrodes for Reproducible Electrochemiluminescence (ECL) Emission on a Paper-Based Platform". Anal. Chem. 2012. 84(6): 3033-3038.
173. M.S. Wu, H.W. Shi, L.J. He, J.J. Xu, H.Y. Chen. "Microchip Device with 64-Site Electrode Array for Multiplexed Immunoassay of Cell Surface Antigens Based on Electrochemiluminescence Resonance Energy Transfer". Anal. Chem. 2012. 84(9): 4207-4213.
174. I.L. Medintz, T. Pons, S.A. Trammell, A.F. Grimes, D.S. English, J.B. Blanco-Canosa, P.E. Dawson, H. Mattoussi. "Interactions Between Redox Complexes and Semiconductor Quantum Dots Coupled via a Peptide Bridge". J. Am. Chem. Soc. 2008. 130(49): 16745-16756.
175. M.D. Swain, J. Octain, D.E. Benson. "Unimolecular, Soluble Semiconductor Nanoparticle-Based Biosensors for Thrombin Using Charge/Electron Transfer". Bioconjugate Chem. 2008. 19(12): 2520-2526.
176. M. Sykora, M.A. Petruska, J. Alstrum-Acevedo, I. Bezel, T.J. Meyer, V.I. Klimov. "Photoinduced Charge Transfer Between CdSe Nanocrystal Quantum Dots and Ru-Polypyridine Complexes". J. Am. Chem. Soc. 2006. 128(31): 9984-9985.
177. M. Malicki, K.E. Knowles, E.A. Weiss. "Gating of Hole Transfer from Photoexcited PbS Quantum Dots to Aminoferrocene by the Ligand Shell of the Dots". Chem. Commun. 2013. DOI: 10.1039/C2CC32895J.
178. D. Dorokhin, N. Tomczak, A.H. Velders, D.N. Reinhoudt, G.J. Vancso. "Photoluminescence Quenching of CdSe/ZnS Quantum Dots by Molecular Ferrocene and Ferrocenyl Thiol Ligands". J. Phys. Chem. C. 2009. 113(43): 18676-18680.
179. M.J. Ruedas-Rama, E.A.H. Hall. "A Quantum Dot-Lucigenin Probe for Cl". Analyst. 2008. 133(11): 1556-1566.
180. I. Yildiz, M. Tomasulo, F.M. Raymo. "A Mechanism to Signal Receptor-Substrate Interactions with Luminescent Quantum

Dots''. P. Natl. Acad. S. USA. 2006. 103(31): 11457-11460.
181. A.J. Morris-Cohen, M.T. Frederick, L.C. Cass, E.A. Weiss. "Simultaneous Determination of the Adsorption Constant and the Photoinduced Electron Transfer Rate for a Cds Quantum Dot-Viologen Complex". J. Am. Chem. Soc. 2011. 133(26): 10146-10154.
182. F. Scholz, L. Dworak, V.V. Matylitsky, J. Wachtveitl. "Ultrafast Electron Transfer from Photoexcited CdSe Quantum Dots to Methylviologen". ChemPhysChem. 2011. 12(12): 2255-2259.
183. I.L. Medintz, M.H. Stewart, S.A. Trammell, K. Susumu, J.B. Delehanty, B.C. Mei, J.S. Melinger, J.B. Blanco-Canosa, P.E. Dawson, H. Mattoussi. "Quantum-Dot/Dopamine Bioconjugates Function as Redox Coupled Assemblies for in Vitro and Intracellular pH Sensing". Nat. Mater. 2010. 9(8): 676-684.
184. X. Ji, G. Palui, T. Avellini, H.B. Na, C. Yi, K.L. Knappenberger, H. Mattoussi. "On the pH-Dependent Quenching of Quantum Dot Photoluminescence by Redox Active Dopamine". J. Am. Chem. Soc. 2012. 134(13): 6006-6017.
185. R. Freeman, T. Finder, R. Gill, I. Willner. "Probing Protein Kinase (CK2) and Alkaline Phosphatase with CdSe/ZnS Quantum Dots". Nano Lett. 2010. 10(6): 2192-2196.
186. J. Callan, R. Mulrooney, S. Kamila, B. McCaughan. "Anion Sensing with Luminescent Quantum Dots–A Modular Approach Based on the Photoinduced Electron Transfer (PET) Mechanism". J. Fluoresc. 2008. 18(2): 527-532.
187. J. Huang, D. Stockwell, Z. Huang, D.L. Mohler, T. Lian. "Photoinduced Ultrafast Electron Transfer from CdSe Quantum Dots to Re-Bipyridyl Complexes". J. Am. Chem. Soc. 2008. 130(17): 5632-5633.
188. S. Ruhle, M. Shalom, A. Zaban. "Quantum-Dot-Sensitized Solar Cells''. ChemPhysChem. 2010. 11(11): 2290-2304.
189. S. Jin, J.-C. Hsiang, H. Zhu, N. Song, R.M. Dickson, T. Lian. "Correlated Single Quantum Dot Blinking and Interfacial Electron Transfer Dynamics". Chem. Sci. 2010. 1(4): 519-526.
190. W. Qin, P. Guyot-Sionnest. "Evidence for the Role of Holes in Blinking: Negative and Oxidized CdSe/CdS Dots''. ACS Nano. 2012. 6(10): 9125-9132.
191. M. Shim, C.J. Wang, P. Guyot-Sionnest. "Charge-Tunable Optical Properties in Colloidal Semiconductor Nanocrystals". J. Phys. Chem. B. 2001. 105(12): 2369-2373.
192. M. Tagliazucchi, D.B. Tice, C.M. Sweeney, A.J. Morris-Cohen, E.A. Weiss. "Ligand-Controlled Rates of Photoinduced Electron Transfer in Hybrid CdSe Nanocrystal/Poly(-viologen) Films". ACS Nano. 2011. 5(12): 9907-9917.
193. A.J. Morris-Cohen, M.D. Peterson, M.T. Frederick, J.M. Kamm, E.A. Weiss. "Evidence for a Through-Space Pathway for Electron Transfer from Quantum Dots to Carboxylate-Functionalized Viologens". J. Phys. Chem. Lett. 2012. 3(19): 2840-2844.
194. D. Dorokhin, N. Tomczak, D.N. Reinhoudt, A.H. Velders, G.J. Vancso. "Ferrocene-Coated CdSe/ZnS Quantum Dots as Electroactive Nanoparticles Hybrids". Nanotechnology. 2010. 21: 285703.
195. M.G. Sandros, D. Gao, D.E. Benson. "A Modular Nanoparticle-Based System for Reagentless Small Molecule Biosensing". J. Am. Chem. Soc. 2005. 127(35): 12198-12199.
196. M.G. Sandros, V. Shete, D.E. Benson. "Selective, Reversible, Reagentless Maltose Biosensing with Core-Shell Semiconducting Nanoparticles". Analyst. 2006. 131(2): 229-235.
197. B.P. Aryal, D.E. Benson. "Electron Donor Solvent Effects Provide Biosensing with Quantum Dots". J. Am. Chem. Soc. 2006. 128(50): 15986-15987.
198. V.S. Shete, D.E. Benson. "Protein Design Provides Lead(II) Ion Biosensors for Imaging Molecular Fluxes Around Red Blood Cells". Biochemistry. 2009. 48(2): 462-470.
199. R. Gill, R. Freeman, J.-P. Xu, I. Willner, S. Winograd, I. Shweky, U. Banin. "Probing Biocatalytic Transformations with CdSe−ZnS QDs". J. Am. Chem. Soc. 2006. 128(48): 15376-15377.
200. R. Freeman, T. Finder, R. Gill, I. Willner. "Probing Protein Kinase (CK2) and Alkaline Phosphatase with CdSe/ZnS Quantum Dots". Nano Lett. 2010. 10(6): 2192-2196.
201. S.C. Cui, T. Tachikawa, M. Fujitsuka, T. Majima. "Photoinduced Electron Transfer in a Quantum Dot-Cucurbituril Supramolecular Complex". J. Phys. Chem. C. 2011. 115(5): 1824-1830.
202. C. Burda, T.C. Green, S. Link, M.A. El-Sayed. "Electron Shuttling Across the Interface of CdSe Nanoparticles Monitored by Femtosecond Laser Spectroscopy". J. Phys. Chem. B. 1999. 103(11): 1783-1788.
203. J. Tian, L. Zhou, Y. Zhao, Y. Wang, Y. Peng, S. Zhao. "Multiplexed Detection of Tumor Markers with Multicolor Quantum Dots based on Fluorescence Polarization Immunoassay". Talanta. 2012. 92(0): 72-77.
204. S.A. Empedocles, R. Neuhauser, M.G. Bawendi. ''Three-Dimensional Orientation Measurements of Symmetric Single Chromophores Using Polarization Microscopy". Nature. 1999. 399(6732): 126-130.
205. I.H. Chung, K.T. Shimizu, M.G. Bawendi. "Room Temperature Measurements of the 3D Orientation of Single CdSe Quantum Dots Using Polarization Microscopy". P. Natl. Acad. S. USA. 2003. 100(2): 405-408.
206. P.K. Chattopadhyay, D.A. Price, T.F. Harper, M.R. Betts, J. Yu, E. Gostick, S.P. Perfetto, P. Goepfert, R.A. Koup, S.C. De Rosa, M.P. Bruchez, M. Roederer. "Quantum Dot Semiconductor Nanocrystals for Immunophenotyping by Polychromatic Flow Cytometry''. Nat. Med. 2006. 12(8): 972-977.
207. O. Kovtun, E.J. Ross, I.D. Tomlinson, S.J. Rosenthal. "A Flow Cytometry-Based Dopamine Transporter Binding Assay Using Antagonist-Conjugated Quantum Dots''. Chem. Commun. 2012. 48(44): 5428-5430.
208. P.O. Krutzik, G.P. Nolan. "Fluorescent Cell Barcoding in Flow Cytometry Allows High-Throughput Drug Screening and Signaling Profiling''. Nat. Methods. 2006. 3(5): 361-368.
209. Luminex Corporation. "Luminex". 2012. www.luminex.com [accessed Nov 12 2012].
210. M.Y. Han, X.H. Gao, J.Z. Su, S. Nie. "Quantum-Dot-Tagged Microbeads for Multiplexed Optical Coding of Biomolecules". Nat. Biotechnol. 2001. 19(7): 631-635.
211. A. Agrawal, C.Y. Zhang, T. Byassee, R.A. Tripp, S.M. Nie. "Counting Single Native Biomolecules and Intact Viruses with Color-Coded Nanoparticles". Anal. Chem. 2006. 78(4): 1061-1070.
212. K.C. Goss, G.G. Messier, M.E. Potter. "Data Detection Algorithms for Multiplexed Quantum Dot Encoding". Opt. Express. 2012. 20(5): 5762-5774.
213. Y.L. Gao, W.L. Stanford, W.C.W. Chan. ''Quantum-Dot-Encoded Microbeads for Multiplexed Genetic Detection of Non-Amplified DNA Samples". Small. 2011. 7(1): 137-146.
214. S. Giri, E.A. Sykes, T.L. Jennings, W.C.W. Chan. "Rapid Screening of Genetic Biomarkers of Infectious Agents Using Quantum Dot Barcodes". ACS Nano. 2011. 5(3): 1580-1587.
215. H.X. Xu, M.Y. Sha, E.Y. Wong, J. Uphoff, Y.H. Xu, J.A. Treadway, A. Truong, E. O'Brien, S. Asquith, M. Stubbins, N.K. Spurr, E.H. Lai, W. Mahoney. "Multiplexed SNP Genotyping Using the Qbead (TM) System: A Quantum Dot-Encoded Microsphere-Based Assay". Nucleic Acids Res. 2003. 31(8): e43.
216. J.D. Joannopoulos, S.G. Johnson, J.N. Winn, R.D. Meade. Photonic Crystals: Molding the Flow of Light. Princeton, NJ: Princeton University Press, 2008. 2nd ed.
217. B.T. Cunningham, R.C. Zangar. "Photonic Crystal Enhanced Fluorescence for Early Breast Cancer Biomarker Detection". J. Biophotonics. 2012. 5(8-9): 617-628.
218. N. Ganesh, W. Zhang, P.C. Mathias, E. Chow, J.A.N.T. Soares, V. Malyarchuk, A.D. Smith, B.T. Cunningham. "Enhanced Fluorescence Emission from Quantum Dots on a Photonic Crystal Surface". Nat. Nanotechnol. 2007. 2(8): 515-520.
219. K.E. Sapsford, S. Spindel, T. Jennings, G.L. Tao, R.C. Triulzi, W.R. Algar, I.L. Medintz. ''Optimizing Two-Color Semiconductor Nanocrystal Immunoassays in Single Well Microtiter Plate Formats". Sensors. 2011. 11(8): 7879-7891.
220. B.T. Cunningham, P. Li, S. Schulz, B. Lin, C. Baird, J. Gerstenmaier, C. Genick, F. Wang, E. Fine, L. Laing. "Label-Free Assays on the BIND System". J. Biomol. Screen. 2004. 9(6): 481-490.
221. S.H. Cao, W.P. Cai, Q. Liu, Y.Q. Li. "Surface Plasmon-Coupled Emission: What Can Directional Fluorescence Bring to the Analytical Sciences?". Annu. Rev. Anal. Chem. 2012. 5: 317-336.
222. J.R. Lakowicz, J. Malicka, I. Gryczynski, Z. Gryczynski, C.D. Geddes. "Radiative Decay Engineering: The Role of Photonic Mode Density in Biotechnology". J. Phys. D: Appl. Phys. 2003. 36(14): R240-R249.
223. C.D. Geddes, J.R. Lakowicz. "Editorial:

Metal-Enhanced Fluorescence". J. Fluoresc. 2002. 12(2): 121-129.
224. O. Kulakovich, N. Strekal, A. Yaroshevich, S. Maskevich, S. Gaponenko, I. Nabiev, U. Woggon, M. Artemyev. "Enhanced Luminescence of CdSe Quantum Dots on Gold Colloids''. Nano Lett. 2002. 2(12): 1449-1452.
225. Y.-H. Chan, J. Chen, S.E. Wark, S.L. Skiles, D.H. Son, J.D. Batteas. "Using Patterned Arrays of Metal Nanoparticles to Probe Plasmon Enhanced Luminescence of CdSe Quantum Dots". ACS Nano. 2009. 3(7): 1735-1744.
226. J.H. Song, T. Atay, S.F. Shi, H. Urabe, A.V. Nurmikko. "Large Enhancement of Fluorescence Efficiency from CdSe/ZnS Quantum Dots Induced by Resonant Coupling to Spatially Controlled Surface Plasmons''. Nano Lett. 2005. 5(8): 1557-1561.
227. P.P. Pompa, L. Martiradonna, A. Della Torre, L. Carbone, L.L. del Mercato, L. Manna, M. De Vittorio, F. Calabi, R. Cingolani, R. Rinaldi. "Fluorescence Enhancement in Colloidal Semiconductor Nanocrystals by Metallic Nanopatterns. Sensors. Actuat. B-Chem. 2007. 126(1): 187-192.
228. K. Leong, Y. Chen, D.J. Masiello, M.T. Zin, M. Hnilova, H. Ma, C. Tamerler, M. Sarikaya, D.S. Ginger, A.K.-Y. Jen. "Cooperative Near-Field Surface Plasmon Enhanced Quantum Dot Nanoarrays". Adv. Funct. Mater. 2010. 20(16): 2675-2682.
229. L. Zhou, F. Ding, H. Chen, W. Ding, W. Zhang, S.Y. Chou. "Enhancement of Immunoassay's Fluorescence and Detection Sensitivity Using Three-Dimensional Plasmonic Nano-Antenna-Dots Array". Anal. Chem. 2012. 84(10): 4489-4495.
230. R. Robelek, L. Niu, E.L. Schmid, W. Knoll. "Multiplexed Hybridization Detection of Quantum Dot-Conjugated DNA Sequences Using Surface Plasmon Enhanced Fluorescence Microscopy and Spectrometry". Anal. Chem. 2004. 76(20): 6160-6165.
231. L.-H. Jin, S.-M. Li, Y.-H. Cho. "Enhanced Detection Sensitivity of Pegylated CdSe/ZnS Quantum Dots-Based Prostate Cancer Biomarkers by Surface Plasmon-Coupled Emission. Biosens". Bioelectron. 2012. 33(1): 284-287.
232. L. Malic, M.G. Sandros, M. Tabrizian. "Designed Biointerface Using Near-Infrared Quantum Dots for Ultrasensitive Surface Plasmon Resonance Imaging Biosensors". Anal. Chem. 2011. 83(13): 5222-5229.
233. H. Chen, J. Xue, Y. Zhang, X. Zhu, J. Gao, B. Yu. "Comparison of Quantum Dots Immunofluorescence Histochemistry and Conventional Immunohistochemistry for the Detection of Caveolin-1 and PCNA in the Lung Cancer Tissue Microarray". J. Mol. Histol. 2009. 40(4): 261-268.
234. C. Chen, J. Peng, H.S. Xia, G.F. Yang, Q.S. Wu, L.D. Chen, L.B. Zeng, Z.L. Zhang, D.W. Pang, Y. Li. "Quantum Dots-Based Immunofluorescence Technology for the Quantitative Determination of HER2 Expression in Breast Cancer". Biomaterials. 2009. 30(15): 2912-2918.
235. Y. Ruan, W.M. Yu, F. Cheng, X.B. Zhang, S. Larre. "Detection of Prostate Stem Cell Antigen Expression in Human Prostate Cancer Using Quantum-Dot-Based Technology". Sensors. 2012. 12(5): 5461-5470.
236. Y. Xing, Q. Chaudry, C. Shen, K.Y. Kong, H.E. Zhau, L. WChung, J.A. Petros, R.M. O'Regan, M.V. Yezhelyev, J.W. Simons, M.D. Wang, S. Nie. "Bioconjugated Quantum Dots for Multiplexed and Quantitative Immunohistochemistry". Nat. Protoc. 2007. 2(5): 1152-1165.
237. J.K. Jaiswal, H. Mattoussi, J.M. Mauro, S.M. Simon. "Long-Term Multiple Color Imaging of Live Cells using Quantum Dot Bioconjugates". Nat. Biotechnol. 2003. 21(1): 47-51.
238. J.B. Delehanty, C.E. Bradburne, K. Susumu, K. Boeneman, B.C. Mei, D. Farrell, J.B. Blanco-Canosa, P.E. Dawson, H. Mattoussi, I.L. Medintz. "Spatiotemporal Multicolor Labeling of Individual Cells Using Peptide-Functionalized Quantum Dots and Mixed Delivery Techniques". J. Am. Chem. Soc. 2011. 133(27): 10482-10489.
239. A. Matsuno, J. Itoh, S. Takekoshi, T. Nagashima, R.Y. Osamura. "Three-Dimensional Imaging of the Intracellular Localization of Growth Hormone and Prolactin and Their mRNA Using Nanocrystal (Quantum dot) and Confocal Laser Scanning Microscopy Techniques". J. Histochem. Cytochem. 2005. 53(7): 833-838.
240. P.M. Chan, T. Yuen, F. Ruf, J. Gonzalez-Maeso, S.C. Sealfon. "Method for Multiplex Cellular Detection of mRNAs Using Quantum Dot Fluorescent in Situ Hybridization". Nucleic Acids Res. 2005. 33(18): e161.
241. J. Lee, Y.-J. Kwon, Y. Choi, H.C. Kim, K. Kim, J. Kim, S. Park, R. Song. "Quantum Dot-Based Screening System for Discovery of G Protein-Coupled Receptor Agonists". ChemBioChem. 2012. 13(10): 1503-1508.
242. C. Chen, S.R. Sun, Y.P. Gong, C.B. Qi, C.W. Peng, X.Q. Yang, S.P. Liu, J. Peng, S. Zhu, M.B. Hu, D.W. Pang, Y. Li. "Quantum Dots-Based Molecular Classification of Breast Cancer by Quantitative Spectroanalysis of Hormone Receptors and HER2". Biomaterials. 2011. 32(30): 7592-7599.
243. X.-Q. Yang, C. Chen, C.-W. Peng, J.-X. Hou, S.-P. Liu, C.-B. Qi, Y.-P. Gong, X.-B. Zhu, D.-W. Pang, Y. Li. "Quantum Dot-Based Quantitative Immunofluorescence Detection and Spectrum Analysis of Epidermal Growth Factor Receptor in Breast Cancer Tissue Arrays". Int. J. Nanomedicine. 2011. 6: 2265-2273.
244. J.A. Liu, S.K. Lau, V.A. Varma, B.A. Kairdolf, S.M. Nie. "Multiplexed Detection and Characterization of Rare Tumor Cells in Hodgkin's Lymphoma with Multicolor Quantum Dots". Anal. Chem. 2010. 82(14): 6237-6243.
245. J. Liu, S.K. Lau, V.A. Varma, R.A. Moffitt, M. Caldwell, T. Liu, A.N. Young, J.A. Petros, A.O. Osunkoya, T. Krogstad, B. Leyland-Jones, M.D. Wang, S.M. Nie. "Molecular Mapping of Tumor Heterogeneity on Clinical Tissue Specimens with Multiplexed Quantum Dots". ACS Nano. 2010. 4(5): 2755-2765.
246. Y.P. Varshni. "Temperature Dependence of the Energy Gap in Semiconductors". Physica. 1967. 34(1): 149-154.
247. J.-M. Yang, H. Yang, L. Lin. "Quantum Dot Nano Thermometers Reveal Heterogeneous Local Thermogenesis in Living Cells". ACS Nano. 2011. 5(6): 5067-5071.
248. A. Diaspro, G. Chirico, M. Collini. "Two-Photon Fluorescence Excitation and Related Techniques in Biological Microscopy". Q. Rev. Biophys. 2005. 38(2): 97-166.
249. G.S. He, L.S. Tan, Q. Zheng, P.N. Prasad. "Multiphoton Absorbing Materials: Molecular Designs, Characterizations, and Applications''. Chem. Rev. 2008. 108(4): 1245-1330.
250. T. Wang, J.Y. Chen, S. Zhen, P.N. Wang, C.C. Wang, W.L. Yang, Q. Peng. "Thiol-Capped CdTe Quantum Dots with Two-Photon Excitation for Imaging High Autofluorescence Background Living Cells". J. Fluoresc. 2009. 19(4): 615-621.
251. D.J. Bharali, D.W. Lucey, H. Jayakumar, H.E. Pudavar, P.N. Prasad. "Folate-Receptor-Mediated Delivery of InP Quantum Dots for Bioimaging Using Confocal and Two-Photon Microscopy". J. Am. Chem. Soc. 2005. 127(32): 11364-11371.
252. M. Geszke, M. Murias, L. Balan, G. Medjahdi, J. Korczynski, M. Moritz, J. Lulek, R. Schneider. "Folic Acid-Conjugated Core/Shell ZnS: Mn/ZnS Quantum Dots as Targeted Probes for Two Photon Fluorescence Imaging of Cancer Cells". Acta Biomater. 2011. 7(3): 1327-1338.
253. C. Tu, X. Ma, P. Pantazis, S.M. Kauzlarich, A.Y. Louie. "Paramagnetic, Silicon Quantum Dots for Magnetic Resonance and Two-Photon Imaging of Macrophages". J. Am. Chem. Soc. 2010. 132(6): 2016-2023.
254. R. Zhang, E. Rothenberg, G. Fruhwirth, P.D. Simonson, F. Ye, I. Golding, T. Ng, W. Lopes, P.R. Selvin. "Two-Photon 3D FIONA of Individual Quantum Dots in an Aqueous Environment". Nano Lett. 2011. 11(10): 4074-4078.
255. M. Stroh, J.P. Zimmer, D.G. Duda, T.S. Levchenko, K.S. Cohen, E.B. Brown, D.T. Scadden, V.P. Torchilin, M.G. Bawendi, D. Fukumura, R.K. Jain. "Quantum Dots Spectrally Distinguish Multiple Species within the Tumor Milieu in Vivo". Nat. Med. 2005. 11(6): 678-682.
256. L.M. Maestro, J.E. Ramirez-Hernandez, N. Bogdan, J.A. Capobianco, F. Vetrone, J.G. Sole, D. Jaque. "Deep Tissue Bio-Imaging Using Two-Photon Excited CdTe Fluorescent Quantum Dots Working within the Biological Window''. Nanoscale. 2012. 4(1): 298-302.
257. W. Jiang, A. Singhal, B.Y.S. Kim, J. Zheng, J.T. Rutka, C. Wang, W.C.W. Chan. "Assessing Near-Infrared Quantum Dots for Deep Tissue, Organ, and Animal Imaging Applications". J. Lab. Autom. 2008. 13(1): 6-12.
258. S. Weiss. "Measuring Conformational Dynamics of Biomolecules by Single Molecule Fluorescence Spectroscopy". Nat. Struct. Biol. 2000. 7(9): 724-729.
259. S. Weiss. "Fluorescence Spectroscopy of Single Biomolecules''. Science. 1999. 283(5408): 1676-1683.
260. T. Pons, H. Mattoussi. "Investigating Biological Processes at the Single Molecule

Level Using Luminescent Quantum Dots". Ann. Biomed. Eng. 2009. 37(10): 1934-1959.
261. M.P. Bruchez. "Quantum Dots Find Their Stride in Single Molecule Tracking". Curr. Opin. Chem. Biol. 2011. 15(6): 775-780.
262. F. Pinaud, S. Clarke, A. Sittner, M. Dahan. "Probing Cellular Events, One Quantum Dot at a Time". Nat. Methods. 2010. 7(4): 275-285.
263. S.R. Opperwall, A. Divakaran, E.G. Porter, J.A. Christians, A.J. DenHartigh, D.E. Benson. "Wide Dynamic Range Sensing with Single Quantum Dot Biosensors". ACS Nano. 2012. 6(9): 8078-8086.
264. C.Y. Zhang, H.C. Yeh, M.T. Kuroki, T.H. Wang. "Single-Quantum-Dot-Based DNA Nanosensor". Nat. Mater. 2005. 4(11): 826-831.
265. C.Y. Zhang, J. Hu. "Single Quantum Dot-Based Nanosensor for Multiple DNA Detection". Anal. Chem. 2010. 82(5): 1921-1927.
266. T. Pons, I.L. Medintz, X. Wang, D.S. English, H. Mattoussi. "Solution-Phase Single Quantum Dot Fluorescence Resonance Energy Transfer". J. Am. Chem. Soc. 2006. 128(47): 15324-15331.
267. M. Dahan, S. Levi, C. Luccardini, P. Rostaing, B. Riveau, A. Triller. "Diffusion Dynamics of Glycine Receptors Revealed by Single-Quantum Dot Tracking". Science. 2003. 302(5644): 442-445.
268. C. Bouzigues, M. Morel, A. Triller, M. Dahan. ''Asymmetric Redistribution of GABA Receptors During GABA Gradient Sensing by Nerve Growth Cones Analyzed by Single Quantum Dot Imaging". P. Natl. Acad. S. USA. 2007. 104(27): 11251-11256.
269. T. Buerli, K. Baer, H. Ewers, C. Sidler, C. Fuhrer, J.-M. Fritschy. ''Single Particle Tracking of alpha 7 Nicotinic AChR in Hippocampal Neurons Reveals Regulated Confinement at Glutamatergic and GABAergic Perisynaptic Sites". PLoS ONE. 2010. 5(7): e11507.
270. M. Heine, L. Groc, R. Frischknecht, J.C. Beique, B. Lounis, G. Rumbaugh, R.L. Huganir, L. Cognet, D. Choquet. "Surface Mobility of Postsynaptic AMPARs Tunes Synaptic Transmission''. Science. 2008. 320(5873): 201-205.
271. Q. Zhang, Y.Q. Cao, R.W. Tsien. "Quantum Dots Provide an Optical Signal Specific to Full Collapse Fusion of Synaptic Vesicles". P. Natl. Acad. S. USA. 2007. 104(45): 17843-17848.
272. Q. Zhang, Y. Li, R.W. Tsien. "The Dynamic Control of Kiss-and-Run and Vesicular Reuse Probed with Single Nanoparticles". Science. 2009. 323(5920): 1448-1453.
273. A.R. Lowe, J.J. Siegel, P. Kalab, M. Siu, K. Weis, J.T. Liphardt. "Selectivity Mechanism of the Nuclear Pore Complex Characterized by Single Cargo Tracking". Nature. 2010. 467(7315): 600-U126.
274. N.P. Wells, G.A. Lessard, P.M. Goodwin, M.E. Phipps, P.J. Cutler, D.S. Lidke, B.S. Wilson, J.H. Werner. ''Time-Resolved Three-Dimensional Molecular Tracking in Live Cells". Nano Lett. 2010. 10(11): 4732-4737.
275. S. Doose, J.M. Tsay, F. Pinaud, S. Weiss. "Comparison of Photophysical and Colloidal Properties of Biocompatible Semiconductor Nanocrystals Using Fluorescence Correlation Spectroscopy". Anal. Chem. 2005. 77(7): 2235-2242.
276. T. Liedl, S. Keller, F.C. Simmel, J.O. Radler, W.J. Parak. "Fluorescent Nanocrystals as Colloidal Probes in Complex Fluids Measured by Fluorescence Correlation Spectroscopy". Small. 2005. 1(10): 997-1003.
277. C. Dong, J. Ren. "Measurements for Molar Extinction Coefficients of Aqueous Quantum Dots". Analyst. 2010. 135(6): 1395-1399.
278. R.F. Heuff, J.L. Swift, D.T. Cramb. "Fluorescence Correlation Spectroscopy Using Quantum Dots: Advances, Challenges and Opportunities". Phys. Chem. Chem. Phys. 2007. 9(16): 1870-1880.
279. J.L. Swift, R. Heuff, D.T. Cramb. "A Two-Photon Excitation Fluorescence Cross-Correlation Assay for a Model Ligand-Receptor Binding System Using Quantum Dots". Biophys. J. 2006. 90(4): 1396-1410.
280. J.L. Swift, D.T. Cramb. ''Nanoparticles as Fluorescence Labels: Is Size All That Matters?". Biophys. J. 2008. 95(2): 865-876.
281. J.L. Swift, M.C. Burger, D. Massotte, T.E.S. Dahms, D.T. Cramb. "Two-Photon Excitation Fluorescence Cross-Correlation Assay for Ligand-Receptor Binding: Cell Membrane Nanopatches Containing the Human mu-Opioid Receptor". Anal. Chem. 2007. 79(17): 6783-6791.
282. H.M. Wobma, M.L. Blades, E. Grekova, D.L. McGuire, K. Chen, W.C.W. Chan, D.T. Cramb. "The Development of Direct Multicolour Fluorescence Cross-Correlation Spectroscopy: Towards a New Tool for Tracking Complex Biomolecular Events in Real-Time". Phys. Chem. Chem. Phys. 2012. 14(10): 3290-3294.
283. M.L. Blades, E. Grekova, H.M. Wobma, K. Chen, W.C.W. Chan, D.T. Cramb. "Three-Color Fluorescence Cross-Correlation Spectroscopy for Analyzing Complex Nanoparticle Mixtures". Anal. Chem. 2012. 84(21): 9623-9631.
284. N. Durisic, A.I. Bachir, D.L. Kolin, B. Hebert, B.C. Lagerholm, P. Grutter, P.W. Wiseman. ''Detection and Correction of Blinking Bias in Image Correlation Transport Measurements of Quantum Dot Tagged Macromolecules". Biophys. J. 2007. 93(4): 1338-1346.
285. A.I. Bachir, D.L. Kolin, K.G. Heinze, B. Hebert, P.W. Wiseman. "A Guide to Accurate Measurement of Diffusion Using Fluorescence Correlation Techniques with Blinking Quantum Dot Nanoparticle Labels". J. Chem. Phys. 2008. 128(22).
286. S. Boyle, D.L. Kolin, J.G. Bieler, J.P. Schneck, P.W. Wiseman, M. Edidin. "Quantum Dot Fluorescence Characterizes the Nanoscale Organization of T Cell Receptors for Antigen". Biophys. J. 2011. 101(11): L57-L59.
287. F.-C. Chien, C.W. Kuo, P. Chen. "Localization Imaging Using Blinking Quantum Dots". Analyst. 2011. 136(8): 1608-1613.
288. National Science Foundation (NSF) Division of Molecular and Cellular Biosciences Awards. ''National Science Foundation: Where Discoveries Begin". 2012. http://www.nsf.gov/awardsearch/showAward?AWD_ID=1052733 [accessed Nov 12 2012].
289. National Science Foundation (NSF)-Funded Collaborative Research Project QSTORM. "Switchable Quantum Dots and Adaptive Optics for Super-Resolution Imaging." 2012. www.qstorm.org [accessed Nov 12 2012].
290. Y. Chen, L. Shao, Z. Ali, J. Cai, Z.W. Chen. "NSOM/QD-Based Nanoscale Immunofluorescence Imaging of Antigen-Specific T-Cell Receptor Responses During an in Vivo Clonal Vγ2Vδ2 T-Cell Expansion". Blood. 2008. 111(8): 4220-4232.
291. J. Chen, Y. Wu, C. Wang, J. Cai. "Nanoscale Organization of CD4 Molecules of Human T Helper Cell Mapped by NSOM and Quantum Dots". Scanning. 2008. 30(6): 448-451.
292. J. Chen, Y. Pei, Z. Chen, J. Cai. "Quantum Dot Labeling Based on Near-Field Optical Imaging of CD44 Molecules". Micron. 2010. 41(3): 198-202.
293. L. Zhong, G. Zeng, X. Lu, R.C. Wang, G. Gong, L. Yan, D. Huang, Z.W. Chen. "NSOM/QD-Based Direct Visualization of CD3-Induced and CD28-Enhanced Nanospatial Coclustering of TCR and Coreceptor in Nanodomains in T Cell Activation". PLoS One. 2009. 4(6): e5945.
294. G.W. Walker, V.C. Sundar, C.M. Rudzinski, A.W. Wun, M.G. Bawendi, D.G. Nocera. ''Quantum-Dot Optical Temperature Probes". Appl. Phys. Lett. 2003. 83(17): 3555-3557.
295. L.M. Maestro, C. Jacinto, U.R. Silva, F. Vetrone, J.A. Capobianco, D. Jaque, J.G. Solé. "CdTe Quantum Dots as Nanothermometers: Towards Highly Sensitive Thermal Imaging". Small. 2011. 7(13): 1774-1778.
296. P. Haro-González, L. Martínez-Maestro, I.R. Martín, J. García-Solé, D. Jaque. "High-Sensitivity Fluorescence Lifetime Thermal Sensing Based on CdTe Quantum Dots". Small. 2012. 8(17): 2652-2658.
297. R.K. Pai, M. Cotlet. "Highly Stable, Water-Soluble, Intrinsic Fluorescent Hybrid Scaffolds for Imaging and Biosensing". J. Phys. Chem. C. 2011. 115(5): 1674-1681.
298. M.J. Ruedas-Rama, A. Orte, E.A.H. Hall, J.M. Alvarez-Pez, E.M. Talavera. "A Chloride Ion Nanosensor for Time-Resolved Fluorimetry and Fluorescence Lifetime Imaging". Analyst. 2012. 137(6): 1500-1508.
299. P.P. Provenzano, K.W. Eliceiri, P.J. Keely. "Multiphoton Microscopy and Fluorescence Lifetime Imaging Microscopy (FLIM) to Monitor Metastasis and the Tumor Microenvironment". Clin. Exp. Metastas. 2009. 26(4): 357-370.
300. Y. Sun, J. Phipps, D.S. Elson, H. Stoy, S. Tinling, J. Meier, B. Poirier, F.S. Chuang, D.G. Farwell, L. Marcu. "Fluorescence Lifetime Imaging Microscopy: In Vivo Application to Diagnosis of Oral Carcinoma". Opt. Lett. 2009. 34(13): 2081-2083.
301. D. Shcherbo, E.A. Souslova, J. Goedhart, T.V. Chepurnykh, A. Gaintzeva, T.W. Shemiakina, II, J. Gadella, S. Lukyanov, D.M. Chudakov. "Practical and Reliable FRET/FLIM Pair of Fluorescent Proteins". BMC Biotechnol. 2009. 9: 24.